Università degli Studi di Verona

Department of Surgery,Dentistry, Pediatrics and Ginaecology

GRADUATE SCHOOL of Life and Health Science

DOCTORAL PROGRAM IN Cardiovascular Science

Cycle XXX

β-adrenergic and adenosine receptors interaction during heart failure in atrial cardiomyocytes

S.S.D MED/23

Coordinator:
Prof. Giovanni Battista Luciani

Tutors:
Prof.Giuseppe Faggian
Prof. Julia Gorelik
Dr. Michele Miragoli

PhD. candidate
Marta Mazzola

Abstract

Heart failure (HF) is still a major cause of morbidity and mortality, contributing significantly to global health expenditure, although there have been significant advances in HF therapy in recent decades. Adrenergic nervous system hyperactivity becomes a major problem in HF, conferring significant toxicity to the failing heart. Adenosine is an important endogenous physiological modulator of the heart function and it has been demonstrated to serve as a negative feedback regulator of sympathetic overstimulation by the β_1-adrenoceptors (β_1ARs). It is well known that the antiadrenergic action of adenosine, through activation of A_1 adenosine receptors (A_1ARs), serves as a mechanism of cardioprotection against cardiotoxicity which may accompany excessive adrenergic stimulation. The study presented here aims to assess, in both atrial and ventricular myocytes, spatial distribution of adrenergic and adenosine receptors in different subcellular microdomains and explore their functional interplay in normal heart and HF. The study aimed to: (1) investigate the functional role of the anti-adrenergic effect of adenosine in normal heart and HF, measuring the cell contractility via IonOptix system; (2) dissect cellular mechanisms**,** elucidating the cyclic nucleotide response to catecholamine stimulation following both global (in the bath) or local (in the nano-pipette) stimulation of either β_1ARs or A_1ARs. The cAMP levels were measured via Förster Resonance Energy Transfer (FRET) for the whole-cell recording and via a combination of FRET and scanning ion conductance microscopy (SICM) for local stimulation and measurement of cAMP within the specific microdomains; (3) study molecular mechanisms of the anti-adrenergic effect of adenosine by quantitative PCR (qPCR) and western blot technique. It was found that A_1ARs agonist significantly decreases cAMP concentration following β_1AR stimulation, in both atrial and ventricular myocytes. In contrast, corresponding reduction in the sarcomere shortening was found exclusively in atrial myocytes. Using animal model, heart failure condition was found to be associated with the significant reduction of the anti-

adrenergic effect of A_1ARs stimulation for both contractility and cAMP production in atrial cardiomyocytes. Such effect could be associated with structural changes occurring during HF conditions, such as t-tubule and/or caveolae degradation. Indeed, with the caveolae disruption a similar situation was observed. In addition, molecular investigation shows that A_1ARs are upregulated in left atrium. This study presents evidence of a population of A_1ARs that are localized specifically within the cholesterol lipid microdomains on the surface of myocytes and suggests that A_1ARs may interact with the β_1ARs in these microdomains. During the HF the antiadrenergic effect of adenosine is significantly lower. The loss of the antiadrenergic effect of A_1ARs could be associated with the loss of cardiac cytoarchitecture occurring during HF conditions that may cause a disruption of adrenergic/adenosine signalling compartmentation and interplay. On the other hand, the increase of A_1ARs density during failing conditions appears to follow the loss of the adenosine effects, suggesting the establishment of a potential compensatory mechanism that could be a driving factor of the failing phenotype.

Table of contents

LIST OF ABBREVIATIONS

A_1AR	Adenosine A_1 receptor
$A_{2A}AR$	Adenosine A_{2A} receptor
$A_{2b}AR$	Adenosine A_{2Ab} receptor
AC	Adenylyl cyclase
AF	Atrial fibrilation
ATP	Adenosine triphosphate
β_1AR	β_1 Adrenergic receptor
β_2AR	β_2 Adrenergic receptor
β_3AR	β_3 Adrenergic receptor
cAMP	3',5'-Cyclic adenosine monophosphate
Cav3	Caveolin-3
CICR	Calcium-induced calcium release
cEpac2	cytosolic Epac2-based cAMP FRET sensor
CFP	cyan fluorescent protein
CGP	CGP20712A
Cav3	Caveolin-3
DADs	Delayed afterdepolarisations
DAG	diacyl glycerol
EC	excitation-contraction
ECG	electro-cardiogram
EM	electron microscopy
EC	excitation-contraction

Epac-1	Epac1-based cAMP FRET sensor
FRET	förster resonance energy transfer
GAPDH	glyceraldehyde 3-phosphatedehydrogenase
Gi	inhibitory g-protein
GPCR	g-protein coupled receptor
GDP	Guanosine diphosphate
GTP	Guanosine triphosphate
Gs	stimulatory g-protein
Gαi	inhibitory alpha subunit of g-protein
Gαs	stimulatory alpha subunit of g-protein
Gβγ	beta-gamma subunit of g protein
HF	Heart failure
IBMX	3-Isobutyl-1-methylxanthine
ICI	ICI 118,551
I_K	potassium current
I_{KATP}	ATP-dependent potassium current
I_{Na}	sodium current
ISO	isoprenaline
IP_3	1,4,5-triphosphate
LTCC	LTCC L-type Ca^{2+} channel
M199	medium 199
MβCD	Methyl-β-cyclodextrin
NCX	Na^+-Ca^{2+} antiporter exchanger

PKA	Phosphokinase A
PLC	PLC Phospholipase C
RyR2	Ryanodine receptor
ROI	Region of interest
SR	Sarcoendoplasmic reticulum
SERCA	SR calcium transport
SICM	Scanning ion conductance microscopy
NCX	Na^{+}-Ca^{2+} antiporter exchanger
PKA	Phosphokinase A
PLC	PLC Phospholipase C

CHAPTER 1. General introduction

1. General introduction

1.1 The cardiovascular system

The cardiovascular system consists of the blood vessels and the heart. The lymphatic system, which does not contain blood, represents an additional third component that is connected to the cardiovascular system. It serves an important exchange function together with the blood vessels. The heart is a muscular, four-chambered organ, about the size of a man's closed fist. It is positioned in the mediastinum (middle of the thoracic cavity) between the lungs, above the diaphragm and in front of the oesophagus. By its rhythmic contraction, the heart acts as a pump maintaining the circulation of the blood to the whole body (Gray, 1918). The heart is composed of four chambers: two atria and two ventricles (Figure 1). The atria are separated by a wall called interatrial septum; whereas the ventricles are separated by the interventricular septum. In each half of the heart, left and right, an atrium is connected to a ventricle; valves allow blood to flow in one direction preventing backflow. The heart is connected to the vascular system wich delivers blood through the body. The purpose of the cardiovascular system is to transport oxygen and nutrients to the cells of the body and remove carbon dioxide and other metabolic waste products. Each pumping cicle, or beat of the heart, consists of two phases - diastole and systole. During the diastole the ventricles are filling with blood and the atria are contracting. Then the systole follows, the ventricles are contracting while the atria are relaxing and filling up with blood (Sonnenblick et al., 1967). The aorta distributes blood to all organs via the arterial system; inside the organs, the vasculature branches out into smaller and smaller vessels, eventually forming capillaries. Recently, it has been shown that the heart has an important signalling function: it synthesizes several hormones. One of these is the atrial natriuretic peptide, which plays an important role in the regulation of blood volume and blood pressure.

The lymphatic system, which is associated with the blood vessels, collects the excess fluid that filters from the vasculature and transports it back into venous circulation (Klabunde, 2011).

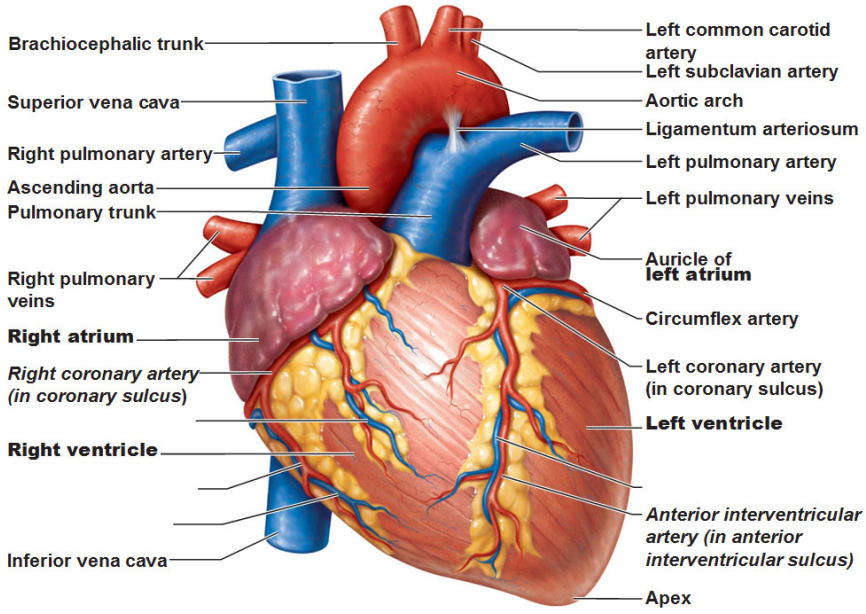

Figure 1: Herat anterior exposure (Netter, 1991)

1.2 The conduction System

Cardiac tissue is an involuntary striated muscle structurally similar to the skeletal one. Despite this similarity, the electrophysiology of the two tissues presents many differences (Hopkins, 2006). Indeed, in the skeletal muscle the action potential that causes contraction is very short (2-3 ms) and is generated by central nervous system. In contrast, the action potential in the heart is not generated by nervous activity, but due to the activity of the specialized areas of cardiac tissue (nodes) which are able to initiate the action potential that then goes directly from cell to cell. Neuronal activity can only modulate the rate of the spontaneous contraction of the heart.

In contractile cells, an action potential leads to a mechanical contraction. Conductive cells are specialized cells that allow the initiation and

propagation of action potentials. The myocardium is a specialized form of muscle, consisting of individual cells joined by electrical connections. Cardiac cells are electrically coupled through gap junctions (Figure 2), which allows action potentials to spread to the adjacent cells, causing an electrical wave of action potentials throughout the whole heart (Carmeliet and Vereecke, 2002). The depolarization wave is followed by a wave of contraction that passes across the atria, then moves into the ventricles.

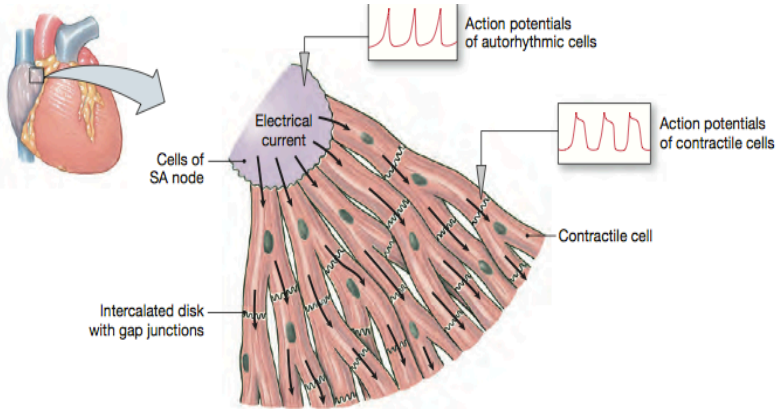

Figure 2: Action potentials of pacemaker cells. Depolarizations of the autorhythmic cells then spread rapidly to adjacent contractile cells through gap junctions (Silverthorn, 2010).

The depolarization begins in the sinoatrial (SA) node that is a small mass of specialized tissue in the right atrium. It is located in close proximity to the opening of the superior vena cava and is electrically coupled with the atrial syncytium. The SA nodal cells are self-excitatory, pacemaker cells. In human, they generate action potentials at the rate of about 70 events per minute. Cardiac impulse travels from the SA node into the atrial syncytium, and the atria begin to contract almost simultaneously. Then the impulse passes along junctional fibers of the conduction system to the atrioventricular node (AV), that is a mass formed by a group of autorhythmic cells. AV node is located in the bottom interatrial septum, beneath the

endocardium. From the AV node, the impulse moves into the ventricles. There are specialized conducting cells, called Purkinje fibers, that transmit electrical signals very rapidly down the atrioventricular bundle (bundle of His) in the ventricular septum (Silverthorn, 2010). The AV bundle fibers divide into left and right bundle branches. The bundle branch fibers continue downward to the apex of the heart, where they divide into smaller Purkinje fibers that spread outward among the contractile cells. The Purkinje fibers transmit impulses rapidly, with speeds up to 4 m/sec, so that all contractile cells in the apex contract nearly simultaneously.

1.2.1 The action Potential

Cardiac myocytes, like neurons, are excitable cells which are able to generate action potentials. Action potential occurs when the membrane quickly depolarizes and then repolarizes back to its resting state. Each of the two types of cardiac muscle cells (myocardial contractile cells and myocardial autorhythmic cells) has a distinctive action potential. The cardiac action potential can in general be subdivided into five phases (Figure 3) although the shapes of the action potential show large variations between different cells, and some phases are not pronounced or may even be absent in some cell types (Carmeliet and Vereecke, 2002).

Phase 0: consists of the initial depolarization phase, which brings the membrane potential quickly from a negative value of about -80 mV during diastole to a positive potential. Voltage-gated Na^+ channels open, allowing Na^+ to enter the cell and rapidly depolarize it. The membrane potential reaches about +20 mV before the Na^+ channels close.

Phase 1: when the Na^+ channels close, the cell begins to repolarize as K+ leaves through open K^+ channels. This is an initial repolarization.

Phase 2 (Plateau): during the plateau phase the membrane potential remains for some times near 0 mV, but during this phase the potential membrane slowly becomes more negative. The action potential then flattens into a plateau as the result of two events: a decrease in K^+

permeability and an increase in Ca^{2+} permeability. Voltage-gated Ca^{2+} channels activated by depolarization slowly open during phases 0 and 1. When they finally open, Ca^{2+} enters the cell. At the same time, some “fast” K^+ channels close. The combination of Ca^{2+} influx and decreased K^+ efflux causes the action potential to flatten out into a plateau.

Phase 3: the plateau ends when Ca^{2+} channels close and K^+ permeability increases once more. The “slow” K^+ channels responsible for this phase are similar to those in the neuron: they are activated by depolarization but are slow to open. When the slow K^+ channels open, K^+ exits rapidly, from the cell restoring its potential.

Phase 4 (Resting membrane potential): myocardial contractile cells have a stable resting potential of about - 80 mV

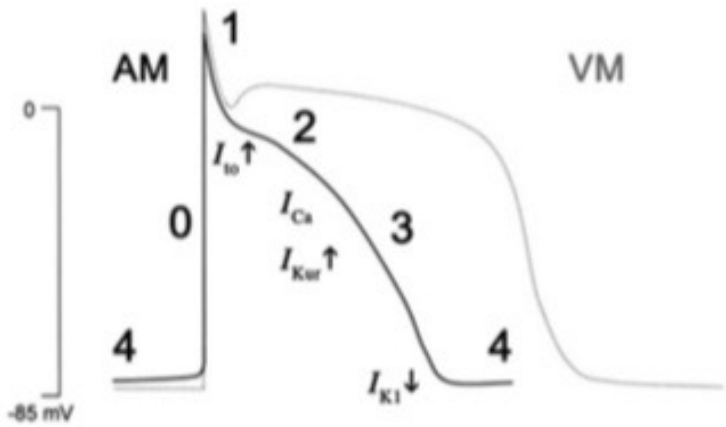

Figure 3: Atrial myocyte (AM, black line) and ventricular myocyte (VM, grey line) action potential (AP) morphology. The atrial AP resting potential is less negative and slowly depolarizes in phase 4 in response to electrical stimulations reaching the threshold for full phase 0 depolarization; the phase2 plateau is abbreviated; and terminal repolarization in phase3 is slower compared to VM. Differences in AP morphology are mainly explained by increased I_{to} and I_{Kur} versus decreased I_{K1} currents, while I_{Ca} currents are overall similar in atrial and ventricular myocytes. Modified figure reproduced from (Sören Brandenburg et al., 2015).

In different cell types a heterogeneity of the action potential, in terms of shape, amplitude and duration was observed. This is due to the differences of the ionic currents (Gossop and Connel, 1975). Many differences are also present between atrial and ventricular cells. Indeed, in the atria, action potential has a less negative resting potential, a shorter plateau, and a slower terminal repolarization (Figure 3). In both atrial and ventricular myocytes, the time and voltage dependent properties of the voltage the voltage-gated inward Na^+ (Na_v) and Ca^{2+} (Ca_v) currents are similar. Otherwise, there are different types of K^+ currents, particularly K_v currents, which contribute to atrial and ventricular action potential repolarization (Gossop and Connell, 1975 and Anumonwo et al., 2001).

1.2.2. Abnormal action potential

During pathophysiological conditions, contractile (i.e., non-pacemaker) cells may undergo spontaneous depolarizations during both phase 3 and in the early phase 4, triggering abnormal action potential. These spontaneous depolarizations, known as afterdepolarization events, are able to trigger, if of sufficient magnitude, self-sustaining action potentials, resulting in cardiac arrhythmias. Afterdepolarizations can either interrupt the process of repolarization or take place after completion of repolarization and are called respectively as early (EAD) or delayed (DAD) afterdepolarizations (Rosen and Schwartz, 1991).

An EAD occurs during phase 3 and is more prone to happen when action potential duration is prolonged. Several mechanisms for EADs are proposed. All of these result in a change in the membrane inward current that delays or interrupts repolarization (Rosen and Schwartz, 1991). The primary mechanism could be, for example, a reduction in the normal repolarizing current, I_K, an abnormal prolonged duration of inward current carried by sodium or calcium channels (Cranefield et al., 1988 and Isenberg et al., 1976).

A DAD occurs at the end of phase 3 or early in phase 4. Such events are

caused by intracellular calcium overload resulting in repetitive release of calcium from the sarcoplasmic reticulum (Cranefield et al., 1988). This particular event appears to be associated with the elevation in intracellular calcium that for example can occur during ischemia or during excessive catecholamine stimulation.

1.3 Genesis of the ECG waves

The electrocardiogram (ECG) is a temporal record of the changes in electrical charge of all four chambers of the heart during each beat (Farraj et al., 2011) (Figure 4).

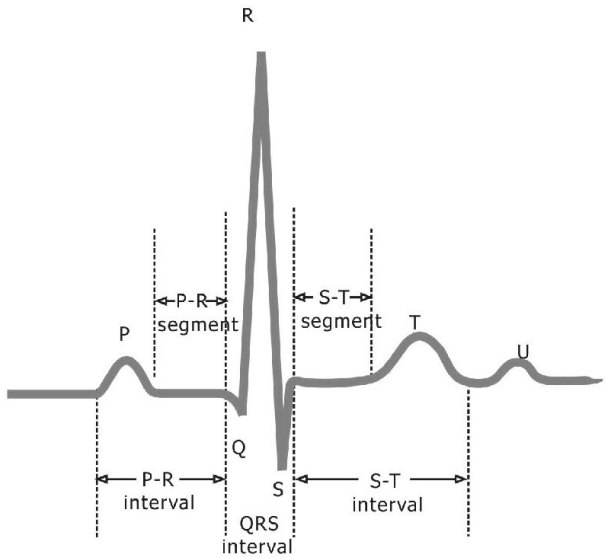

Figure 4: A typical one-cycle ECG tracing. (http://www.ni.com/white-paper/6349/en/).

There are two major components of an ECG: waves and segments. Waves appear as deflections above or below the baseline. Segments are sections of baseline between two waves. Intervals are combinations of waves and segments. The first wave is the P wave, which corresponds to depolarization of the atria. The first half of the P wave is largely due to the

right atrium activation, while the second half largely corresponds to the left atrial depolarization (Carmeliet, 2002). The next three waves (QRS complex) represent the progressive depolarization of the ventricles. Because of the larger tissue mass, the QRS complex is larger than the P wave. Ventricular activation is the product of two temporally overlapping events, endocardial activation and transmural activation (Velimirovic, 2006). In a normal ventricle, the QRS segment is followed by a long period where all ventricular cells are depolarised during the plateau of the action potential. This complex is therefore followed by an isoelectric interval, ST segment, starting at the end of QRS complex and ending at the beginning of the T wave, which signals the ventricular repolarisation. T wave represents ventricular repolarization and is asymmetric, with a slow upstroke and a more rapid downstroke. The beginning of T wave is caused by the decline of the plateau of the epicardial action potential, while the peak of the T wave correlates in time with the full repolarization of the epicardium. Since the duration of the plateau of the ventricular action potential strongly depends of action potential frequency, the duration of the QT interval (measured from the beginning of QRS to the end of the T wave) is also strongly frequency-dependent. In order to evaluate the duration, it needs to be corrected for frequency. The T wave may be followed by an additional low-amplitude wave known as the U wave. This wave, usually less than 0.1 mV in amplitude, normally has the same polarity as the preceding T wave. Its electrophysiologic basis is uncertain; it may be caused by the late repolarization of the Purkinje fibers or by delayed repolarization in areas of the ventricle that undergo late mechanical relaxation.

1.4 Role of cardiomyocytes in the heart

The specialized striated muscle of the heart is formed by numerous coupled cardiomyocytes; they amount to 70% of the myocardium by volume (Vliegen et al., 1991) and roughly 30% in number. These cells represent the first source of contractile power in the heart, conferring the production of force

to drive the deoxygenated blood around the pulmonary circulation (right atrium and right ventricle) and oxygenated blood to the other organs of the body (left ventricle and left atrium). Mammalian cardiomyocytes are highly organized cells, in general with one or two nuclei and have a diameter of approximately 25 μm and a length of 100 μm. The complexity of the membrane architecture of cardiomyocyte is a specific feature that is directly related with its specific function. Cardiomyocytes are able to form a branching network of cells, referred to a functional syncytium. Individual cardiomyocyte connect to each other by a specialized zone of the cell membrane called intercalated disk. When isolated cardiomyocytes are viewed under the light microscope, it is possible to see distinct repeating lines and bands across the cell body, each of which represent a different component of the contractile protein complex. The segment between two Z-lines is called sarcomere and it represents the basic contractile unit of the cardiomyocyte.

Under physiological condition the length of each sarcomere should be between 1.6 (contracted) and 2.2 μm (relaxed). Transverse tubules (or T-tubules) and intercalated disks are responsible for electro-mechanical coupling of myocytes and the transduction of the electrical stimulation. In particular, T-tubules permit the synchronous contraction of the cells, while intercalated disk allows a coordinated propagation of the action potential throughout the heart. Atrial and ventricular cardiomyocytes present several differences. For example, atrial cardiomyocytes typically show one central elongated nucleus, otherwise in ventricular cardiomyocytes two nuclei are usually present (Figure 5 a)). In ventricular cells, a well-developed T-tubule system is present, and the T-tubule features are placed perpendicular to the long axis of the cell along each Z-line with branching between adjacent tubules (Wagner et al., 2011 and Soeller et al., 1999). Differently, in atrial cells that possess T-tubular structures, the system runs mostly along the long axis of the cell and appears disorganized (Figure 5 b)) compared with the well-developed system of ventricular cells (Kirk et al., 2003; Ohler et al., 2009 and Smyrnias et al., 2010). Also, in atrial cells each of the two nuclear

pole regions is associated with a voluminous Golgi complex, several granules, vesicles, and mitochondria (Nutt et al., 1969 and Forbes et al., 1988). The cytoplasm of a myocyte contains high number of mitochondria of variable length that intercalate between the myofilaments every 0.2–0.5 µm (Nutt et al., 1969). Denser transversal packing of mitochondria between myofilaments is observed in atrial compared to ventricular cardiomyocytes. In addition, atrial cardiomyocytes have high density of Golgi complexes, which is related to atrial myocytes being secretory active and producing specific secretory vesicles (Forbes et al., 1988). Consequently, atrial myocytes have high rate of plasma membrane exchange and protein recycling and trafficking, via both clathrin and Cav3-associated membrane invaginations, coated pits and caveolae, respectively (Newman et al., 1992).

Dysfunction of the plasma membrane microdomain formation and recycling may lead to a formation of a critical substrate for potential disease.

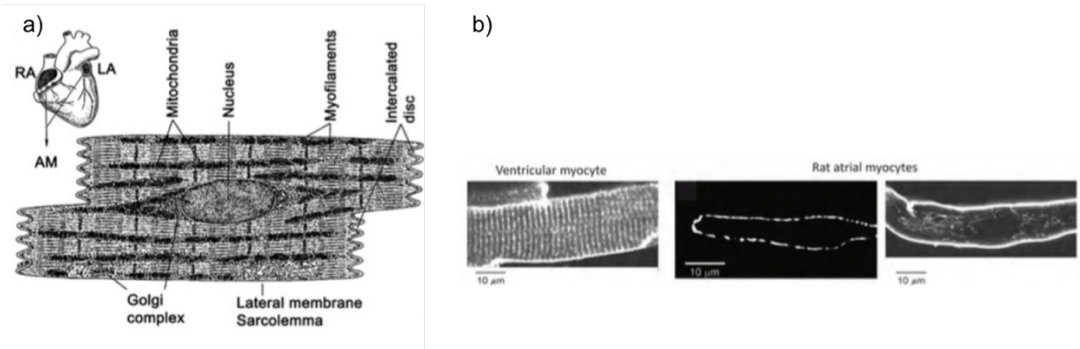

Figure 5: a) Left (LA) and right (RA) atria each contain atrial myocytes, which are elongated brick-like cells with surface boundaries defined by the lateral surface membrane (sarcolemma) and the intercalated disks shown on its short sides. The EM drawing represents a section parallel to the myofilaments through the central nucleus and nuclear poles, each abutted by perinuclear Golgi complexes, numerous granules, and

mitochondria. Note the densely packed myofilaments and mitochondria in the cytoplasm, which further contains scattered Golgi complexes near the sarcolemma (Forssmann et al., 1998) **b)** Di-4 or di-8-ANEPPS membrane staining of rat ventricular and atrial myocytes showing a regular T-tubule network in ventricular myocytes, an atrial myocyte where T-tubules are absent, and an atrial myocyte with a substantial transverse axial tubule system exhibiting prominent longitudinal components (Trafford et al., 2012).

1.5 Cardiomyocytes excitation-contraction coupling

The excitation-contraction (EC) coupling is the most important pathway to obtain a linear contraction of individual cardiomyocytes. The ubiquitous second messenger Ca^{2+} is essential in cardiac electrical activity in order to directly activate the myofilaments, which causes the contraction (Bers, 2001). Mishandling of Ca^{2+} in myocytes plays a central role in both the contractile dysfunction and the onset of arrhythmias (Pogwizd et al., 2001). Action potential of cardiomyocytes induces the opening of voltage-dependent calcium channels also named L-type calcium channels (LTCC) located in the sarcolemma. This opening elicits small increase of intracellular Ca^{2+} level which triggers the opening of cardiac ryanodine receptors (RyR2) on the sarcoplasmic reticulum (SR). The SR is the major component for the intracellular Ca^{2+} store and subsequently releases higher levels of Ca^{2+} into the cytosol. This process is known as Ca^{2+} induced Ca^{2+} release (CICR) (Fabiato and Fabiato, 1979). The Ca^{2+} present in the cytosol is able to bind the myofilament Troponin C and the Troponin complex that together with Tropomyosin, leads the actin and myosin filaments from sliding along each other. Such process produces the contraction in the cardiomyocytes (Carafoli, et al., 2001). Subsequently the relaxation occurs gradually when Ca^{2+} detaches from Troponin C. The removal of Ca^{2+} from the cytosol is made by reabsorption of Ca^{2+} in the SR by a specific Ca^{2+}-ATPase (SERCA2A) in addition to extrusion across the sarcolemma via Na^{+}/ Ca^{2+} exchanger (NCX) (Figure 6).

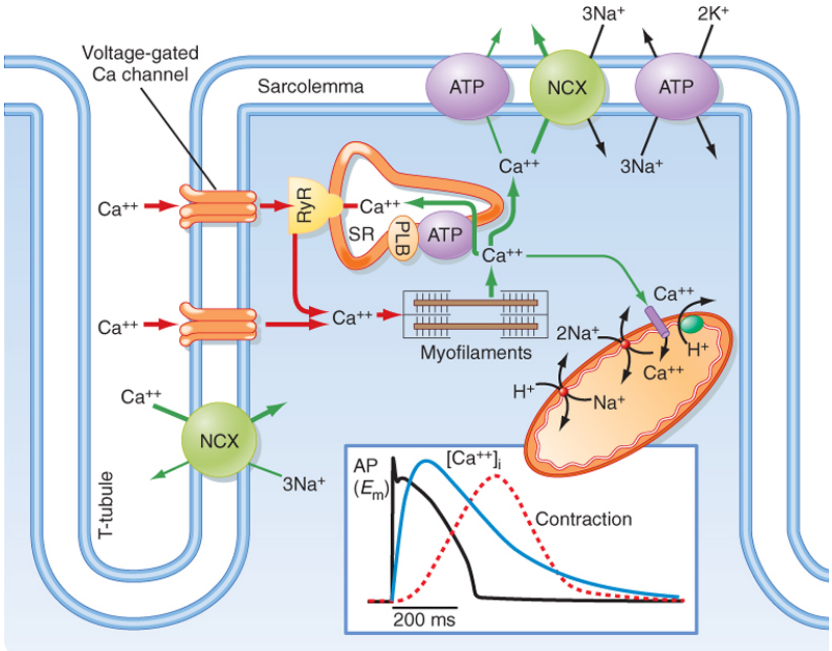

Figure 6: Ca^{2+} cycling and excitation-contraction-coupling related molecules in cardiomyocytes 2+ transport in ventricular myocytes. Inset shows the time course of an action potential, Ca^{2+} transient and contraction measured in a rabbit ventricular myocyte at 37°C. NCX, Na+/Ca2+ exchange; ATP, ATPase; PLB, phospholamban; SR, sarcoplasmic reticulum (Donald et al., 2002).

1.6 The unique features of atrial cardiomyocytes during EC coupling

Atrial cardiomyocytes exhibit unique calcium signaling features compared to ventricular cells. In the rat atrial myocardium, compared to ventricle, the calcium transient is smaller, but the mechanism for the reuptake trough SR is more robust. One reason of such difference is due to the overexpression of SERCA2 in these type of cells (Dobrev et al., 2009). Despite this robust mechanism of Ca^{2+} reuptake, defects in Ca^{2+} handling may occur, resulting in an abnormal release of Ca^{2+} from intracellular stores. Such events lead to spontaneous local increases in Ca^{2+} concentration, but with the consequent unrelated electrical stimulation. The local Ca^{2+} leaks, referred as Ca^{2+} sparks, activate the NCX on the sarcolemma. The results of such

process is the presence of Na^+ influx, which triggers a wave of abnormal membrane depolarizations called delayed afterdepolarizations (DADs). DADs are diastolic membrane depolarization events that occur after normal repolarization, but before the next depolarization event. They are associated with arrhythmogenic electrical activity and may trigger reentry initiating atrial fibrillation (AF). Another specific feature of atrial myocytes is that they possess two different populations of RyRs, one called junctional RyRs located in the sarcolemma and non-junctional RyRs located inside the cell (Mackenzie et al., 2001). Though the junctional RyRs represent the smallest fraction of the total of these receptors, they are crucial during atrial EC-coupling, initiating the CIRC. In addition, there is evidence that in atrial myocytes LTCCs are expressed around the periphery of the cell (Bootman et al., 2011). This is the only place where LTCCs and RyRs are placed close to each other and are able to form the dyads. Indeed, in atrial myocytes Ca^{2+} activation triggers SR Ca^{2+} release only through RyR2 located in the subsarcolemmal (i.e., junctional) SR. The Ca^{2+} wave then propagates from the junctional SR to the cell center, activating with some delay central ("corbular") SR compartments. In addition, atrial myocytes possess inositol 1,4,5-trisphosphate type-2 receptors (IP3R2), which are located in the junctional SR in close vicinity to RyR2, amplifying CICR and facilitating Ca^{2+} wave propagation to the cell centre (Figure 7). This concept is quite important because it is thought that one of the cause of abnormal Ca^{2+} leaks in atrial cells is due to the misregulation of RyR2 phosphorylation or abnormal coupling between the LTCCs and RyR2 (Kockskämper and Pieske, 2006). To better understand and investigate this process, a careful investigation of the upstream modulators such as the G-protein coupled receptors is required.

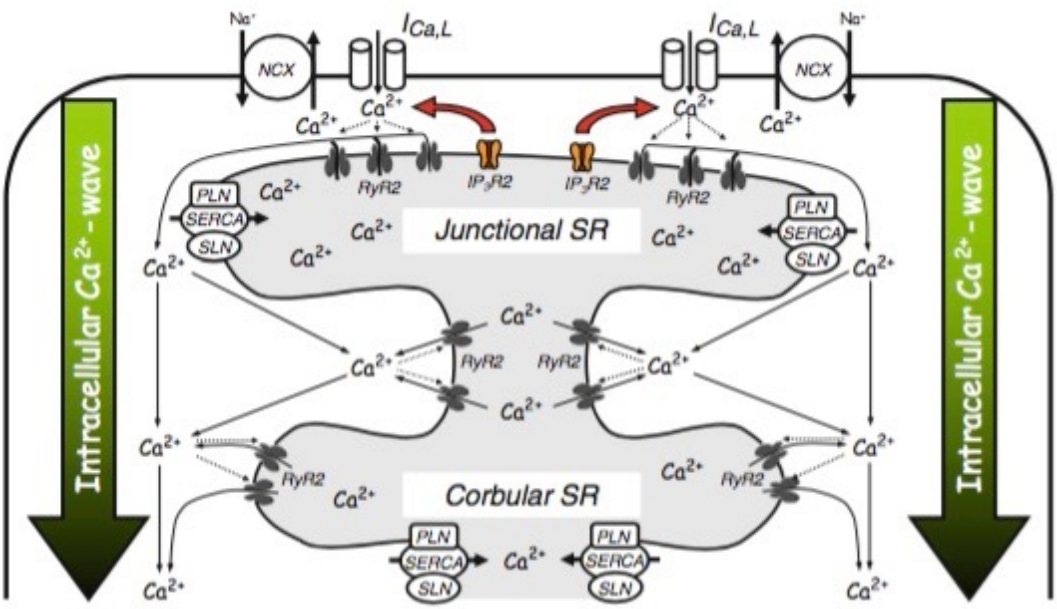

Figure 7: Subscellular architecture of excitation contraction coupling in the atrium. During each action potential Ca^{2+} influx through sarcolemmal L-Typ Ca^{2+} channels ($I_{Ca,L}$) triggers a larger ryan- odine receptor (*RyR2*) mediated Ca^{2+} release from the subsarcolemmal sarcoplasmic reticulum (*junctional SR*). The released Ca^{2+} diffuses into the cell interior and activates RyR2 located in internal SR compartments (*corbular SR*), thereby creating a centripetal Ca^{2+} wave. During diastole cytosolic Ca^{2+} is extruded from the cell through Na^{+}-Ca^{2+} exchanger (*NCX*) or pumped back into the SR by SR- Ca^{2+} ATPase (*SERCA*), which is regulated by phospholamban (*PLN*) and sarcolipin (*SLN*). The SR Ca^{2+} release through RyR2 is amplified by inositol 1,4,5-trisphosphate type-2 chan- nels (IP_3R2). See text for further details (Dobrev et al., 2009).

1.7 G-protein coupled receptors (GPCRs)

GPCRs represent one of the biggest protein family of cell-surface receptors in the mammalian genome (Fredriksson et al., 2003). Their primary function is to transduce extracellular stimuli into intracellular signals. They are formed by a sequence of seven α helices with high hydrophobicity, which form seven transmembrane (7TM) spanning domains (Fredriksson et al., 2003). GPCRs are activated by extracellular ligands which induce a conformational change in the receptors and facilitate their ability to interact with guanine-nucleotide binding proteins (G proteins). G-proteins are

formed by 3 different subunits: α, β and γ. When they are in the inactivate state, they are bound to guanidine diphosphate (GDP). When the receptors are coupled with G-protein, the conversion of GDP to GTP take place, resulting with the dissociation of the G α subunits from β and γ which is necessary to initiate the signalling cascade. Gα is present in three different varieties: stimulatory (Gs), inhibitory (Gi), the phospholipase C activating (Gq) and G12/13 (Audet, 2012). In general, Gs stimulates adenylate cyclase (AC) that increases cAMP level, Gi ihibits AC decreasing cAMP level, and Gq acts via cAMP-independent pathway. Upon the binding to the target protein, GTP is hydrolysed within the Gα which returns it to its basal conformation allowing it to re-associate with Gβγ and GPCRs. In the large family of the GPCRs the adrenergic and the adenosine receptors play a key role in the regulation of the cardiac function (Figure 8).

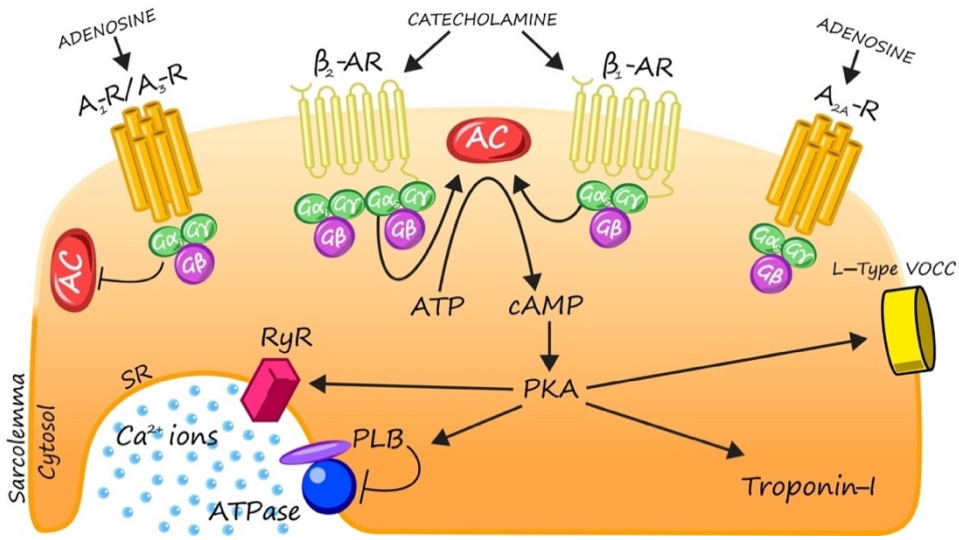

Figure 8: Schematic representation of the β -adrenergic and adenosine pathways. Upon the ligand binding (catecholamines: adrenaline, noradrenaline, dopamine and adenosine respectively) they transduce the signal inducing intracellular phosphorylation events via the activation of cAMP. Their targets such as RyRs and PLB have a key role in the regulation of cardiac excitation-contraction coupling.

1.7.1 β-adrenergic receptors

The heart has an intrinsic ability to spontaneously generate electrical impulses and regular muscle contractions, these processes are tightly controlled by the autonomic nervous system. The autonomic nervous system consists of two main branches: sympathetic and parasympathetic. The activation of the sympathetic nervous system acts on the chronotropic, inotropic and lusitropic effect, acting at the level of heart rate, contractility and relaxation rate, respectively. This activation is caused by the action of the catecholamines (norepinephrine and epinephrine, also known as noradrenalin and adrenalin) on the adrenergic receptors (AR) (Hill, 2006). Mammalian heart express nine AR subtypes that are implicated in different cellular mechanisms. The β-ARs play a key role in the regulation of heart function and three different subtype have been distinguished: β_1AR, β_2AR and β_3AR. In the human heart the most aboundant receptor is the β1AR; the β1/β2 ratio is 70-80%: 30-20% in the ventricle. In the atrium the ratio is 60-70% to 40-30% (Wallukat, 2002). Both β_1AR and β_2AR predominantly bind to Gs and stimulate AC, an enzyme which catalyses the synthesis of the secondary messenger cAMP from ATP. Under some particular conditions β_2AR is able to bind Gi, in a process known as stimulus trafficking or biased agonism (Amin et a.,l 2011) leading to the reduction in the AC activity; however, Gβγ can also be involved in β_2AR signalling and modulate molecules involved in the control of cellular homeostasis (Warne et al., 2008). The β_3AR binds to the Gi and its functional role in the heart is very disputable. Specific subcellular localizations and signaling pathways of β_3ARs are known to be different from β_1- and β_2ARs. The β_1ARs are implicated in the process for cardiomyocyte contraction by playing a key role in positive lusitropic and inotropic effects. They were found in both sarcolemma and T-tubular network. In contrast, β_2ARs are found exclusively in the T-tubular system, where they are involved only in the inotropic response (Nikolaev et al., 2010); Otherwise they are generally

associated with smooth muscle relaxation (Amin et al., 2011). The classic pathway includes the activation of adenylyl cyclase via Gs, resulting in an elevation of the cAMP level. The first target for cAMP is protein kinase A (PKA). PKA is very important for the cardiac function as it can phosphorylate a wide range of proteins involved in the EC coupling: L-type calcium channels (LTCC), phospholamban, Troponin I, RyR2, myosin binding protein-C, etc (Lohse et al, 2003). All of these are important for the contractile phenomenon by increasing Ca^{2+}-influx (LTCC), increasing Ca^{2+} reuptake into the SR (phospholamban and SERCA) and with the modulation of the myofilament Ca^{2+} sensitivity (troponin I) (Lohse et al., 2003). In contrast, β_2ARs have been found to affect LTCC phosphorylation and opening, without effect on the others cardiac contractile proteins (Kushel et al., 1999).

In addition, β_1ARs can stimulate apoptosis via a cAMP-dependent pathway, while stimulation of β_2AR is involved in the process of apoptosis inhibition via a Gi-coupled pathway (Communal et al., 1999). Several studies showed cardiac βAR system alterations during HF (Brodde et al., 1993). These changes include a reduction of the β1AR which correlates with the severity of disease. In contrast, no change in number of β_2ARs expressed has been reported in HF. The reason why this downregulation occurs and is specific only for the β_1AR receptor subtype remains unclear.

1.7.2 Adenosine receptors

An another type of GPCR that is involved in the regulation of the cardiomyocytes functionality is represented by adenosine receptors. Adenosine is a purine nucleoside catobolite of ATP that is ubiquitously present in the whole body; it is implicated in numerous functions in mammalian organ system. Adenosine is able to modulate cell metabolism through several mechanisms, with the most direct being its rephosphorylation to AMP via adenosine kinase to help restore and maintain ATP level in the cytoplasm (Lasley, 2011). Adenosine can be

generated through two primary pathways: hydrolysis of 5'-AMP or metabolism of s-adenosylhomocysteine. The first one is the most important mechanism to generate adenosine; it involves 5'-AMP, which is derived from adenine nucleotides but also potentially from cAMP, and as a consequence it is extremely regulated (Deussen, 1989). Several studies show the intracellular 5′-AMP pool is the major source of adenosine under both baseline conditions and during ischemia or hypoxia (Borst and Schrader, 1991, Headrick, et al., 1992). Adenosine is generated in both intra and extracellualr compartments, and its level rises in the cytoplasm in response to physiological and pathological stimuli (Headric et al., 2013). Adenosine mediates a wide range of actions in the heart, improving the cellular energy balance and promoting the cellular resistance to stress or injury (Olsson et al., 1990). For these reasons, adenosine has been described in 1985 as a "retaliatory metabolite" (Newby et al., 1985). Indeed, it is released as a protection for the heart against excessive external stimulation. In addition, under pathological conditions (ischemia or hypoxia), heart cells may in a sense 'retaliate' via receptor-mediated effects of greatly enhanced adenosine release, which induce short and long-term resistance to stress (Headrick et al., 2011). On the other hand, the release of adenosine is not exclusive to stress or injury conditions; adenosine is released in response to even mild perturbations in energy state, being sensitive to a wide range of regulatory molecules such as catecholamines and mediators derived from cAMP cascade (Deussen, 1989). Under physiological or mild perturbations conditions, adenosine acts in a process that appear to be directed to optimize the balance between energy utilization and generation enhancing O_2 and substrate delivery (Figure 9) (Headrick et al., 2011). All of these changes in adenosine levels are crucial for a number of cardiovascular functions, including heart rate, cardiac impulse conduction, coronary dilatation, vasculogenesis and cardiovascular growth/remodeling (Mallet et al., 1996). Being a cardio-protective nucleoside adenosine also decreases the heart rate (Hisatome, 2007). These different responses, however, can be modified in different

pathologies in the heart and such dysfunctions can potentially contribute to shifts in resistance to and progression of heart disease (Mallet et al., 1996).

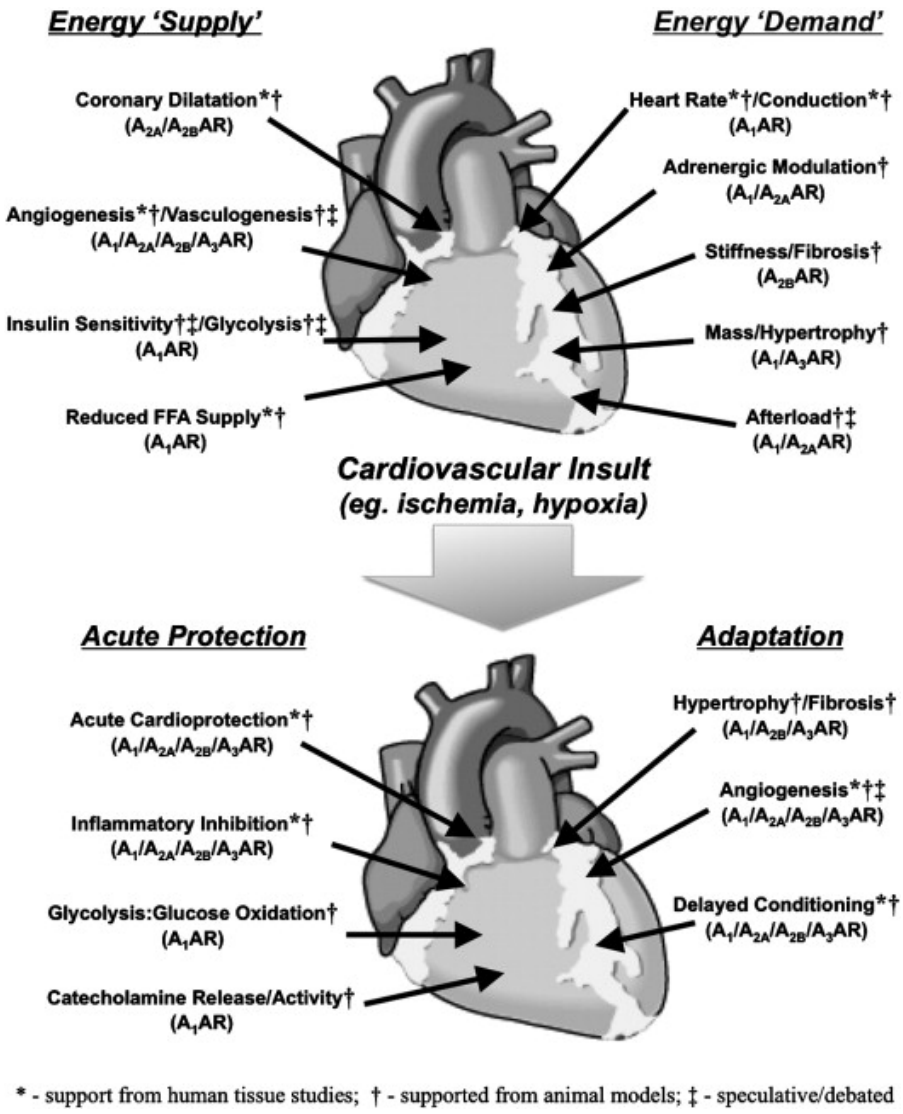

Figure 9: Simplified depiction of proposed regulatory roles of adenosine and ARs in modulating/optimizing the balance between myocardial energy 'supply' and 'demand' (upper panel), and the impact of ARs in ameliorating injury and promoting adaptation (lower panel) during and following myocardial insult (Headrik et al., 2011).

The importance of adenosine in multiple heart functions generated a substantial interest for a pharmacological approach to adenosine receptors, with the purpose to better understand their interactions and their effects in both physiological and pathological conditions.

Adenosine regulates cardiac function through four different type of adenosine receptors: A_1, A_{2A}, A_{2B} and A_3ARs (Fredholm et al., 2011). The adenosine receptors were initially classified based on pharmacologic responses to adenosine analogues, both A_1 and A_3ARs inhibiting adenylate cyclase, and the A_2AR sub-type activating it. Later A_2AR was sub-divided in two groups based on different level of affinity (high for A_{2A} and low-affinity for A_{2B}). All AdRs are expressed in the heart (Yang et al., 2007 and Chandrasekera et al., 2010), with different levels of mRNA. Both murine heart cardiomyocytes and HL-1 cell line express A_1ARs at the highest level followed by A_{2a}AR, whereas A_{2b} and A_3ARs are expressed at a much lower level (Epperson et al., 2009).

1.7.2.1 A_1 adenosine receptors

A_1AR has high affinity for adenosine and is the most conserved subtype across species (Fredholm et al., 2000). It is expressed throughout the body, with high level in the brain and atria. Variations in regional expression of A_1AR have been found in the heart, with higher levels in atria than in ventricles (Bohm et al., 1989, Musser et al., 1993, Kapicka et al., 2003). Activation of the A_1AR inhibits adenylyl cyclase activity and PKA through activation of G_i proteins (Calker et al., 1979 and Londos et al., 1980), decreasing the phosphorylation of RyRs, other contractile proteins and reducing Ca^{2+} transient amplitude and cell contractility (Fenton et al., 1991 and Dobson, 1983). Investigation of the A_1AR effects in the heart gave conflicting results. On one hand there is evidence of the cardio-protective effect of A_1AR stimulation during the conditions of hypoxia and Ischemia (Fenton e Dobson, 1987, Fenton and Dobson, 1993, Yu et al., 2011); on the other hand other studies show a relation between A_1AR stimulation and

cardiac arrhythmias (Robin et al., 2011 and Lach et al., 2011). This could be explained by the fact that A_1AR, while acting mostly through Gi protein, it can also couple with G_s activating AC or with $G_{q/11}$, stimulating inositol phosphate production (Headrick et al., 2013). A_1AR have been reported to protect against the injury due to myocardial ischemia and reperfusion by inhibiting adenylyl cyclase and activating ATP-dependent potassium channels (Liang and Gross, 1999; Light et al., 2000 and Miura et al., 2000). In addition to myocardium, indirect evidence supports a possible role for A_1AR in the coronary circulation (Maczewski et al., 1998). The firs known effector of A_1AR was inhibition of AC; acetylcholine also inhibits AC in the heart tissue and because acetylcholine activate potassium channels through a G-protein in atria, Kurachi et al studied the effect of adenosine finding that it can activate the same potassium channels like acetylcholine (Kurachi et al., 1986).

1.7.2.2 A_{2a} adenosine receptors

Another high affinity adenosine receptor, A_{2a}AR, is widely distributed in the body. The highest level of expression is found in brain, spleen, thymus, and an intermediated level of expression is noticed in the heart and the lung. A_{2a}AR is coupled with Gs protein and is implicated in the coronary vasodilatory mechanism, and its cardio-protective effect looks to be associated with an anti-inflammatory response (Wilson and Mustafa, 2009). Some studies evidence that A_{2a}AR, especially in smaller species, such as rat and guinea pig, can modulate intracellular calcium handling in a cAMP-dependent pathway (Dobson and Fenton, 1997). However, other studies could not find a relationship between A_{2a}AR and RyR2 opening and in addition is some species expression of A_{2a}AR in the heart was not detected (Hove-Madsen et al., 2006). Besides, cardiac fibroblast express A_{2a}AR, which have been shown to be important for the modulation of the fibroblast proliferation and fibrosis (Epperson et al., 2009). They are also present I

coronary vessels, mediating dilation of both endothelial and vascular smooth muscle cells (Hein et al., 1999 and Teng et al., 2005).

1.7.2.3 A_{2b} adenosine receptors

The A_{2b}AR has the lowest affinity for adenosine compared to other three receptors. The expression is high in the colon and cecum and low expression is found in the heart. It regulates signaling via $G_{S\alpha}$ to stimulate AC activity, and also via $G_{q/11}$ to activate PLC. Some studies indicate A_{2b}ARs are expressed in myocytes and A_{2b}ARs are reported to modify ventricular function in mice (Morrison et al., 2002; Chandrasekera et al., 2010). A_{2b}ARs are also expressed in cardiac fibroblast and mediate the vasodilation effect in mice (Morrison et al., 2002) and rats (Hinschen et al., 2003) via NO and K_{ATP} channel dependent processes (Teng et al., 2008).

1.7.2.4 A_3 adenosine receptors

The A_3ARs show the most variable expression pattern across the species (Fredholm et al., 2000). Similar to A_1AR, this subtype is able to couple with G_i protein with the consequent inhibition of AC, and G_{q11} with the modulation of PLC and Ca handling (Lasley, 2011). The highest expression is found in the lung and liver and very low level in the heart. Myocardial A_3AR levels appear to be very low, with the absence of the protein in murine myocardium (Black et al., 2002). They act principally at the level of the arterial and in the other vascular smooth muscle cells (Zhao et al., 1997).

1.8 Adenosine signaling pathways and regulation

Generally, adenosine receptors signaling occurs through inhibition or stimulation of AC; although now there is evidence that different pathways,

such as phospholipase C (PLC), Ca^{2+} and mitogen-activated protein kinases (MAPKs), are also involved. In general, when there is the stimulation of the receptor, the subunit releases guanosine diphosphate (GDP), allowing the binding of guanosine triphosphate (GTP); the G protein complex dissociates into two components: α subunit and βγ subunit (Figure 10). Gαi and Gαs have been associated with inhibition and stimulation of AC, respectively (Figure 10). The activation of the Gαs pathway is important in the modulation of calcium handling (Schroder et al., 1983). Gβγ on the other hand regulates adenosine action in the cell nucleus by modifying the expression of genes involved in cell growth and remodeling (Feldam et al., 2007 and Wettschureck et al., 2005).

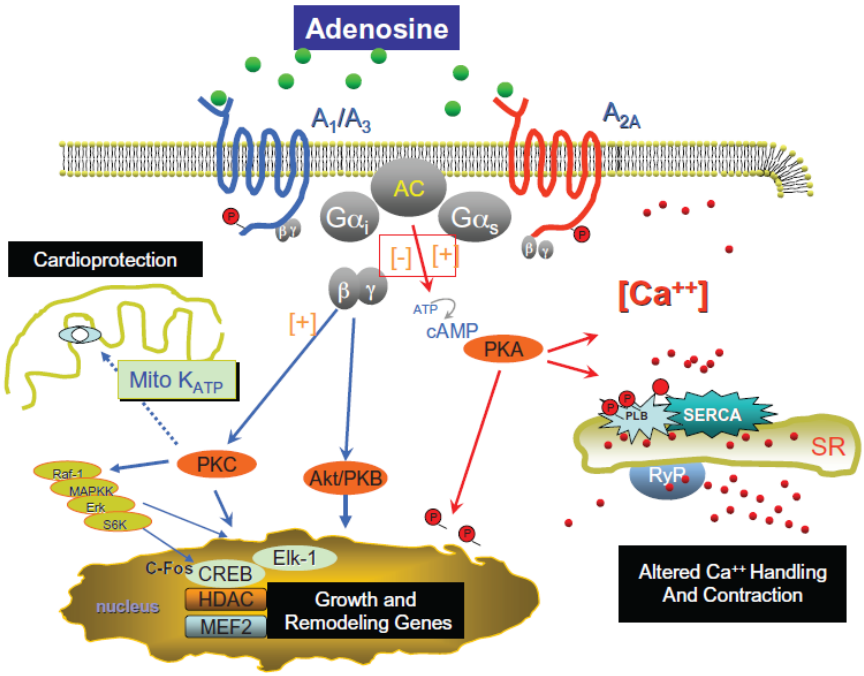

Figure 10: Signalling pathway of adenosine receptors. Extracellular adenosine functions as signaling molecule by engaging cell surface adenosine receptors (A_1, A_{2A}, A_{2B} and A_3ARs). A_1AR and A_3AR are coupled to adenylyl cyclase (AC) by the inhibitory G-protein subunit (Gαi). With this patway a reduction of cAMP levels occurs. In contrast, the A_{2A}AR and A_{2B}AR can induce AC by the stimulatory G-protein subunit (Gαs) and therefore can induce intracellular cAMP levels. Activation of A_1AR stimulates phosphatidylinositol 3-

kinase (PI3K)/AKT pathway. (Feldam et al., 2007).

The cAMP-dependent pathway is for sure the predominant mechanism in which these receptors work. However, other second-messenger system, such as phosphatidylinositol 3-kinase, tyrosine kinase and phospholipase C (PLC), can also be activated by AdRs (Ansari et al., 2008; Peart and Headrick, 2007; Tawfik et al., 2005). This pathway and its role in mediating the effect of adenosine on at the level of the coronary vasculature have not been clearly understood. Additionally, crosstalk between the cAMP/PKA pathway and the PLC/PKC pathway has also been reported (Germack and Dickenson, 2004). Currently, the mechanism of these two second-messenger systems has reserved more attention in studies of ARs mechanism of action in the heart.

1.9 β-adrenergic receptors and membrane microdomains

The first evidence that not all cAMP signals are equal, in terms of the downstream responses they elicit, was provided almost three decades ago when studies in isolated perfused hearts showed that isoproterenol (ISO) and prostaglandin E1 (PGE1), although elevating intracellular cAMP to comparable levels and similarly affecting the PKA activity ratio, had very different effects on PKA substrates (Zaccolo, 2009). Over the years, a wide range of studies for the functional compartmentalization of the cAMP signal has accumulated and recently we have the possibility to obtain a better understanding of the spatial distribution of βAR signalling in the heart at nanoscale. Xiao et al. first suggested that βAR subtypes induce compartmentalized cAMP signal in cardiomyocytes (Xiao et al., 1994). Based on cAMP signalling distribution, the authors concluded that the activation of LTCCs appears to be in close proximity with β_2ARs at the stimulation site, whereas the β1AR stimulation of LTCCs requires cAMP diffusion (Xiao and Lakatta, 1993). Later the development of genetically

encoded biosensors allowed the visualization of compartmentalized cAMP in neonatal cardiomyocytes directly (Zaccolo and Pozzan, 2002), which opened a new era of studying the exact mechanism of localized βAR signals. In the ventricular cardiomyocytes the production of cAMP induced by β_2ARs stimulation appears to be confined in the T-tubules wile the production of cAMP induced by β_1AR stimulation is found in both sarcolemma membrane and T-tubules (Nikolaev et al., 2010). These studies confirm the concept that the activation of β_1ARs leads to an extensive distribution of cAMP signal troughout the cell, while the activation of the β_{2a}ARs leads to local signaling action. Local degradation of cAMP makes the signaling to be within the confined region, where it is required, and this represents an important aspect of cAMP compartmentation. This is a very important concept, opening different possibility for the investigation.
In atrial cells, A_1AR localization has not been confirmed yet, but its presence has been reported in the crest/caveolae domains (Figure 11). Phosphodiesterases (PDEs) are enzymes belonging to a family of hydrolases which catalyse the hydrolysis of the cyclic phosphate bond of the cAMP. There are 11 phosphodiesterase sub-families (Conti and Beavo, 2007), and 7 of them are active in the heart: PDE1, PDE2, PDE3, PDE4, PDE5, PDE8 and PDE9 (Vandeput et al., 2007 Mongillo et al., 2006, Ahmad et al., 2015 and Lee et al., 2015). These PDEs have different specificity towards either cAMP or CGMP or both, and are located in distinct intracellular microdomains.

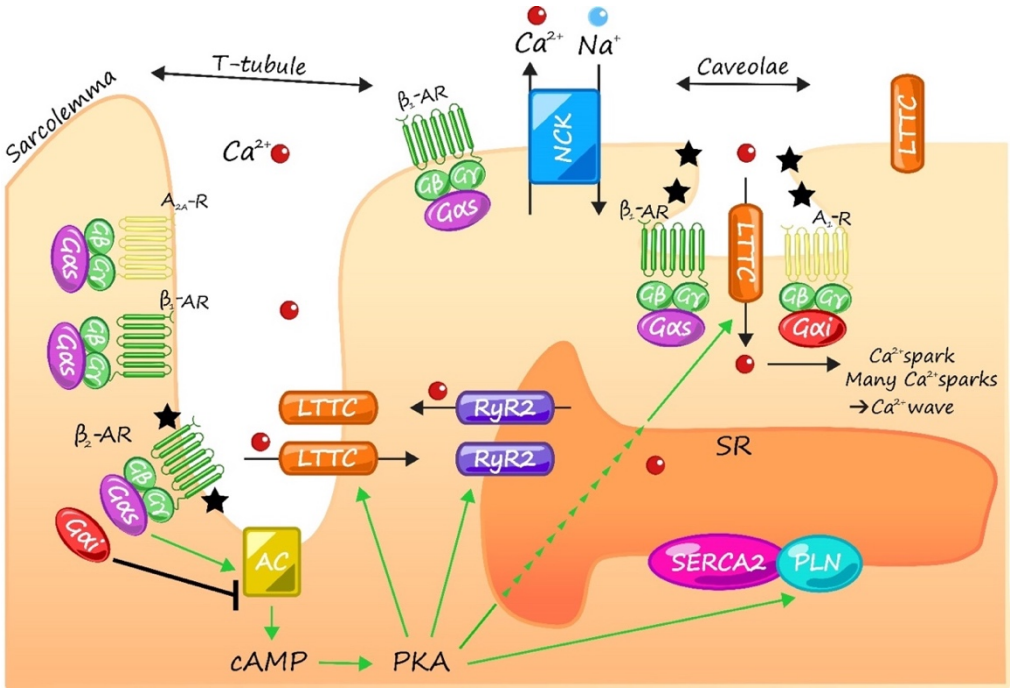

Figure 11: Microdomain distribution of adrenergic and adenosine receptors in atrial cardiomyocytes. β_1AR is possibly expressed both in the cell crest and in the T-tubular network. It could be (or not) in close proximity to Cav3 lipid raft-forming proteins (stars). β_2AR is preferentially expressed in the T-tubular network and is exclusively found within Cav3 domains. Catecholamines and adenosine could positively (via Gs proteins) or negatively (via Gs proteins) act on the AC-mediated cAMP production and thus regulate the action of PKA. PKA phosphorylates a number of targets such as the LTCC, RyR2, phospholamban, troponin I and myosin-binding protein C, which are important for the process of cardiomyocyte contraction or relaxation.

1.10 Adenosine receptors and membrane microdomains: Caveolae

One of the mechanism proposed for the regulation of the subcellular signaling is the concept of the compartmentation at the level of the cell membrane. These compartments, or microdomains often reside in the specialized plasma membrane domains lipid rafts. The presence of the structural protein caveolin delineates a specialized type of lipid raft, caveola,

a flask-shaped invagination (50–100 nm) of the membrane (Lasley, 2011). Caveolae were first discovered in the 1950 (Palade, 1953) and are known to play an important role for the organization of the signal transduction pathways; caveolae were named based on their morphology, appearing as “little caves”. The shape of the caveolae can also be modulated according with the phsysiological state of the cell (Palade and Bruns, 1968). Cholesterol is the major component of caveolae and its depletion makes caveolae flat shaped and eventually caveolae disappear from the plasma membrane (Simionesciu, 1983 and Rothberg et al., 1992). Chang et al. showed that a critical amount of cholesterol is required for the correct formation and maintenance of caveolae (Chang et al., 1992). There are three different isoforms of caveolin: caveolin 1, 2 and 3. They have different level of expression in the body. In the cardiac myocytes the most expressed isoform is the caveolin3 (Cav3) (Ferruccio et al., 2001 and Song et al., 1996), which seems to be essential for the formation of caveolae in cardiomyocytes (Galbiati et al., 2001). Cav3 is crucial for the function of caveolae in cardiomyocyte, and it was found to be present in T-tubules and plasma membrane domains. Cav3 was found to be co- localized with T-tubular membrane as an intermediator for the EC coupling process, supporting the interaction between T-tubule and RyRs (Calaghan and White, 2006). Patel et al. reported that G-proteins and members of G-protein signaling pathways are located in caveolae, showing their central role in the spatial control of the signaling inside the cardiomyocytes (Head et al., 2005). Recent evidence shows that adenosine receptor signaling could be regulated via membrane micro-domains and also that this regulation may involve the localization of these receptors in the caveolae. Different studies show A_1AR to be localized in lipid raft/caveolae (Lasley, 2011 and Cavalli et al., 2007**).** Cavalli et al. observed that A_1AR appear to co-immunoprecipitate with caveolin-3, and immunofluorescence additionally showed that A_1AR co-localise with caveolin-3 in cardiomyocytes (Cavalli et al., 2007). A_1AR could be co-immunoprecipitated with Cav3 in adult rat ventricular cardiomyocytes (Garg et al., 2009). Despite observations about

the localization of the adenosine receptors in close proximity with the caveolae structure, the role of this specific localization and the effect that can occur remain unclair.

1.11 Microdomain distribution of GPCR: T-tubule

Ventricular cardiomyocytes possess an intricate transverse tubular system of membrane invaginations, which are able to form a network reaching deep inside the cell, creating a distinct and important microdomain (Gorelik et al., 2013). All healthy ventricular myocytes have a well-developed and regular transverse T-tubular system. The T-tubular network present in mammalian ventricular cardiomyocytes, was first reported in 1956 by Linder and colleagues by using the electron microscopy (Linder et al., 1956). Later, using the two-photon live-imaging, Soeller and Cannell showed the complexity of the T-tubules which invaginate from the sarcolemma and form a network of periodically aligned tubules, variable in diameter (Soeller and Cannel, 1999). T-tubules play a crucial role in cardiac excitation-contraction coupling as they allow for the conduction of the electrical impulses to the center of the cardiomyocyte. T-tubules are known to be rich in ion channels and receptors that are involved in many processes important for mycocytes functionality (Orchard et al., 2009). For example, LTCCs are located in T-tubules in close proximity to the sarcoplasmic reticulum which is a large internal store of Ca^{2+} that is released during CICR (Sipido & Cheng, 2013). T-tubules form a coupling with the SR membrane, known as dyads that are able to conducts action potential into the cell (Kaftan et al., 1996). This leads to the synchronous Ca^{2+} release that occurs throughout the cell with each depolarization (Soeller and Cannell, 1999). As it has been demonstrated recently, functional LTCCs are predominantly placed in the T-tubules of adult ventricular cardiomyocytes (Bhargava et al., 2013). βARs, that are important for the contractile process, are preferentially located in T-tubules: some of the β_1ARs and exclusively all β_2ARs.

In contrast to ventricular myocytes, in atrial cells the scenario is more complex. Initially, it has been accepted that only ventricular myocytes possess a real T-tubule organization that facilitates the synchronous rise in Ca^{2+}, whereas atrial myocytes lack any such organization on their surface (Brette et al., 2002). The idea that only ventricular cells have T-tubules and that T-tubules are absent or less developed in atrial was largely disputed (Cordeiro et al., 2001 and Huser, 1996). In the last years, increasing amount of evidence shows that large mammalian species such as sheep, cows, horses and humans, possess atrial myocytes with well-developed T-tubular structures (Richards et al., 2011). Other evidence shows that some atrial myocytes possess a rudimentary T-tubule system compared to the ventricular one (Trafford et al., 2013). Currently, it has been accepted that approximately one third of rat atrial myocytes possess a T-tubular system (Frisk et al., 2014). There is evidence suggesting a correlation between the cell size and the presence of a well-developed T-tubule system. In this concept, smaller atrial myocytes (about 12.2 µm average width) possess disorganized or no T-tubules, while the bigger atrial cells (17.1µm average width) can have a well-developed T-tubule system; however, this system is not as prominent as in ventricular cells (Glukhov et al., 2015) (Figure 12).

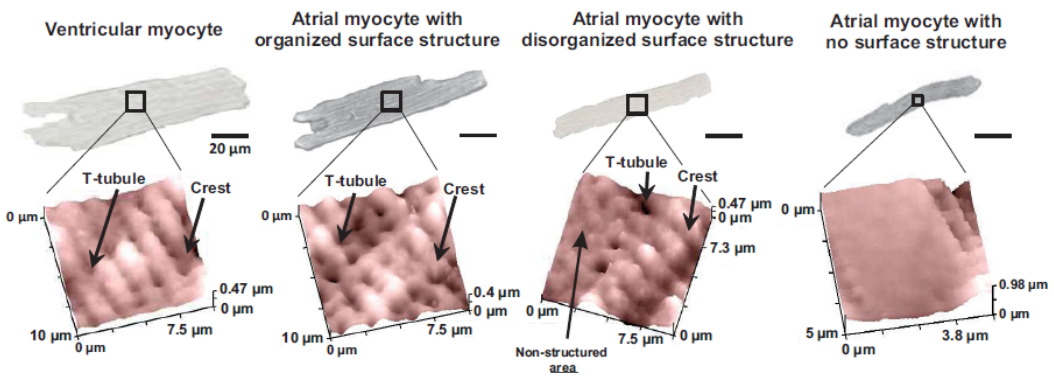

Figure 12: Optical images and topography scans (zoomed areas) of a ventricular cell and atrial cells with various degrees of organization of surface structures. T-tubules, crests, and non-structured areas are indicated by arrows. (Glukhov et al., 2015).

The formation of T-tubules and their maintenance during adulthood is not yet fully understood; however, it seems to involve various molecules. These molecules include Cav3 (Woodman et al., 2002), bridging integrator 1 (BIN1) that may induce the curvature in membrane (Hong et al., 2010), tropomyosin (Vlahovich et al., 2009), telethonin (Tcap) and junctophilins for the correct association between T-tubule and SR (Han et al., 2013). In cardiomyocytes, a relationship between caveolae and T-tubule system has been suggested but not clearly defined. A study hypothesized that the formation of transverse-axial tubular system was derived from the repetitive generation of caveolae, which form "beaded tubules" (Forbes et al., 1984). Additionally, in the skeletal muscle, the loss of caveolae and the abnormalities in the spatial organization of the T-tubule system have been noted in the Cav3 knockout model (Galbiati et al., 2001). More investigations are required to clearly understand the role of caveolae in the possible development and maintenance of the T-tubule system in the heart and the possible change and relationship in disease.

During the end stage of HF, in human and rodent ventricular myocytes, a disruption of the T-tubule network has been shown (Lyon et al., 2009). This dysfunction is able to create a critical substrate for the incorrect βAR and Ca^{2+} signalling (Nikolaev et al., 2010). The spatial relationship between T-tubule, LTCCs, RyRs and SR has a crucial role in terms of efficacy and stability of CICR. Congestive HF is characterized by a reduction of T-tubule density in rodent failing hearts (Louch et al., 2006 and Song et al., 2006). Experimental disruption of T-tubule network produces changes that are similar to those observed in HF, with a lack of synchronous release of Ca^{2+} that leads to a slow Ca^{2+} transient (Lipp et al., 1996, Brette at al., 2005 and Brette at al., 2004). Generally different cardiac pathologies are associated with the progressive change of the T-tubule system. In this study, we will focus our attention on cardiac remodeling in HF and atrial fibrillation since they are the major causes of morbidity and mortality.

1.12 Interation between β-adrenergic receptors and adenosine receptors

β-adrenergic and adenosine receptors are co-expressed in several cell types such as the mammalian heart. It has been reported that A_1ARs and, equally, both β_1 and β_2ARs may function as homo-and heterodimers. A_1AR can heterodimerize with A_{2a}AR and with D_1-dopamine and $mGlu_{1\alpha}$-glutamate receptors leading to various functional ramifications (Ciruela et al., 2006 and Ginés et al., 2000). The β_1 and β_2ARs are also able to form a functional homodimers with numerous receptors such α2A-adrenergic, δ-opioid, and somatostain receptors (Xu J et al., 2003). β_1ARs can also heterodimerize with β_2ARs increasing β_2ARs internalization (Lavoie et al., 2002). Additionally, adenosine and β-adrenergic receptors can functionally interact in a process in which A_1AR inhibits the contractile response following the β-adrenergic receptor stimulation. Such process is well known as anti-adrenergic effect of A_1AR (Song et al., 1996). However, the possibility that these receptors can interact with each other has not been extensively investigated. Chansraesekera et al. first reported that A_1AR can heterodimerize with the family of βARs (Chandrasekera et al., 2013). These results suggest that the co-expression of A_1ARs with β_1 or β_2ARs resulted in the formation of functional heterodimers. The formation of such complex results in altered pharmacological and signaling properties of the participant proteins. In addition, this data suggests that these receptors may form such constitutive heterodimers in the human heart. Using co-immunoprecipitation analysis, the authors revealed that A_1ARs form a stable heteromeric complex only when two types of receptors were co-expressed in the same cell. The inability of these receptors to co- immunoprecipitate from cells that singly express these receptors indicate that the observed process of heterodimerization is not due to aggregation artifacts, which may occur during detergent solubilization. Double-label immunofluorescence results (Chandrasekera et al., 2013) indicated that A_1ARs and β_1ARs co-localize at

the plasma membrane. However, the co-localization does not confirm the heterodimerization. Such study could have physiological relevance in the cells where these two receptors are co-expressed, including the cardiovascular system.

1.13 Adrenergic receptors during pathologies

During the progression of heart failure the functionality of the cardiomyocytes and the βAR signalling pathways are subject to drastic alterations. Furthermore, because the cardiac efficiency in such condition diminishes, the sympathetic nervous system is increasingly activated in an attempt to maintain cardiac output (Esler et al., 1997). Excessive stress by overstimulating βARs activates a complex network of pathways, which interact and are able to initiate myocardial hypertrophy to preserve cardiac function. Several studies demonstrate that cardiac hypertrophy is an adaptive process that improves ventricular function in response to the growing workload (Chien et al., 1991). However, on the other hand cardiac hypertrophy could be a precursor for the onset of heart failure. The prolonged adrenergic stimulation may also induce electrophysiological disturbances in the heart, resulting in arrhythmia (Haft, 1974). Chronic adrenergic stimulation may act at the level of the expression of some components implicated on the βAR signal. Several studies show alteration of the cardiac β-AR system in failing hearts, with persistent β_1AR stimulation and the consequent cAMP production leading to a maladaptive cell remodelling (Brodde 1993, Brodde and Michel 1999, Engelhardt et al., 1996). These alterations include a significant reduction of β_1AR subtype (correlated to disease severity), whereas the levels of the β_2AR subtype remained unchanged (Engelhardt et al., 1996). In addition, there is a significant increase (up to 200%) of Gαl levels, and significantly elevated βAR kinase 1 (βARK1) activity (Freedman and Lefkowitz, 2004). To compensate for this β_1ARs are increasingly desensitized, internalized and degraded during the progression of the pathology (Xiang, 2011). The

reason why this downregulation in heart failure occurs exclusively for the β_1AR subtype is not clear. In contrast the β_2AR remain same in number but move from their specific position in the T-tubules to the whole sarcolemma (Nikolaev et al., 2010). This redistribution during HF leads to a change in the compartmentation of cAMP and may contribute to the failing myocardial phenotype.

Even though all of these changes are well documented by different studies, their interpretation is often ambiguous. These changes may be interpreted as beneficial helping to protect the heart from the detrimental effect chronic βAR stimulation. On the other hand, they may be interpreted as deleterious as they can lead to further deterioration of heart failure. Depending of these different interpretations different therapeutic approaches and strategies could be used, in order to inhibit or, on the contrary, stimulate the βAR system.

1.14 Adenosine receptors during pathologies

Despite the beneficial effect of adenosine in the heart (described above), we hypothesized that adenosine and adenosine receptors could play a crucial role in the development of cardiac dysfunction, hypertrophy, and failure. This concept could be explained by the fact that in the cardiac scenario, adenosine receptors activate a cascade of downstream signaling molecules, where the most part of them are implicated in in cardiac hypertrophy, apoptosis, or the regulation of calcium fluxes (Figure 10). These signaling molecules include: Akt, protein kinase C (PKC), the nuclear regulatory proteins MEF2, CERB, HDAC, and c-Fos, the mitochondrial K_{ATP} channels, and the protein kinase A (PKA) signaling system that regulate the function of the calcium regulatory proteins phospholamban and Ca^2ATP-ase (Feldman et al., 2011). Although there is some scientific evidence about the role of A_1AR during cardiac pathologies, mechanism of its action remains clairly unknow. Indeed, the possible involvement of adenosine and adenosine receptors in the modulation of Ca^{2+} handling and the specific

effect of the signaling pathway through adenosine receptors in failing heart remain unknown.

1.15 Heart Failure and atrial fibrillation

Heart failure, often referred to as congestive heart failure (CHF), is a global term used to describe a physiological condition in which the heart is unable to pump sufficiently blood flow to the body's need. HF is associated with progressive structural and functional modification resulting in inefficient cardiac function. Such condition is present in acute state or could be a develop that lead in a chronic state.

A wide range of cardiovascular diseases such as arterial hypertension, atrial fibrillation, valve disease, and cardiomyopathy can contribute to CHF, and are the major causes of mortality worldwide causing more than 7.4 millions deaths annually (this number is expected to rise in the next year) (World health organization, 2015). A complex links with other cardiovascular disorders, e.g. atrial fibrillation (AF) is present (Anter et al., 2009). AF is the most common type of cardiac arrhythmia and is characterized by rapid and irregular beat of the heart. The incidence of AF increases with advancing age, with an annual incidence per 1,000 person-years of about 3.1 cases in men and 1.9 cases in women 55 to 64 years of age, rising to 38.0 and 31.4 cases in men and women 85 to 94 years of age (Benjamin et al., 1994). The clinical risk factors for AF include advancing age, diabetes, hypertension, CHF, valve disease, and myocardial infarction. The association between AF and HF was appreciated almost a century ago (Mackenzie, 1914). However, the exact pathophysiological mechanisms underlying such association have not been fully understood (Anter et al., 2009 and Knollman et al., 2008). Prevalence of AF increases 6-fold when CHF is present (Anter et al., 2009) and there are several evidences showing the prevalence of AF in HF trials (Ehrlich et al., 2002 and Benjamin et al., 1998). In the healthy heart, the pacemaker cells within the sino-atrial node initiate every heart beat (Levick, 2010). After that, there is a process that converts this electrical signal into

the mechanical contraction of the cardiomyocytes: “cardiac excitation-contraction coupling”. Into this process the calcium ions (Ca^{2+}) play an important role; the electrical signal goes through the atrial causing them to contract and fill the ventricles with blood. Every dysfunction in any part of this coupling process can lead to abnormally beat or to fibrillate, resulting in inefficient blood supply for the body (Knollman et al., 2008). During pathological conditions, pathophysiological interaction between atrial and ventricular tissue may occur. During AF, the alterations occurred in atrial tissue can also influence the ventricular function and may lead and non-regular ventricular rhythms. The effects of AF on ventricular function and the consequences of LV dysfunction on the atria lead to a vicious circle, in which AF promotes ventricular dysfunction, these dysfunction causes atrial remodeling that further promotes AF (Iwasaki and Nattel, 2011).

1.16 Hypothesis and aims

The cardiac contraction is generated by the highly orchestrated activity of numerous proteins, including regulatory receptors and ion channels. Cardiomyocytes express a wide range of regulatory receptors, such as adenosine and β-adrenergic, the two very important receptor subtypes in the heart. The previous paragraphs highlighted the current knowledge about adenosine and β-adrenergic receptors distribution and functionality in the cardiomyocytes and in the heart. In particular, it is evident from the previous knowledge that these receptors are spatially compartmentalized in a variety of distinct subcellular mircrodomains. The membrane microdomains, including caveolae and T-tubules, are responsible for the specificity of different receptor pathway necessary for the correct physiological activity of the cells. We hypothesize that the receptor compartmentation at the cell membrane will impact on the subcellular signallling following stimulation of the receptor.

It is well known that adenosine plays a key role in the protection of the heart from excessive β-adrenergic stimulation (anti-adrenergic effect), which may cause cardiac hypertrophy. Specifically, A_1 adenosine receptor subtype antagonizes the β-adrenergic receptor signal in the heart. For these reasons, it would also be interesting to understand how the interaction between these two receptors takes place in the membrane microdomains of the cardiomyocytes, in normal heart and in heart failure. During the pathological remodeling, the architecture and the structural integrity of the cells are drastically altered, inducing the redistribution of the receptors (Nikolaev et al., 2010) that leads to a change of the compartmentation of cAMP and may contribute to the failing myocardial phenotype. However, the exact mechanism of the molecular remodelling that usually occurs during heart failure has not been described yet. We hypothesize that protective effect of adenosine against excessive catecholamine stimulation is lost in failing cardiomyocytes, where structural disruption of microdomains leads to molecular remodeling.

The main aims of this thesis are:

1) To explore the functional role of the anti-adrenergic effect of adenosine in healthy and disease hearts. Investigate the anti-adrenergic effect of A_1 adenosine receptor agonist on cell contraction in both healthy atrial and ventricular rat cardiomyocytes. Study heart failure associated changes in adenosine A_1 receptors effect, by using a 16-weeks post-myocardial infarction rat model of heart failure.

2) To dissect cellular mechanisms of the anti-adrenergic effect of adenosine on the cAMP level. Study the A_1ARs effect on whole-cell cAMP level using FRET measurements in control Epac-1 mice, in both atrial and ventricular myocytes. Investigate the A_1AR dependent cAMP signalling during heart failure. Characterise microdomain-specific localization of anti-adrenergic effect of adenosine in atrial cardiomyocytes.

3) To study molecular mechanisms of the anti-adrenergic effects of adenosine, in control and during failing conditions, by using a rat model of heart failure (16-weeks post-MI).

4) To translate the observed findings from the animal model into human atrial cardiomyocytes. Compare cell contraction and whole-cell cAMP level, and investigate the molecular mechanisms that occur during different pathologies in several group of human patients.

CHAPTER 2. Materials and Methods

CHAPTER 2. Material and Methods

2.1 Animals

Procedures involving animals and their care conformed to institutional guidelines in compliance with the criteria of Animals in Scientific Procedures Act 1986 (ASPA, 1986).

2.1.1 Sprague Dawley Rats

The study population used in this work consisted of both male and female out-bred, wild type rats (Rattus Norvegicus), obtained from Harlan Laboratories (Wyton, UK). This strain is one of the most common used outbred strain present in research. The animals were placed in special cages at a density of 4-6 per cage until the onset of the experiments, in a temperature-controlled room at 20-24°C, with 12-hour light/dark. Male were sacrificed for the adult cardiomyocytes isolation when >250g, female when >190g.

2.1.2 Rat Heart Failure Model

To study the remodelling of GPCR signalling in single cardiomyocyte in the settings of cardiac pathology, a model of chronic myocardial infarction (MI) in adult Sprague-Dawley rats was used. This model was obtained via the ligation of the left anterior descending coronary artery to induce chronic MI, as previously described (Lyon et al., 2009). Briefly animals were anaesthetised and placed in ventral recumbence; the dorsal mid-lumbar region was shaved and the antibiotic agent was applied. The chest and the pericardium were opened surgically and a suture was made around the left anterior descending artery to bound and constrict the blood flow. As a control, sham animals were used, in which no constriction of the blood flow

occurred, but the suture was bound only loosely around the artery. After this process, animals were placed back to the special cage until the complete recovery. The parameter of the ejection fraction volume was determined at 4, 8 and 16 weeks post the surgical procedure via echocardiography recordings to obtain an indicator of wall contractile function.

2.1.3 EPAC-1 mice

Both male and female mice of FVB/N strain were also obtained from Harlan Laboratories (Wyton, UK). Male mice of this strain that transgenically homozygously expressed the cAMP-sensing FRET construct Epac-1, were given from Professor Viacheslav Nikolaev, Hamburg University, Germany. All males were separated and placed in a cage alone, females were housed at a density of 5-6. All animals were maintained on a 12-hour light/dark cycle. They were sacrificed for the adult cardiomyocytes isolation when >20g. The transgenic mice were prepared by cloning the DNA sequence of the Epac1-camps Sensor into pB-βAKT vector between KpnI and EcoRV restriction sites (Nikolaev et al., 2006). This process allows the uniform distribution and expression of the Epac-1 sensor in all tissues.

2.2 Human patients

2.2.1 Patients screening

Patients examined during this work were enrolled from routine cardiac surgery. The permission to obtain heart tissue biopsy was received from the respective patients. The clinical information (anamnesis data, electrocardiogram and echocardiography data etc) were used to establish the main cardiac disease and to allow the classification of the patients in different groups. Human biopsies were collected either during mitral valve (MV) surgery or during bypass surgery as well as from dilated (DCM) and

ischemic cardiomyopathy (ICM) heart transplant with and without left ventricle assistant devices (LVADs). For reasons of patient anonymity identification and personal data are not available in this thesis.

2.2.2 Biopsy storing

Tissue was obtained from human subjects in agreement with the Declaration of Helsinki developed for the medical community by the World Medical Association (WMA). The study performed was approved by a UK institutional ethic committee (Ref: 12/WA/0196 + 11/LO/1874).
Biopsies were collected during cannulation for coronary artery bypass grafting (CABG) or valves replacement operation from both the right and left atria. Excised tissue was placed in cold low calcium solution adjusted for human tissue storing (see in section 2.3.4 details for composition), until the transport to laboratory. Collected tissue was immediately used for cardiomyocytes isolation. In addition, to investigate possible molecular mechanisms, small pieces of tissue were frozen and stored at −80°C (where this was possible depending on the size of the tissue), for future PCR and Western Blot analysis.

2.3 Cardiomyocytes isolation

2.3.1 Rat ventricular Cardiomyocytes isolation

Sprague-Dawley rats were anesthetized with 5% isoflurane- 95% O2; heparine was injected to prevent blood coagulation, and then they were humanely killed by cervical dislocation. The chest and the pericardium were opened to fully expose the thoracic cavity. Heart and lungs were promptly removed and placed in ice cold Krebs-Henseleit (KH) Buffer (119mM NaCl, 4.7mM KCl, 0.94mM MgSO4, 1mM CaCl2, 1.2mM KH2PO4, 25mM NaHCO3, 11.5mM glucose; 95% O2, 5% CO2). The tissue was moved into a Petri-dish with ice cold KH solution. Lungs and thyroid pericardial fat were

removed from the heart, leaving only the aorta intact to allow a clear view for the cannulation. Heart was cannulated using the aorta with the Langerdoff settings. The first part of the isolation protocol was to perfuse the all heart with KH at 37°C for 5 minutes. After this time the KH buffer was switched to a low calcium ($LoCa^{2+}$) buffer (12-15μM CaCl2, 120mM NaCl, 5.4mM KCl, 5mM MgSO4, 5mM pyruvate, 20mM glucose, 20mM taurine, 10mM HEPES, 5mM nitrilotriacetic acid (NTA); 100% O2). Rapid cessation of beating confirmed that the $LoCa^{2+}$ buffer had removed calcium from the heart and that perfusion was going properly. After 5 minutes of $LoCa^{2+}$ administration, a solution containing 1mg/ml Collagenase II and 0.6mg/ml Hyaluronidase (C+H) in enzyme (Enz) buffer (12-15μM CaCl2, 120mM NaCl, 5.4mM KCl, 5mM MgSO4, 5mM pyruvate, 20mM glucose, 20mM taurine, 10mM HEPES,150μM Ca2+) was perfused into the heart for 10 minutes. Later, when the enzymatic degradation was finished, the perfusion system was switched off and the all heart was placed in a petri-dish and dissected. The right ventricular free wall and atria were removed. Left ventricle was minced and placed in a fresh falcon tube with C+H. The samples were shaken mechanically at 35oC for 5 minutes; at this point the supernatant was filtered through 200-μm nylon mesh and replaced with new buffer for isolation. This process was switched off after 30 minutes and then the resulting digested tissue was centrifuged for 1 minute at 700 rpm. The supernatant was removed and discarded, in contrast the pellet was resuspended in Enz buffer without the enzymes until the beggining of the experiments (Nikolaev et al., 2010).

2.3.2 Rat atrial Cardiomyocytes isolation

Similar to ventricular isolation, for rat atrial cardiomyocytes isolation, the heart was extracted and cannulated using Langendorff apparatus. In the first part of the protocol, the heart was perfused with KH solution for 5 minutes, then with the $LoCa^{2+}$ for additional 5 minutes, as for ventricles.

The most important difference between the two types of isolation was that the collagenase step was preceded by 19-20 minutes of perfusion with a solution containing Enz buffer plus proteinaise (Type XXIV, Sigma, 7.8 mg/ml). After this, the atria were removed, cut into small pieces, re-suspended in enzyme solution, containing only collagenase (1 mg/ml), placed in falcon tube and shaken in a water bath at 37°C for 6 minutes. Then the tissue was filtered through a 200-μm nylon mesh and the digested tissue was centrifuged for 3 minutes at 600 rpm. The supernatant was removed and discarded, as before, and the pellet was left in fresh Enz buffer without the enzymes until the beggining of the experiments.

2.3.3 Epac- mouse cell isolation

Mice, were anesthetized and then were killed by cervical dislocation. As described before, the heart and lungs were removed and placed into ice cold KH solution. After heart remotion, lungs, tymus and the other tissues were also dissected away from the aorta; given the small size of heart the aorta was cannulated with the useful help of a stereomicroscope and the perfusion with KH solution started for 5 minutes at the temperature of 37°C via the Langerdoff apparatus. After this step, the perfusion of KH solution was switched off and the perfusion with the $LoCa^{2+}$ solution started for another 5 minutes. When the perfusion with $LoCa^{2+}$ solution was finished, we switched to a solution containing Enz buffer plus proteinase (3.8 mg/ml) for an additional 4-6 minutes, depending on the size of the heart. The last step of the protocol included the perfusion of the heart with the Enz solution containing collagenase (1 mg/ml) for 5 minutes. At the end the heart was removed, atrial and ventricular tissues were separately triturated and filtered in 3 different tube (right atrium, left atrium and left ventricle) and leaved for at a least 10 minutes. Thus, the supernatant was discarded and the pellet was suspended with a fresh enzime-free buffer. The tubes containing the cells were left at room temperature until the beginning of the cell plating procedure.

2.3.4 Human atrial cardiomyocyte isolation

After the collection, the human tissue were placed in cold $LoCa^{2+}$ solution, adjusted for human tissue storage ((pH 6.95) (Ca^{2+} (12mM), $MgSO_4$ (5mM), KCl (5.4mM), NaCl (120mM), Glucose (20mM), 4-(2-hydroxyethyl)-1-piperazineethanesulfonic acid (HEPES, 10mM), nitrilotriacetic acid (NTA, 5mM), taurine (20mM) and pyruvate (5mM)). Atrial cardiomyocytes were isolated by enzymatic dissociation and mechanical disaggregation using modification of Harding's isolation protocol (Workman et al,. 2001). The tissue was leaved in the cold human LowCa solution and minced in small pieces of 1-2 mm. Once cut into small pieces, tissues were quickly transferred into a new falcon tube, containing 10ml of oxygenating $LoCa^{2+}$ solution and manually shaken for 3 minutes to remove blood clots; this step was repeated three times until the small pieces of tissue looked clean. After the cleaning processes, tissue was placed into a new tube with Enz buffer plus protease (Type XXIV, Sigma, 0.36mg/ml) and collagenase (type V Sigma, 0.5mg/ml). The solution was bubbled with oxygen (95%) and mechanically shaken for at least 10-15 minutes, until the tissue started to looks white/translucid. The cardiac tissue was filtered with the nylon mesh 200 um used for all type of isolation describe before. The tissue was then digested with collagenase (1 mg/ml). After 2/3 step of 10 minutes each, the tissue was filtered and the all solution was centrifuge at 600 rpm for 3 minutes. The supernatant was then removed, leaving the cell pellet at the bottom. At this time, a fresh Enz solution was transferred in the tube and the cells were leaved until the onset of the experiments (Voigt et al., 2013).

2.3.5 Cardiomyocytes plating and culture

After isolation, cardiomyocytes were plated on to laminin-coated glass bottom dishes (MatTeK Corporation, Ashland, USA) or laminin-coated glass

coverslips (Thermo Scientific, VWR International, # 12392108). Laminin is a heterotrimeric protein of glycoproteins with high molecular weight ~400 kDa forms extracellular matrix and the basal membrane in many tissue, including heart. Laminin was applied (10/20 μL for each dish) and was left to dry to the bottom of each dishes. After checking the laminin dry (at least 10-15 minutes later the plating), the cells were placed on the top and leaved for at least 1 hour before experiments. This is the time needed for the cells to attach to the bottom of each dishes (Kleinman et al., 1985; Lundgren et al., 1988 and Boateng et al., 2005). Cardiomyocytes isolated from mice were used in the same day of isolation and for this after the plating they were fast used for the experiments. Rat cardiomyocytes, after the plating were incubated at 37°C and 5% CO_2 in the presence of modified M199 culture medium. They can also be used on the same day of the experiments for contraction recordings. Modified M199 culture medium was made up from 500 ml M199 medium in addition with creatine 5mM, taurine 5mM, carnitine 5mM, 1g bovine serum albumin, ascorbate 100mM and penicillin/streptomycin 100mM. Human isolated cardiomyocytes were used on the same day of the isolation or were first incubated for 1h in recovery medium (M199 with the addition of fetal bovine serum 10ml/L) and then leaved in the presence the modified M199 medium in which was add the adenovirus FRET biosensors for 48h.

2.4 Functional investigation of cardiomyocytes

2.4.1 Ionoptix System

The Ionoptix system was based around a Myocam camera (Ionoptix Corp. Milton, MA). attached to an inverted microscope (Nikon TE-200) This camera was connected to a PC to allow the view of the cell in the real time (Figure 2.1). The images of the cells were acquired during different protocols and analyzed with the IonWizard 8 software package. The cells were suspended in a specific chamber and placed on the microscope; then were field stimulated (50 V, 0,2 Hz for human cells, 0,5 Hz for rat cells, and

1 Hz for mouse myocytes) by constant depolarizing pulses from platinum electrodes placed on opposite sides of the cell chamber connected to a simulator. During experiments cells were perfused with KH solution at the temperature of 37°C using a peristaltic pump. Depending on protocol the all pharmacological agents were added in KH buffer for at least 10 minutes.

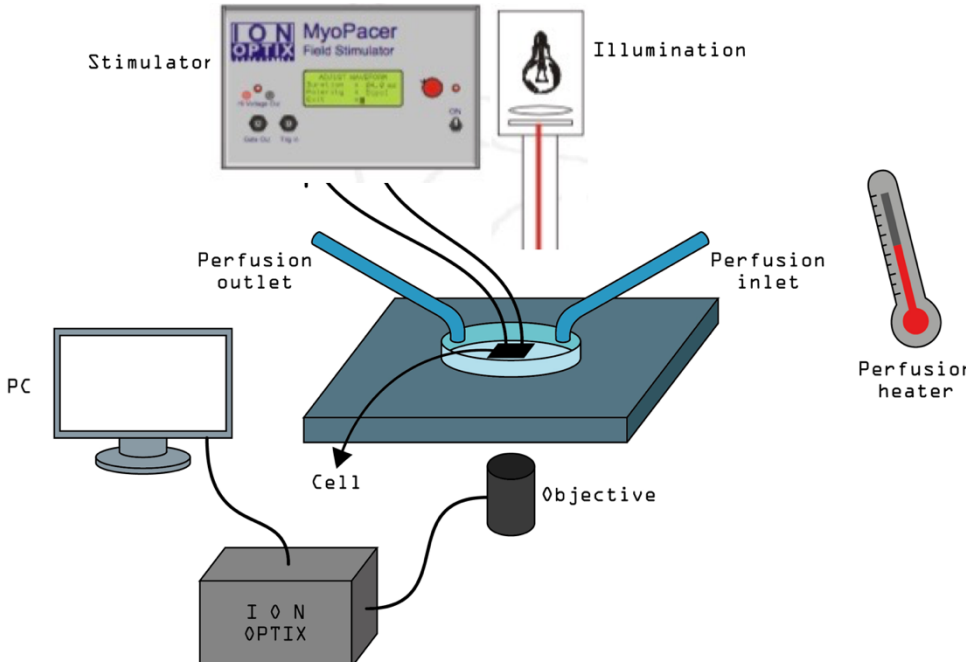

Figure 2.1: Schematic rapresentation of the Ion Optix system used for the measurement of isolated cardiomyocyte shortening upon pacing.

The cells had been selected for experimental protocols when following the subsequent morpho-functional parameters:

- Rod-shaped,
- no spontaneous contraction
- stable contraction and relaxation during 10 minutes of the baseline recording.

The cells length at the baseline were representative as the length of the cell during the diastole (before the application of the electrical stimulation). When the pacing current was applied we were able to observe the shortening of each cells; the differences between the cell length during the contraction and relaxation is defined as cell shortening. This value was used to measure the contractile amplitude. Another parameter that we were able to measure was the lusitropy effect by the value named R50 or R90. This parameter was the value of the time taken from the cells to restore 50% or 90% of the shortening produced by the electrical stimulation (Figure 2.2). For our investigation, we used different pharmacological agents and different protocols that will be discussed in the next chapters.

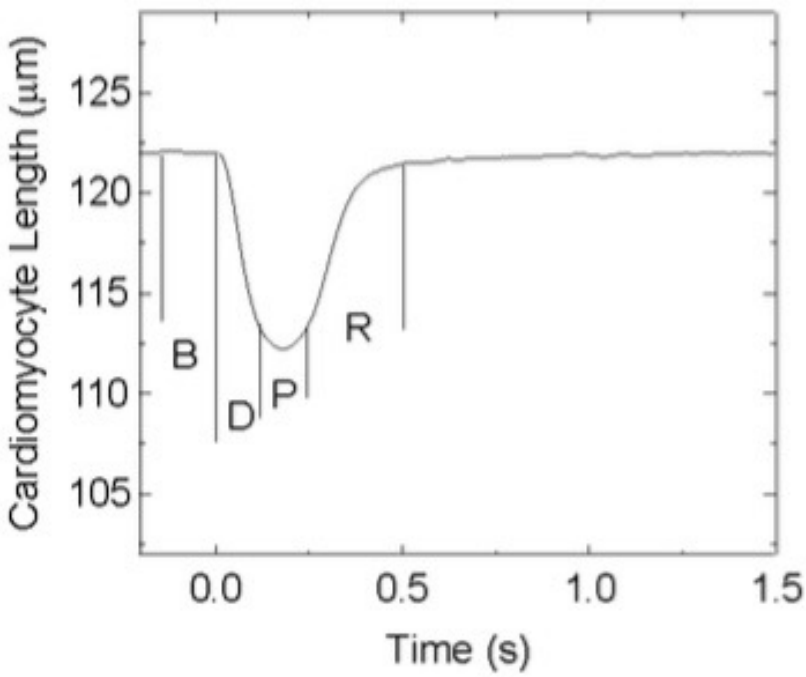

Figure 2.2: Phases of displacement transient: Examples of baseline (B), deflection (D), peak (P), and recovery (R) phases of the transient.

2.4.2 Forster resonance energy transfer (FRET)

FRET technique is based on the physical phenomenon of partial, non-radiative energy transfer between two fluorophores with partially overlapping excitation and transmission energies when in close proximity (several nm). A “donor” in electronic excited state transfers energy to an “acceptor” of lower energy via non-radiative transfer. The energy transfer efficiency is dependent on the sixth power of the distance between the donor and the acceptor, making the technique extremely sensitive to small changes in distance. Our system consisted of an ORCA-ER camera (Hamamatsu Photonics) attached to an inverted Nikon TE2000 microscope (Nikon) equipped with 100W halogen lamp light source, Lambda 10-B shutter (Sutter Instruments) with a 436/20nm excitation filter and a DualView beamsplitter (Photometrics) which consists of DM505 dichroic mirror and filters (D535/40 and D430/30) to separate YFP and CFP images, which were projected to the camera sensor simultaneously (Figure 2.3). The images collected using the Micromanager 1.4 program and the ratio of YFP to CFP was calculated using a custom-made plug-in.

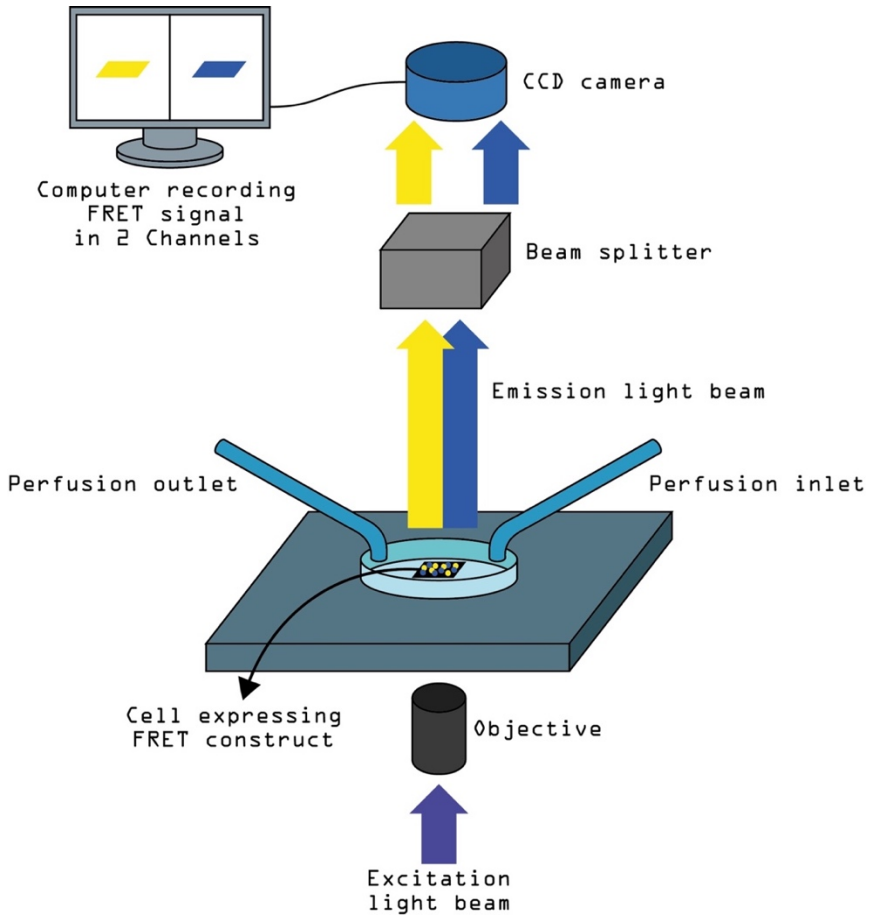

Figure 2.3: Schematic figures of the FRET Microscopy system used for isolated cardiomyocyte cAMP level measurement

Solutions were applied to cells directly in the dish. Reagents and all FRET microscopy studies were performed utilizing a HEPES based FRET buffer (NaCl 144mM, HEPES 10mM, MgCl2 1mM, KCl 5mM – pH7.4).

2.4.3 EPAC-1 sensor

Trasgenic mouse expressing the EPAC-1 sensor was generated previously (Nikolaev et al, 2006). The sensor construct is based on cyan fluorescent protein (CFP) fused to the cAMP binding domain of the type 1 exchange protein activated by cAMP (EPAC1) and yellow fluorescent protein (YFP).

Upon cAMP binding and the resulting conformational change, a reduction in Forster resonance occurs, which indicates cAMP presence. The advantages of using these mice; include, firstly, that the sensor is expressed equally in all cells, and, secondly, freshly isolated cells can be investigated without the need of transfecting and associated adverse effects of a prolonged cell culture.

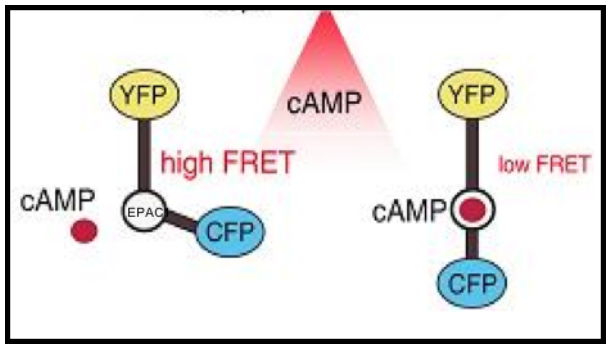

Figure 2.4: FRET measurement principle of relative cAMP levels. Left hand side: In the absence of cAMP the FRET donor CFP gives part of its energy in a non-radiative fashion to the proximal, FRET acceptor YFP. Right hand side: The presence and binding of cAMP leads to a conformational change of the FRET biosensor, which removes YFP from the proximity of CFP, which in turn can no longer transfer any energy onto YFP**.** (Modified from Nikolaev et al., 2010)**.**

2.4.4 RII –EPACsensor

The sensor part of the RII-EPAC sensor is formed by the EPAC1 cAMP binding domain fused to the regulatory subunit of PKA-RII and flanked by CFP and YFP as in the above mentioned cytoplasmic sensor. The sensor protein binds to the cellular components associated with the particulate fraction of cellular PKA. The cAMP that reach this sensor could be able ro influence the contractility, considering that the RII compartment contains the PKA that is responsible for the modulation of the cell contraction. This sensor is a kind gift of Professor Manuella Zaccolo (Oxford University).

2.4.5 Culture of cardiomyocytes for FRET

Immediately after cells isolation, the cells were placed on laminin-coated 25mm coverslips or mattek dish. 45 minutes later, dead and non-attached cells were washed out and the coverslips were cultured in Mdeium199 (0.5mg/ml BSA, 0.66mg/ml creatine, 0.66mg/ml taurine, 0.32mg/ml carnitine at 37oC and 5%CO2). Coverslips were removed from the culture media for use, washed with a buffer solution containing 144mM NaCl, 5.4mM KCl, 1mM MgCl2, 2mM CaCl2 and 10mM HEPES, pH=7.3, and clipped into a 200µl 25mm coverslip holder containing the same solution. For the rat cells the adenovirus expressing the FRET construct was introduced into the culture medium at a specific concentration and left with the cells for at least 48 hours.

2.4.6 Scanning Ion Conductance Microscopy (SICM)

For the structural characterization of cells, SICM was used. This technique is a non-invasive, nano-scale resolution methodology that was invented by Hansma et al. in 1989; in this methodthe glass nano-pipette is used as a scanning probe for the non-contact visualization of the cell surface of living cells (Hansma et al., 1989). Initially, SICM was used only for the visualization of the smooth surface. Recent introduction of the hopping mode of SICM overcame this restriction and enabled the visualization of the protruding nano-structures such as microvilli (Novak et al., 2009). Hopping mode SICM was used to visualize the surface of cardiomyocytes in the present study. The pipette was generated with the P-2000 laser puller (Sutter Instrument) in which borosilicate glass capillary BF100-50-7.5 (IntraCel) were inserted to create a nanopipette with the necessary tip size (with 80-100MΩ resistance) to resolve nano-scale structures present on the

cardiomyocyte surface, like the T-tubule openings and crests. The dish with cells was placed on top a piezoelectric stage, which can move in the x and y direction. The nano pipette was filled with the electrolyte solution and then an electrode was placed inside. The nano-pipette was fixed in a pipette holder attached to a piezo-actuator that can move in Z direction (up and down); then the nano-pipette was brought into solution above the cells and an ion current was established between the nano-pipette and the electrode in the bath. (Figure 2.6). A feedback system that registers the ion flow between the two electrodes is controlled via the dedicated software IonView (IonScope, UK) and in the same time the nanopipette vertical position at each scanning position in X/Y dimensions was recorded, which generated a topography image of the cell surface. Another advantage was that through the nano-pipette we could apply an agonist or an antagonist to the particular receptor located on a specific structure on the surface of the cells, which was identified while scanning. This was achieved via pressure application to the pipette (Nikolaev et al., 2010 and Miragoli et al., 2016) or by reversal of the electric polarity of the two electrodes, releasing charged substances (such as isoprenaline).

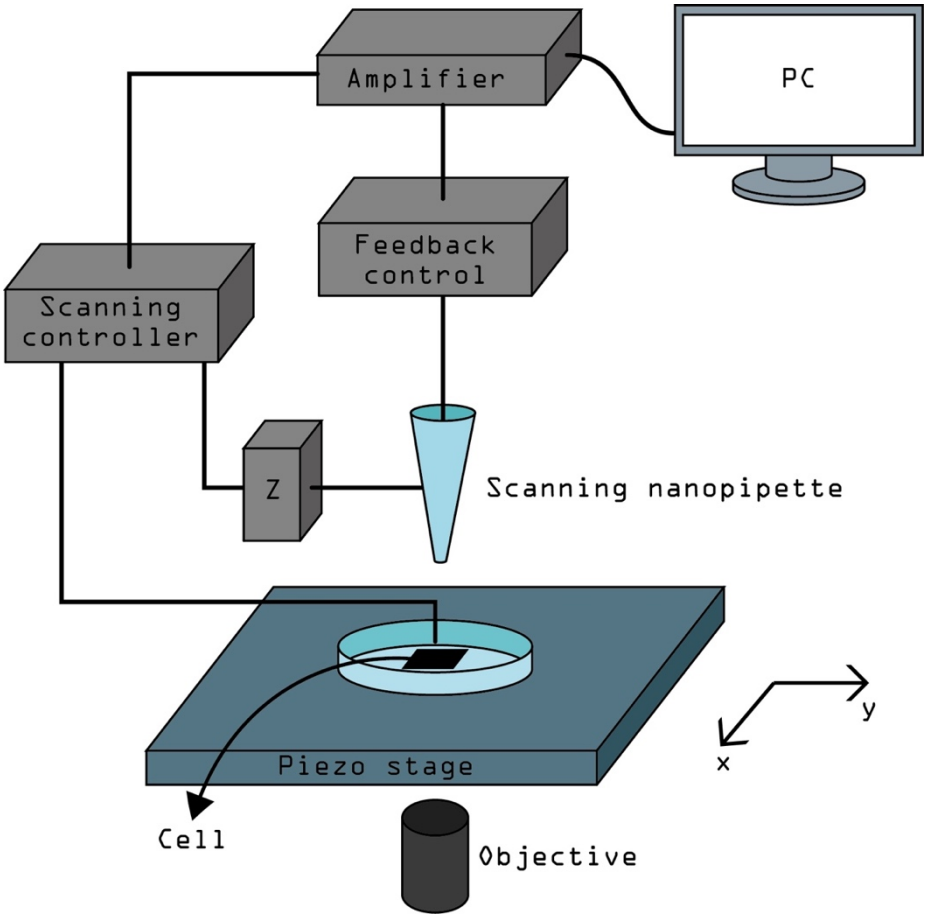

Figure 2.6: Schematic representation of the SICM microscopy system used for isolated cardiomyocyte atrial cardiomyocytes visualization

For this work we used a custom-made combination of a SICM/FRET microscope (see materials and methods chapter 4). Briefly the SICM allows to check the cellular topography and to apply different drugs to a specific area of interest; in addition, because the system was in a combination with the FRET, after the application of the substance trough the nanopipette, we were able to investigate the local effect after that application. With this modality (SICM/FRET) we provide a specific way for looking at the GPCR functionality and cAMP compartmentation.

2.5 Molecular investigation

2.5.1 Real-time polymerase chain reaction

To explore the possible change occurring during heart failure conditions, the mRNA expression profiles of key cardiac contractile proteins, was investigated. Particularly we measured the expression levels for both β_1 and β_2 adrenergic receptors, all three adenosine receptors subtype and cav3. In this thesis, we had the possibility to study the mRNA expression profiles of these receptors in control and rat heart failure model tissue and also in human patients. We divided the human patients in four groups: healthy (no HF, no AF) human patients, HF and AF human patients, HF human patients and AF human patients (see chapter 6). Total RNA was extracted from around 30 mg of atrial tissue with the use of specific KIT for the extraction. For rat atrial tissue, we just extracted the RNA from all atria together or from each atrium separately; for human tissue, when it was storing in Krebs solution we kept one small piece, 30 mg (if this was possible). The RNA was measured using the Thermo Scientific NanoDrop 1000 Spectrophometer and the PCR analysis was performed using SYBR Green JumpStart taq ReadyMix (Sigma) in an Eppendorf Mastercycle EP Realplex machine. Relative expression analysis was performed using the $\Delta\Delta^{Ct}$ method.

2.5.2 Western blot analysis

To study the protein levels in both disease and control conditions, Western blot analysis was performed. We were able to check the protein levels of A_1 adenosine receptors and Cav3. Atrial tissue was snap-frozen in liquid nitrogen. Tissues were lysed in lysis buffer to allow the protein extraction.
50 µg of extracted proteins were loaded on 4-20% Midi-Protean TGX precast gels (BioRad) (see chapter 6 for protocols details). Western blot analysis was performed using the following antibodies: Caveolin 3 (cav3)

(BD), A1 adenosine receptor (A1adoR) (Alomone Lab), GAPDH (Cellsignaling). Immobilon Chemiluminescent Substrate (Millipore) was used to develop blots using a Chemidoc MP Imaging System (Bio-Rad).

CHAPTER 3. Effect of adrenergic and adenosine stimulation on cardiomyocytes contraction.

CHAPTER 3. Effect of adrenergic and adenosine stimulation on cardiomyocytes contraction.

3.1 Introduction

Adenosine action in the heart is mediated by four G-protein coupled receptors: A_1AR and A_3AR, which act via G_i, and A_{2a}AR and A_{2b}AR which act via G_s. All four receptors subtype are expressed in the heart, with different mRNA levels (Headrick et al., 2013). In the heart the most expressed receptor is A_1AR, followed by A_{2a}AR whereas much lower expression of A_{2b}AR and A_{3A}R is noted.

Adenosine receptors mediate a wide range of actions, regulating faithfully cardiovascular function, improving cellular energy balance and promoting cellular resistance to stress or injury (Headrick et al., 2013). However, adenosine receptors activation is not restricted to conditions of stress; they are involved in various responses, from modulation of coronary flow and contraction to cardio-protection, being sensitive to even mild perturbation in energy state and cell signaling pathways.

Adenosine is produced and released mainly during myocardial ischaemia and reperfusion and has multiple actions in the heart; it is produced not only by cardiomyocytes, but also by endothelial cells. Adenosine is known to be cardio-protective with the following effects: it attenuates the release of cathecolamines, βARs-mediated myocardial hypercontraction and myocardial Ca2+ overload via adenosine A1 receptors (Masafumi and Masatsugu, 2000). On the other hand, it increases coronary blood flow via A2 adenosine receptors (Masafumi and Masatsugu, 2000). These effects are able to inhibit and delay the deleterious consequences of ischemia/reperfusion injury in the heart. For these reasons, adenosine could be implicated in the process of cardio-protection and could also attenuate the severity of the heart failure. Adenosine is physiologically present in the heart and has been

reported to attenuate the isoprenaline-induced increase in cardiac force of contraction in several species (Schrader et al., 1977 and Rockoff and Dobson, 1980), in a process well known as anti-adrenergic effect. Such effect can occur in the presence of adenosine alone (direct effect) or in the presence of an additional stimulation (indirect effect). Adenosine anti-adrenergic effect is mediated via A_1AR, and involves Gαi inhibition of PKA activated by β-adrenergic receptor pathway (Dobson, 1983) and modulation of β_1ARs stimulated Gs cycling (Fenton and Dobson, 2007). It is also known that the A_1ARs could act upon β-adrenergic responses in a PKC-dependent process (Dobson et al., 2008) involving Gβγ (Fenton et al., 2010).

Bohm et al. investigated the antagonism between adenosine and isoprenaline influence on the force of contraction in both atrial and ventricular muscle preparations from guinea-pig hearts. They observed that adenosine added 5 minutes after isoprenaline, decreased force of contraction and abolished completely the positive inotropic effect of isoprenaline on atrial muscle preparations. The situation was similar in the ventricular muscle preparation, but the effect was much smaller then in the atrial preparation (Bohm et al, 1984). A similar result was observed by Geoffrey et al. The authors studied the effects of adenyl compounds on rat atrium and ventricle muscle. They reported that adenosine produced negative inotropic effects on the rat atrium but the same effect was not present in the ventricle muscle (slightly enhanced the contractile force but this effect was not significant) (Geoffrey et al., 1983). These experiments clearly show that the anti-adrenergic effect of adenosine is much more robust in atrial muscle compared to ventricle. Changes in adrenergic control were studied in several disease model. For examples in spontaneously hypertensive rats the effect of A_1ARs stimulation followed adrenergic activation was completely abolished (Tang et al., 1998). Furthermore, Chansraesekera et al. first reported that A_1ARs can heterodimerize with the family of beta adrenergic receptors (Chandrasekera et al., 2013). These results suggest that the co-

expression of A_1ARs with β_1 or β_2-adrenergic receptors resulted in the formation of a functional heterodimers. This complex presents altered pharmacological and signaling properties of different pathways.

One mechanism proposed for the regulation of the cellular signaling is the compartmentalization at the cellular membrane level. Significant evidence has accumulated that adenosine receptor signaling could be regulated by membrane microdomains (Lasley, 2010). Such specific regulation may include the localization of adenosine receptors in caveolae or lipid rafts. Although the observations of the localization of A_1ARs in caveolae membranes, the role that this specific localization could play on adenosine signal pathway remains unclear.

Given that the adenosine receptors in the heart activate a cascade of downstream signaling molecules, many of which are implicated in cardiac hypertrophy, apoptosis, or the regulation of intracellular calcium flux, we hypothesize that such receptors could play a crucial role in the development of cardiac dysfunction, such as heart failure. Additionally, considering that adenosine seems to attenuate the detrimental neurohumoral factors in the pathophysiology of heart failure, it may become a new drug for the treatment of congestive heart failure. However, the modulation of adenosine and its anti-adrenergic effect during heart failure is not fully investigated. Since adenosine was investigated as cardio-protective agent during the condition of heart failure, it became important and interesting to analyze the adenosine receptors activity in different situations.

To study atrial and ventricular remodeling during disease, we used the 16 weeks of post–myocardial infarction rat model of heart failure (see material and methods in the next section). This model encloses many features of heart failure conditions that happens in patients, including the remodeling of the organ, characterized by left ventricle dilatation, reduced ejection fraction, and raised filling pressures. To study the possible role played by cholesterol on the regulation of micro-domain distribution of GPCRs in cardiomyocytes, incubation before experiments

with 10 mM of methyl-β-cyclodextrin (MβCD) for 30 minutes at room temperature was done. This incubation resulted in ≈60% depletion of caveolae, with no changes in cell topography and T-tubules density (Glukhov et al., 2015).

During this project, we tried to better understand how adenosine stimulation modulate β-adrenergic signaling in both atrial and ventricular cardiomyocytes in different conditions. For this, the aim of this set of experiments was to explore the functional role of the anti-adrenergic effect of adenosine in control and heart failure conditions.

The main objectives of the chapter are:

- To study the cellular effects of A_1 adenosine receptor stimulation in healthy atrial myocytes.

- To compare the anti-adrenergic effect of A_1 adenosine receptor stiumulation on cell contraction in healthy atrial and ventricular rat myocytes.

- To study heart failure (HF) associated changes in the adenosine effects in 16-weeks post-myocardial infarction rat model of heart failure.

- To study the changes in the adenosine effects in healthy atrial and ventricular rat cardiomyocytes after the depletion of cholesterol.

3.2 Materials and Methods

3.2.1 Animals

In these experiments both male and female Sprague Dawley Rats were used (8-10 weeks old, weight ~250 g).

3.2.2 Rat Post-Infarction HF Model

For the study of single cardiomyocytes during their progression towards heart failure a model of chronic myocardial infarction (MI) in adult Sprague-Dawley rats was generated. The rat model of HF was generated by ligation of the left anterior descending coronary artery. Cardiomyocytes were isolated after sixteen weeks post-MI. This model of heart failure was validated from our group on 2009 (Lyon et al., 2009). 16-weeks after myocardial infarction, all animals had a significant increase of the heart weight/body weight ratios (g/kg) compared to with sham-ligated controls (HF vs. Sham: 4.7 ± 0.2 vs. 3.8 ± 0.1, $P < 0.01$, $n = 6$ in each group), reflecting hypertrophy of the viable left ventricular myocardium. Serum brain natriuretic peptide (BNP) levels were undetectable in sham controls and elevated in HF rats [205 ± 43 pg/mL vs. undetectable (<80 pg/mL), $P < 0.01$]. Pressure–volume (PV) analysis (Fig. 2 *B–D*) demonstrated ventricular dilatation [left ventricular end-diastolic volume (LVEDV): 258 ± 27 μL vs. 173 ± 8 μL, $P < 0.01$], with reduced ejection fraction and elevated end-diastolic pressure: [left ventricular ejection fraction (LVEF): 32% ± 4% vs. 76% ± 2%, $P < 0.001$; left ventricular end-diastolic pressure (LVEDP): 24.0 ± 3.3 mm Hg vs. 8.5 ± 0.5 mm Hg, $P < 0.001$]. Dynamic measures of contractile function [end-diastolic PV relationship (EDPVR);; 0.60 ± 0.12 mm Hg/mL vs. 1.89 ± 0.24 mm Hg/mL, $P < 0.01$; time-varying maximal elastance (Emax): 1.4 ± 0.2 mm Hg/mL vs. 3.1 ± 0.5 mm Hg/mL, $P < 0.05$; preload recruitable stroke work (PRSW): 61 ± 21 mm Hg vs. 110 ± 11 mm

Hg, $P < 0.05$] and ventricular compliance [end-diastolic PV relationship (EDPVR): 0.11 ± 0.01 mm Hg/mL vs. 0.03 ± 0.01 mm Hg/mL, $P < 0.01$] were also significantly impaired in these animals, consistent with the HF phenotype.

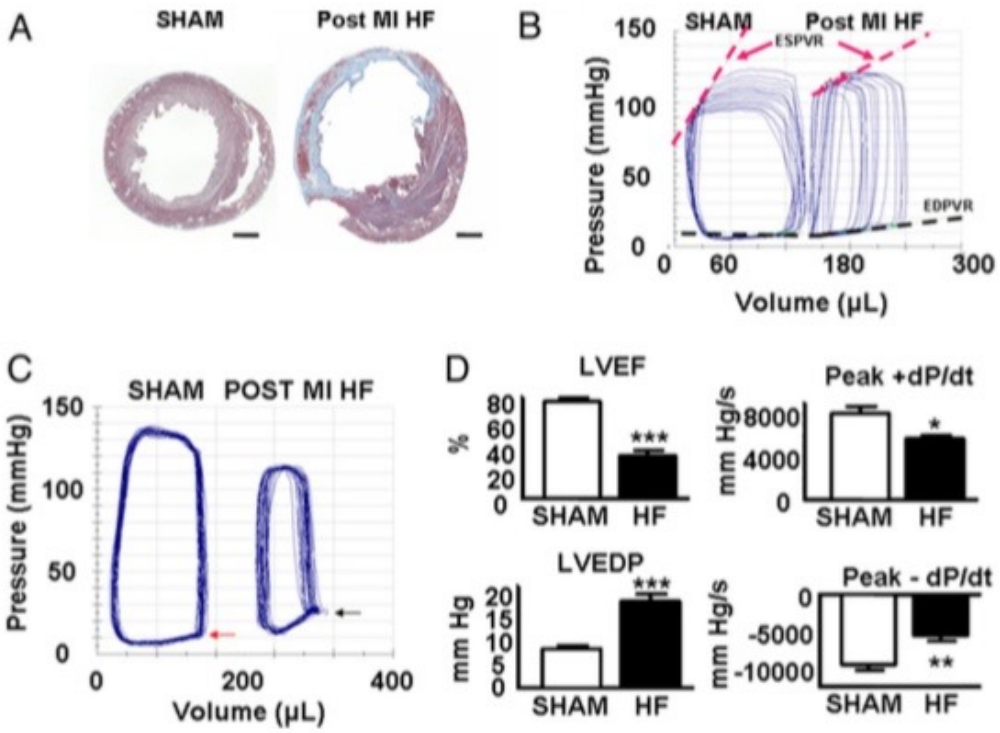

Figure 3.1. The rat chronic post–myocardial infarction (MI) HF model. (A) Midventricular 10-µm section from a sham control rat heart (Left) and a chronically infarcted rat heart (Right) after staining with Masson's trichrome. (Scale bar, 2 mm.) (B) Representative in vivo PV loops during transient inferior vena caval occlusion from an HF rat and a Sham control. ESPVR (red broken lines) and EDPVR (black broken lines) relationships are presented. (C) Representative in vivo steady-state PV loops demonstrating increased ventricular volumes and elevated end- diastolic pressure in HF rats (black arrow) compared with Sham controls (red arrow). (D) Steady- state PV data demonstrating decreased LVEF, increased LVEDP, and reduced peak velocities of pressure change (dPdt) during isovolumic contraction (Peak + dPdt) and isovolumic relaxation (Peak − dPdt) in rats with HF. *, P < 0.05; **, P < 0.01; ***, P < 0.001 (Lyon et al., 2009)

3.2.3 Atrial and Ventricular cardiomyocytes isolation

Cells were isolated from rats as described in Chapter 2 (General materials and methods). Both left and right atrial appendages were placed all together in falcon tube with enzymes (Enz) solution (without proteinase and collagenase). Right ventricular tissue was removed and discarded; left ventricular tissue was kept for contraction experiments in a falcone tube with Enz solution.

3.2.4 Solutions

All solutions used during contraction measurement experiments were made in KH buffer (see general methods in chapter 2). The following drugs were used: Isoprotenerol; ICI 118, 551; CGP20712A; methyl-β cyclodextrin, supplied by Sigma Aldrihc (Poole, UK); 2-MeCCPA: supplied by Tocris (Milan, Italy).

3.2.5 IonOptix studies for cardiomyocytes contractility

Atrial and ventricular rat cardiomyocytes were isolated and stored in a $LoCa^{2+}$ buffer (see general methods in chapter 2) until the beginning of the experiments. A specific perfusion chamber was made with the use of the 22 mm glass cover slip to plate the cells, the chamber was perfused with KH buffer. All solutions used during these experiments were saturated with oxygen/CO2 mixture (95%/5%) and the temperature in the chamber was constantly kept at 37 degrees celsius. The cells were left on the cover slip for around 5-10 minutes in static conditions to allow for the cardiomyocytes to settle on the bottom of the chamber. After this time, the perfusion was resumed. At this point visual screening of the cells was performed to select

good candidates for the experiments. The choice criteria were rod-shaped (live) cells; cells that do not contract without expernal electrical stimulation. Once a cell was selected, electrical pulses of 50V, 20msec were introduced through a field stimulator at the frequency of 0.5Hz. The chosen cell was visualized by the IonOptix imaging software, in the edge detection mode. Two markers for the cell edges were positioned manually by the operator. The cell shortening was then recorded. Baseline was usually recorded for at least 10 minutes to ensure that the cell responds constantly to the pacing and the shortening is uniform and stable, and then different agonist/antagonist were applied as described in the specific protocols.

3.2.6 Investigation of contractile responsiveness of cardiomyocytes to A1 adenosine receptors after β1 adrenergic stimulation.

Cells were perfused with KH buffer for two minutes to establish a steady-state condition for recording. After this, a specific β2AR blocker, ICI118,551 (ICI, 100 nM) was adminisered for 10 minutes to obtain a stable baseline. Using this selective antagonist, introduced in the solution, we were sure that any changes in the contractility were related only to β1ARs activity. Indeed, the subsequent part of the protocol included the addition of Isoproterenol (100 nM) to the perfused solution, for the selective stimulation of the β1ARs. 2-MeCCPA (1 μM), a specific agonist of the A1 adenosine receptors, was applied in the solution to investigate the effect of the activation of these receptors after a specific previous β1 adrenergic stimulation (Figure 3.2). This protocol was repeated in 3 different group of cells for both atrial and ventricular cardiomyocytes:

- Atrial and ventricular control (healthy cardiomyocytes)

- Atrial and ventricular HF (16-week post-myocardial infarction rats)

- Atrial and ventricular cells treated with Methyl-β-cyclodextrin (MβCD)

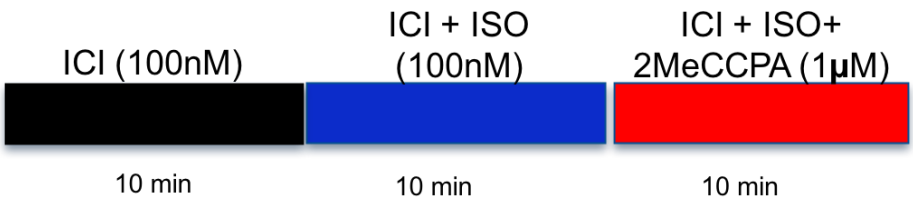

Figure 3.2: Protocol of whole-cell β_1-adrenergic stimulation of rat atrial cardiomyocytes**.**

3.2.7 Effect of cholesterol depletion and consequent caveolar disruption on rat atrial cardiomyocytes AARs responsiveness

Atrial and ventricular cardiomyocytes were incubated for an hour in the presence of 10 mM methyl-β-cyclodextrin (MβCD). MβCD has a high affinity for cholesterol and allows its removal from the cell membrane, causing collapse of the caveolae microdomain. The treated cells were then assed using the protocol described in 3.2.6 section.

3.2.8 Investigation of contractile responsiveness of cardiomyocytes to A_1 adenosine receptors stimulation

In the following protocol, we aimed to investigate the direct effect of A_1ARs activation (without any beta-adrenergic stimulation). For this purpose, the baseline was recorded for 10 minutes, as in the previous protocol, but this time no β-adrenergic receptors specific blocker was added in the solution. After this step, 2-MeCCPA (1 μM) was added to see if the effect of A_1ARs

was also present without a previous β_1-adrenergic stimulation (Figure 3.3)

Figure3.3: Protocol of whole-cell A1 adenosine receptors stimulation

3.2.9 Statistical analysis

Cell contractility was analyzed by initially testing baseline, treatment 1 with Isoproterenol and treatment 2 with A_1ARs agonist for each cell type with an unpaired t-test. Subsequently, fold increase or fold decrease between cell types were analyzed with an unpaired Mann-Whitney test (Non-Gaussian data) or unpaired t-test.

3.3 Results

3.3.1 A_1 adenosine receptor agonist shows anti-adrenergic effect in healthy atrial cardiomyocytes

In order to assess the effect of A_1AR agonist after β_1ARs stimulation we measured cell shortening of atrial cardiomyocytes with the use of IonOptix microscope technique. Figure 3.4 shows the cellular shortening of atrial cardiomyocytes isolated from control rats. These control cells show a significant increase in cell shortening following the addition of isoproterenol (68.6 ± 7.5 %, P<0.001) and a significant decrease in shortening (80.0 ± 3.7%, P<0.001) after the application of 2-MeCCPA (A_1ARs agonist).

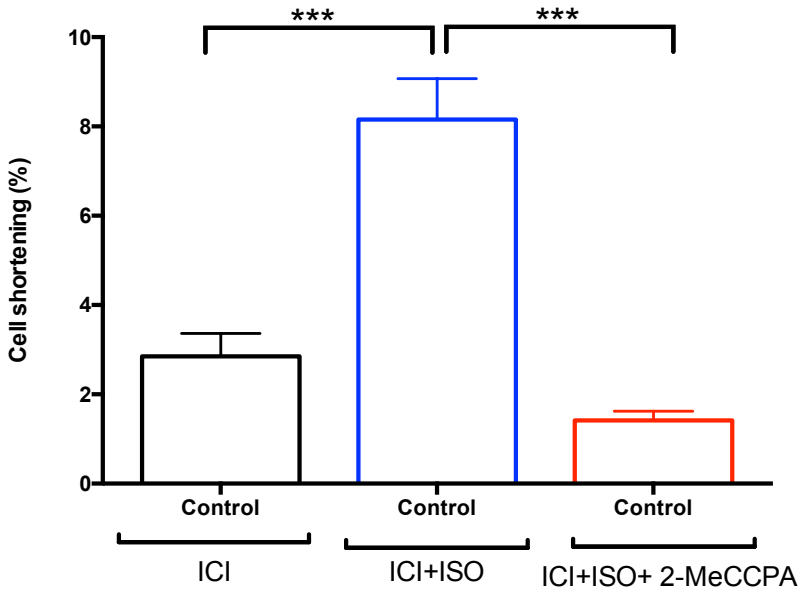

Figure3.4: Rat atrial cardiomyocytes shortening at baseline (ICI) and after selective β_1AR stimulation (ICI 50nM +ISO 1μM) (n=19 f control) as well as after specific stimulation of the A_1ARs (ICI+ISO+2-MeCCPA) (n=8 control) *P<0.05; **P<0.01 ;***P<0.001.

The decrease in cell shortening after A_1AR agonist application is quite in agreement with respect to previous published studies of the adenosine anti-adrenergic effect in atrial tissue.

3.3.2 Heart Failure remodelling leads to a significant reduction of the anti-adrenergic effect of A_1ARs agonist.

The same protocol was repeated for failing atrial cardiomyocytes, isolated from HF-model rats. The reason why we used the same protocol was to compare and to investigate if there were any differences of the anti-adrenergic effect after the application of A_1ARs agonist during HF condition compared to the control one. Data from these experiments show the same trend that we observed in the control rat atrial cardiomyocytes: a significant increase (44.8 ± 6.8 %, P<0.05) in cell shortening following the addition of isoproterenol and a significant decrease (46.07 ± 6.01%, P<0.05) after the application of 2-MeCCPA (Figure 3.5).

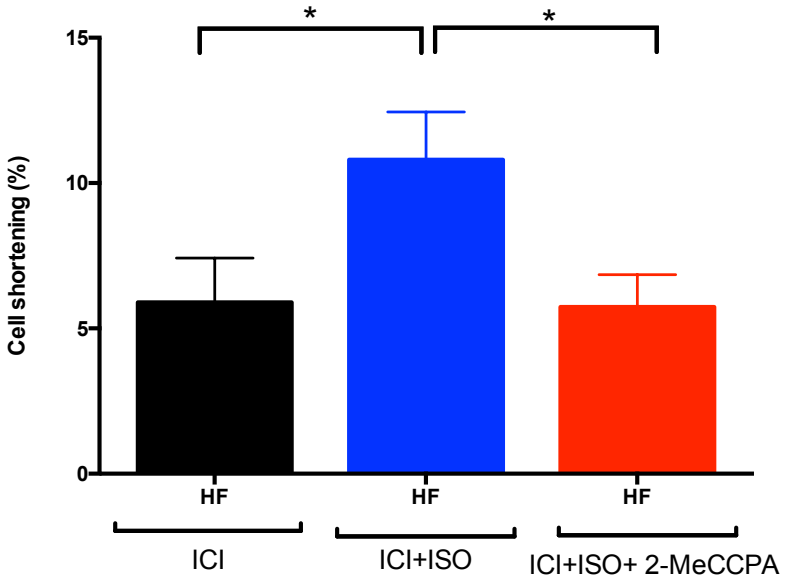

Figure 3.5: Rat atrial cardiomyocyte from MI model: shortening at baseline (ICI) and after selective β_1AR stimulation (ICI 50nM +ISO 1μM) (n=7 HF) as well as after the specific stimulation of the A_1ARs (ICI+ISO+2-MeCCPA) (n=7 HF) *P<0.05; **P<0.01; ***P<0.001.

As evidenced from the results (Figure 3.4 and 3.5), in both control and failing cardiomyocytes, the application of A_1ARs agonist led to a significant effect

on cell shortening, reducing the previous increase obtained from the selective stimulation of β_1ARs. Figure 3.6 a) shows the fold increase after isoproterenol administration in failing atrial cardiomyocytes compared to control cardiomyocytes. The second part of the Figure, 3.6 b) shows the fold decrease after A_1ARs agonist application. We used the parameter fold increase and fold decrease to calculate how much was the increase or decrease after the administration of the specific agonists during failing condition compared to the control. Figure 3.6 shows that both fold increase and decrease are significantly lower in failing atrial cardiomyocytes compared to control cardiomyocytes, while failing cardiomyocytes contract more at the baseline.

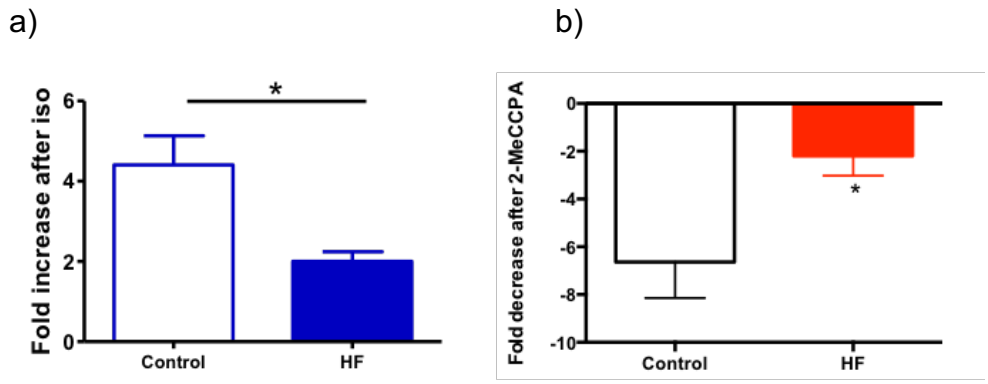

Figure 3.6: Relative change in shortening after selective induction of β_1ARs and A_1ARs. a) fold increase after ISO application and **3.6 b**) fold decrease after 2-MeCCPA administration, comparision between control and failing cardiomyocytes. $P<0.05$.

A_1ARs stimulation does not show any statistical differences in the time that the cells take to reach 50% and 90% of their length (R50), a characterization of cellular relaxation, in both control and failing cardiomyocytes (Figure 3.7 and 3.8 respectively).

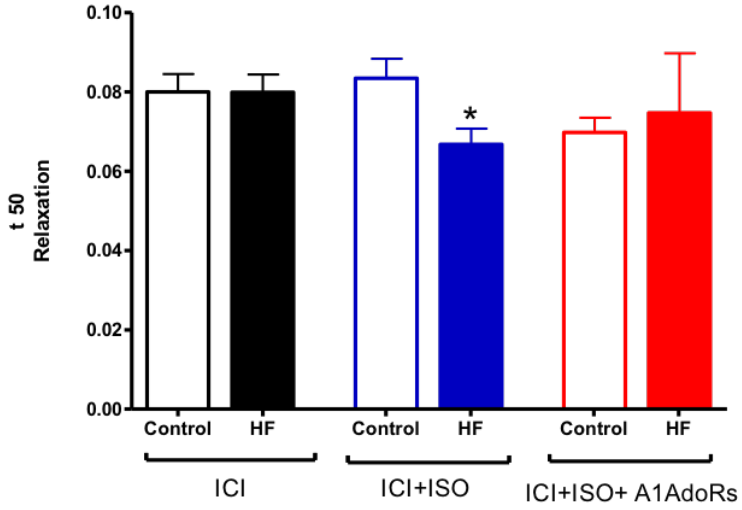

Figure 3.7: Lusitropic response (R50 %) of isolated rat atrial cardiomyocytes induced by β_1AR stimulation (ICI+ ISO) and A1ARs stimulation (2-MeCCPA) in both atrial control and failing cardiomyocytes P<0.05.

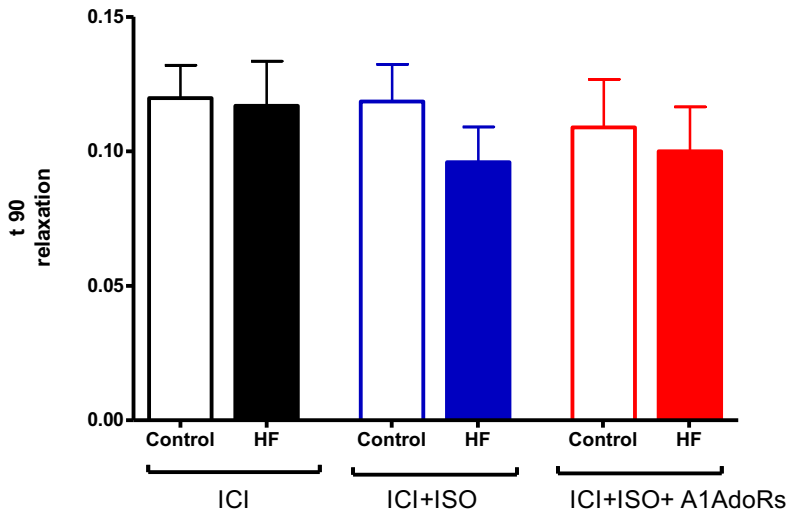

Figure 3.8: Lusitropic response (R90 %) of isolated rat atrial cardiomyocytes induced by β_1ARstimulation (ICI+ ISO) and A1ARs stimulation (2-MeCCPA) in both atrial control and failing cardiomyocytes.

3.3.3 Depletion of cholesterol leads to a significant reduction of the anti-adrenergic effect of A1Rs agonist.

Caveolae are cholesterol containing microdomains which have been shown to play a key role in the localization, compartmentation and control of both βARs and adenosine receptors functionality in cardiomyocytes. The protocol described in section 3.2.7 was employed to assess the A_1AR responses of cholesterol depleted atrial cardiomyocytes. Indeed, atrial cardiomyocytes were incubated for an hour in the presence of MβCD agent to remove the cholesterol from the membrane. After this time the experiment started, with same protocol used in control and failing cardiomyocytes. Significant increase in cell shortening was observed for atrial cardiomyocytes treated with MβCD upon isoproterenol stimulation (65.4 ± 8.07 %, P<0.001) (Figure 3.7). This increase in cell shortening was followed by a significant reduction (69.8 ± 3.7 %, P<0.001) after the stimulation of A_1ARs by 2-MeCCPA, confirming that the anti-adrenergic effect of adenosine was also present in the treated cells (Figure 3.8).

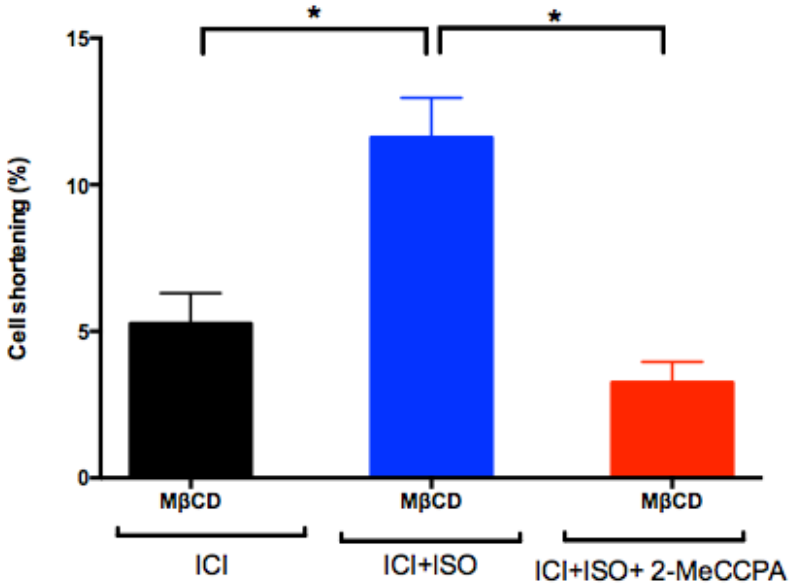

Figure 3.8: Rat atrial cardiomyocyte treated with MβCD: shortening at baseline (ICI) and after selective β_1AR stimulation (ICI 50nM +ISO 1μM) (n=10) as well as after the specific stimulation of the A_1ARs (ICI+ISO+2-MeCCPA). *(n=7 MβCD).* *P<0.05; **P<0.01; ***P<0.001.

We aimed to investigate if there was a difference in the anti-adrenergic effect of A_1ARs agonist between control and treated cells, similar to what we found for the failing atrial cardiomyocytes. We calculated the fold decrease in shortening after application of A_1ARs agonist. We also calculated the fold increase in contraction after the application of isoproterenol, but no significant changes were observed (Figure 3.9 a). Figure 3.9. b shows the comparison of the anti-adrenergic effect given by 2-MeCCPA administration, between control and treated cardiomyocytes. It is possible to observe that the effect given by the selective stimulation of A_1ARs was significantly lower in MβCD treated cells compared to control.

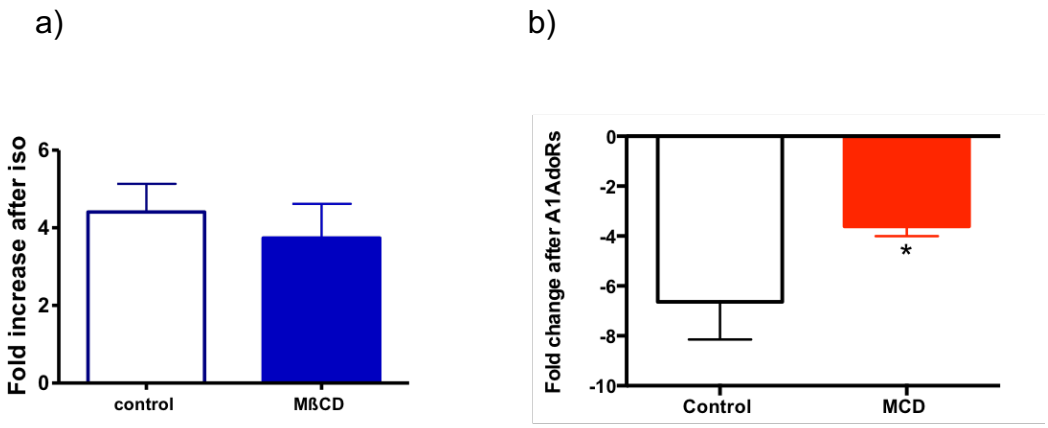

Figure 3.9: Relative change in shortening after selective induction of β1ARs and A1ARs in cholesterol-depleted cells. a) fold increase after isoproterenol application in both control and MβCD treated cells and b) fold decrease after 2-MeCCPA application.

3.3.4 A_1 adenosine receptor agonist does not show any anti-adrenergic effect in ventricular cardiomyocytes, either healthy, failing or cholesterol-depleted.

The cell shortening of ventricular cardiomyocytes was measured to assess the A_1ARs agonist effect after β_1 stimulation, using the same protocol that we used for all different types of rat atrial cardiomyocytes. Figure 3.10 shows the cell shortening after the same protocol we described before (see 3.3.3 section). It is clear that a significant increase after isoproterenol administration is present (66.8 ± 4.1%, P<0.001), but in contrast to what we observed in atrial cardiomyocytes, no significant change in shortening after the application of 2-MeCCPA was recorded (13.8 ± 4.5%, NS).

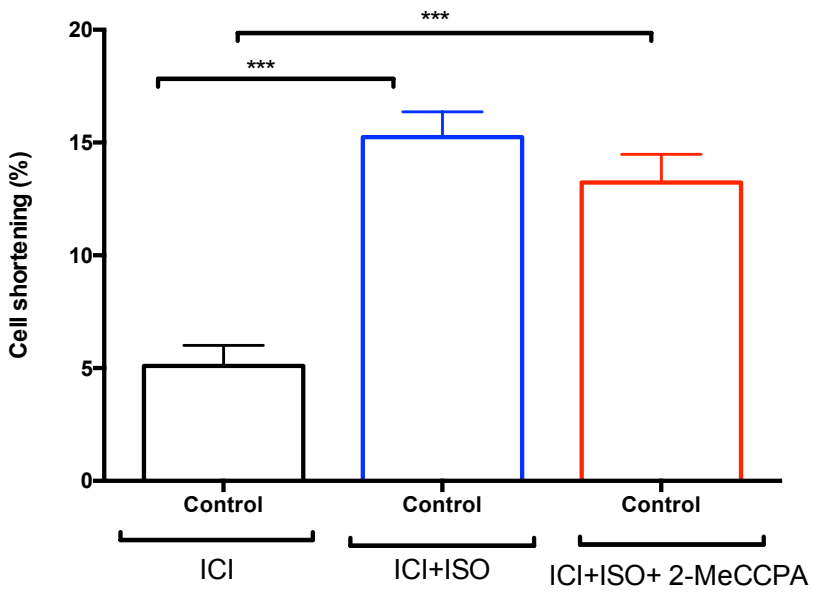

Figure 3.10: Rat ventricular cardiomyocyte shortening at baseline (ICI) and after selective β1AR stimulation (ICI 50nM +ISO 1μM) (n=15 control) as well as after the specific stimulation of the A1ARs (ICI+ISO+2-MeCCPA) (n=11 control). *P<0.05; **P<0.01; ***P<0.001.

For the ventricular cells, despite no significant anti-adrenergic effect was observed, we checked if any change occurred during the HF condition. For this, we repeated the same protocol in isolated left ventricular cardiomyocytes as show in Figure 3.11. We also checked the situation after the cholesterol depletion using metilcyclodestrin incubation for 1 hour (Figure 3.12). As we can see from the Figures 3.11 and 3.12, there was no significant reduction after the application of A_1AR agonist in both groups of cells compared to the control condition (4.9 ± 2.2 %, NS, for failing cardiomyocytes and 4.3 ± 2.1 %)

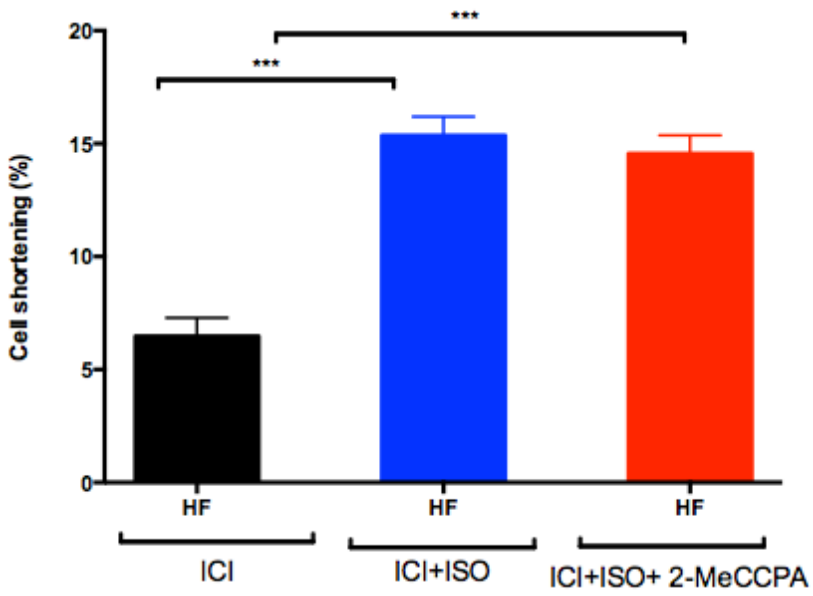

Figure 3.11: Rat venctricular cardiomyocyte from MI model: shortening at baseline (ICI) and after selective β1AR stimulation (ICI 50nM +ISO 1μM) (n=7 HF) as well as after specific stimulation of the A_1ARs (ICI+ISO+2-MeCCPA). *(n=7 HF).* *P<0.05; **P< 0.01; ***P<0.001.

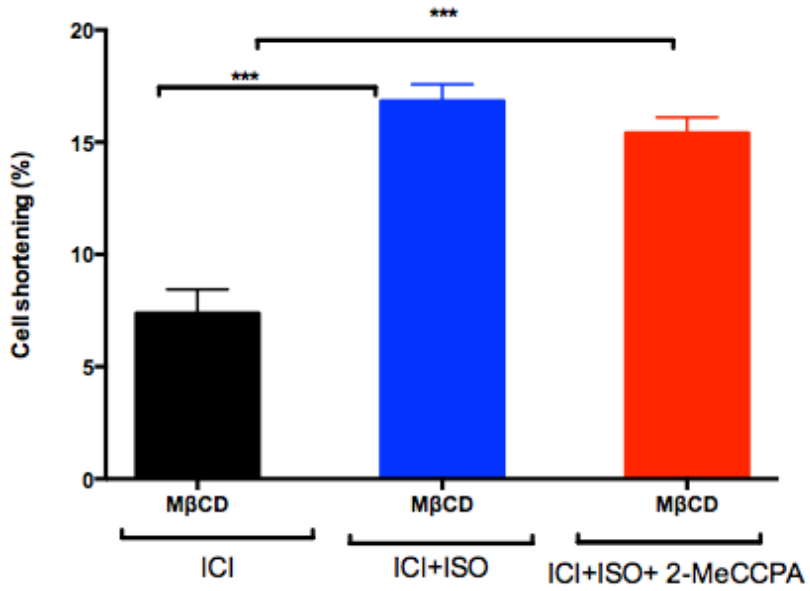

Figure 3.12: Rat ventricular cardiomyocyte treated with MBCD: shortening: baseline (ICI) and after selective β1AR stimulation (ICI 50nM +ISO 1μM) (n=7 HF) as well as after specific stimulation of the A_1ARs (ICI+ISO+2-MeCCPA). *(n=7 MβCD)* *P<0.05; **P<0.01; ***P<0.001.

3.3.5 A1ARs stimulation leads to a direct reduction of contractile responses of rat atrial cardiomyocytes

In light of the previous results, it emerges that the anti-adrenergic effect caused by the A_1AR agonist is clearly present in all type of atrial cardiomyocytes used in our experiments. On the contrary an opposite situation was observed in all type of ventricular cardiomyocytes we tested. After this first part of results, we wanted to investigate if adenosine has any effect in the cardiomyocytes without a previous beta-adrenergic stimulation. To answer to this question we used the protocol describe in section 3.2.7 of materials and methods. Briefly, we recorded 10 minutes of baseline without any β-adrenergic blocking and stimulation, and then we applied A_1AR agonist for 10 minutes. Given that ventricular cells didn't show any anti-adrenergic effect after the administration of A_1AR agonist, for this purpose

we decided to use only atrial cardiomyocytes. In Figure 3.12 cell shortening of atrial control cardiomyocytes is shown. A significant decrease (59.4±6.3 % for control and 33.3±5.4 %), after the application of 2-MeCCPA to elicit A_1ARs response, was observed.

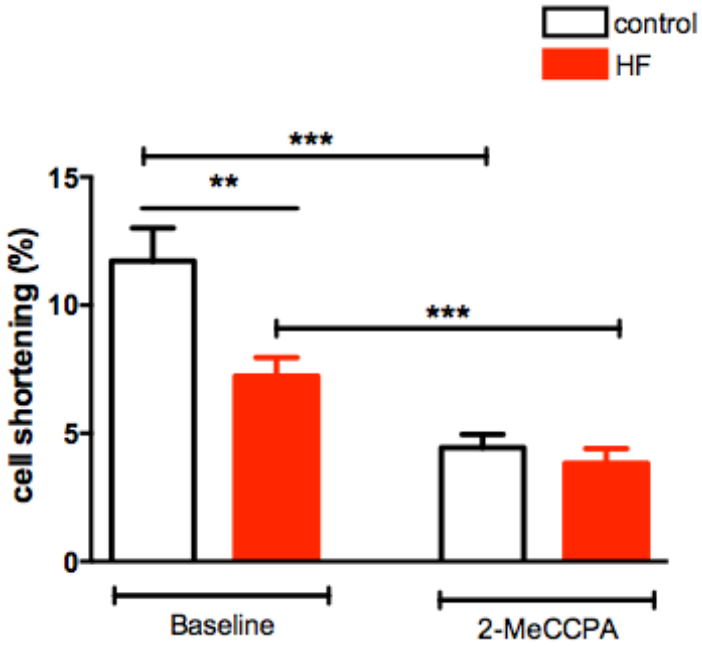

Figure 3.12 Comparison of the shortening of rat atrial cardiomyocyte control and HF cells at baseline and after specific stimulation of the A1Rs (2-MeCCPA). *(n=15 control and n=15 HF)* *P<0.05; **P<0.01; ***P<0.001.

We repeated the same protocol in failing atrial cardiomyocytes to investigate the possible changes occurring during the pathology (Figure 3.12). Figure 3.12 shows that in atrial failing cells the application of 2-MeCCPA also lead to a decrement of baseline contraction (57.9+4.8 %) However, when we calculated the fold decrease after the application of the specific agonist to quantify the effect, we saw the such effect was significantly lower in failing cardiomyocytes compared to control cardiomyocytes 3.13.b).

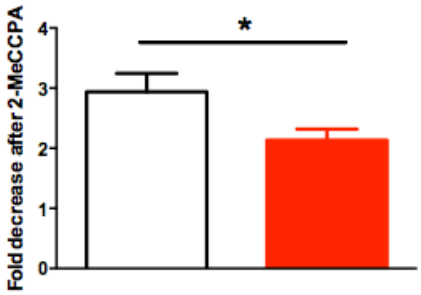

Figure 3.12. Fold decrease after 2-MeCCPA application in control and HF model. *P<0.05

3.5 Key concepts:

- A_1 adenosine receptor agonist shows anti-adrenergic effect in atrial healthy cardiomyocytes.

- While decreased, the anti-adrenergic effect of A_1 adenosine receptor stimulation is present in both atrial failing cardiomyocytes and MβCD treated cardiomyocytes.

- In contrast to atrial myocytes, A_1 adenosine receptor agonist stimulation doesn't show any anti-adrenergic effect in ventricular control, failing and MβCD treated cardiomyocytes.

- A_1 adenosine receptors show a direct inhibition effect, leading to a reduction of cell contraction, in both control and failing atrial cardiomyocytes; in the failing cells this effect is signifacnlty lower.

3.6 Discussion and Conclusions

The aims of this set of experiments was to test the effect of a selective stimulation of A_1 adenosine receptors after β_1-adrenergic stimulation in both atrial and ventricular cardiomyocytes in three different condition: control, HF model and MβCD treated cells.

At cellular level, we observed that A_1AR agonist shows an anti-adrenergic effect in healthy atrial cardiomyocytes (indirect effect) (Figure 3.4). The situation was completely different in the ventricular cardiomyocytes: the anti-adrenergic effect was abolished (Figure 3.9). The anti-adrenergic effect was also not present in all group of ventricular cells we used (control, HF model and MβCD treated cardiomyocytes) (Figure 3.9, Figure 3.10 and Figure 3.11). Our results are consistent with other reports where adenosine does not modify contractile properties of the ventricle muscle in several species such as guinea-pig (Johnson and McKinnon, 1956; Gerlach et al.,1979), cat (Shah et al., 1974), dog (Lammerant and Becsei, 1973) rabbit (Endoh and Yamashita,1980) and rat (Geoffrey et al., 1983). However, adenosine has been shown to have anti-adrenergic effect on ventricular preparation on other studies. Indeed, adenosine shows a depressant effect on the spontaneous rate of ventricular pacemaker cells of the guinea-pig (Szentmiklósi et al., 1980; West et al., 1982). However, in our study no evidence was found for the action of A_1 adenosine receptor agonist on β_1ARs mediated positive inotropic effects in rat ventricular cardiomyocytes. The difference between atrial and ventricular cardiomyocytes could be explained by the greater density of A_1 adenosine receptors in the atrium than in the ventricle. Similar conclusions were drawn from their study by Linden and colleagues. They observed in rat myocardium differences in density level between the two parts of the heart. They reported a density of 30 fmol/mg protein and 23 fmol/mg protein in atria and ventricles, respectively (Linden et al., 1985).

This thesis contributes also to the growing amount of evidence that GPCRs, in particular βARs and adenosine receptors, have distinct microdomains

compartmentation patterns and interaction, not exclusively in ventricular but also in atrial cardiomyocytes. Since we did not see any effect of A_1ARs agonist after β_1ARs stimulation in ventricular cardiomyocytes, we checked if the A_1AR agonist has effect on its own, without previous β-adrenergic stimulation, only in atrial cardiomyocytes. Our results (Figure 12) show that A_1AR agonist produces a direct effect, reducing basal contractility in the absence of β-adrenergic stimulation. This result is also consistent with some studies that showed that adenosine inhibits the basal contraction in the absence of catecholamine in the heart (Rockoff and Dobson, 1980 and Evans et al., 1982). Both direct and indirect effects of A_1AR agonist were observed in atrial cardiomyocytes, in all different experimental groups we used: control, failing and MβCD treated cells. We also observed that the indirect effect of A_1AR agonist was significantly diminished in both failing and MβCD treated cardiomyocytes. Highly localized activation of signaling pathways within the different subcellular microdomains could be a key reason for these differences. Subcellular microdomains are referred to caveolae, invaginations of the plasma membrane enriched in cholesterol, in which the components of various signalling pathways are located, including G-protein. In our caveolae disruption experiments, all cells were incubated with 10mM of MβCD (Kinsonk et al., 1995), causing the collapse of caveolae. Our results in Figure 7 and Figure 8 present that in MβCD treated atrial cardiomyocytes the anti-adrenergic effect of A_1ARs agonist was significantly decreased compared to control conditions. Experiments with MβCD demonstrate that cholesterol plays an active role in the distribution and functionality of both A_1AR and β_1ARs. This result suggests a relationship of the localization of A_1ARs in caveolae microdomain, since when we removed caveolae from the cardiomyocytes, the functionality of the receptors on the inhibition of contraction was significantly reduced.

Similar results were reported by Lasley et al. They found that in ventricular cardiomyocytes, A_1AR receptor is localized in lipid raft/caveolae (Lasley et al., 2000). Later, the observation about this localization between A_1ARs and caveolae, was subsequently reported by two other groups (Cavalli et al.,

2007 and Garg et al., 2009). Even though some observations that cardiac A_1ARs are localized in caveolae structure, the role that this specific localization could play in A_1AR signaling in both atrial and ventricular cardiomyocytes remains unclear. Additionally, using the electron microscopy technique, our group previously reported that atrial cardiomyocytes have three times more caveolae per µm of the cross-section of the membrane, compared to ventricular cardiomyocytes (Glukhov et al., 2015 and Wright et al., 2014).

All of these considerations demonstrate the importance and the complexity of the microdomain specific modulation of signaling at the plasma memnrane. The microdomain-specific distribution of GPCRs in the rat atrial cardiomyocyte that we hypothesize is the following: β_1ARs is suggested to be expressed in both cell crest and T-tubule system, with or without being in close proximity to caveolae; β_2ARs are preferentially expressed in T-tubule system in close proximity with Cav-3 domain; the cell-wide expression of A_1ARs has not been confirmed yet, although its presence in crest caveolae has been reported.

Our results also show that the effect of A_1ARs activity is significantly decreased in HF model atrial cardiomyoctes (figura 3.5). Such situation was found both when the agonist was applied alone under basal conditions (direct effect) and also when it was applied following a selective β_1AR stimulation (indirect effect). However, no studies have addressed subtype-specific adenosine signaling and its regulation in failing cardiomyocytes.

Recently, our group and others have shown that during the development of heart failure after myocardial infarction, a dramatic remodelling of the intracellular T-tubule network occurs in ventricular myocytes. Such remodelling is characterized by T-tubule system disorganization at earlier stages, and the loss of cell surface T-tubular openings in severe chronic HF (Wagner et al., 2012 and Lyon et al., 2009). These conditions may lead to a redistribution of the receptors from membrane areas with T-tubules to areas detubulated. As in ventricular cardiomyocytes, HF causes profound remodeling of the atrial T-tubular system. Our group also demonstrated that

HF leads to a profound degradation of the T-tubule system in atrial cardiomyocytes, decreasing the proportion of structured myocytes and reducing the T-tubule density (Glukhov et al., 2015). Interestingly, Glukhov et al. found similar caveolae density in failing and control cardiomyocytes. This remodeling can potentially lead to some reorganization event of the receptors and the exaggeration of Ca^{2+}-handling abnormalities.

CHAPTER 4 Investigation of influence of β-adrenergic and adenosine stimulation on cAMP signalling in atrial cardiomyocytes in normal heart and during heart failure.

CHAPTER 4 Investigation of influence of β-adrenergic and adenosine stimulation on cAMP signalling in atrial cardiomyocytes in normal heart and during heart failure.

4.1 Introduction

In the previous chapter we assessed the contractile responsiveness to A_1AR agonist following β_1AR stimulation. In atrial cardiomyocytes, the stimulation of A_1ARs leads to both direct and indirect effects. In contrast, no effect was observed in ventricular cardiomyocytes. Additionally, the A_1AR agonist effect statistically diminished in atrial cardiomyocytes during heart failure and in cardiomyocytes after cholesterol depletion. This may suggest that there is difference between the receptor expression densities and functionality between different conditions.

3′ ,5′ -cyclic adenosine monophosphate (cAMP) is an important second messenger that plays a critical role in the regulation of cardiac function. Stimulation of cardiac contractility by catecholamines and their receptors, in particular βAR and adenosine receptors, leads to generation of cAMP, that acts in distinct subcellular micro-domains (Fischmeister et al., 2006; Zaccolo et al., 2009; Perera and Nikolaev, 2013). In terms of contractility, several cAMP micro-domains exist around calcium handling proteins such as L-type calcium channels, ryanodine receptors and phospholamban which rare important for the regulation of the activity of the cardiac sarcoplasmic reticulum calcium ATPase 2a (Bers, 2002; Lompre et al., 2010). Advent of fluorescence resonance energy transfer (FRET) based biosensors allowed to monitor the level of cAMP in intact cells in real-time (Sprenger and Nikolaev, 2013). Recent development of several biosensors and also making a transgenic mice expressing the cAMP biosensor enabled cAMP measurements in adult ventricular cardiomyocytes. This study

showed spatial differences between β1- and β2-adrenergic-induced cAMP signals (Nikolaev et al., 2006). To determine both position and function of these receptors, in this chapter an alternative approach is used, by combining SICM with measurements of cAMP production by FRET, after local receptor stimulation (see chapter 2-general materials and methods). Utilizing this technique, our group recently showed that there is a clear segregation of the β_1- and β_2ARs location on the plasma membrane of healthy ventricular cardiomyocytes. While the β_1ARs are located throughout the sarcolemma β_2ARs are distributed in the T-tubule openings of cardiomyocytes (Nikolaev et al., 2010). In addition, both T-tubule density and regularity are severely lost or altered during the progression of HF in both ventricular and atrial cardiomyocytes (Glukhov et al., 2015; Wagner et al., 2012; Wei et al., 2012). The micro-domain distribution of GPCRs in atrial cardiomyocytes and their possible remodeling during HF condition has not been investigated before. This chapter aims to study the cellular mechanisms of the anti-adrenergic effect of adenosine by monitoring the cAMP level produced following specific stimulation.

The main objectives of this chapter are:

1. To study the anti-adrenergic effect of adenosine on the whole-cell cAMP level in control EPAC1-TG mice, in both atrial and ventricular cells.

2. To characterize microdomain-specific localization of anti-adrenergic effect of adenosine on cAMP level, in control atrial EPAC1-TG mouse myocytes.

3. To investigate the adenosine A1 receptor stimulation effect on the whole-cell cAMP level in control and HF rat atrial cells.

4. To compare the anti-adrenergic effect of adenosine on whole-cell cAMP level in control and failing atrial cardiomyocytes.

5. To study the possible role played by cholesterol on the microdomain-

specific localization of anti-adrenergic effect of adenosine on cAMP level, with incubation with 10 mM MβCD for 30 minutes at room temperature before experiments.

4.2 Material and methods

4.2.1 Animals

In these experiments male EPAC1-transgenic mice and both male and female Sprague Dawley Rats were used in these experiments.

4.2.2 Atrial and Ventricular cardiomyocytes isolation

Cells were isolated from rats and mice as described in Chapter 2 (General materials and methods). Both left and right atrial appendages were placed all together in falcon tube with enzymes solution (without proteinase and collagenase). Right ventricular tissue was removed and discarded; left ventricular tissue was kept for the experiments.

4.2.3 Solutions

All solutions used during FRET measurement experiments were made in FRET buffer (see general Materials and Methods, chapter 2).
Isopotenerol, ICI118,551, CGP20712A, adenosine, and MBCD were from Sigma Aldrich (Poole, UK), 2-MeCCPA and IBMX were supplied by Tocris (Milan, Italy), M199 culture medium was supplied by Thermo Fisher.

4.2.4 Rat Post-Infarction HF Model

To study the single cardiomyocytes during their progression towards HF a model of chronic MI in adult Sprague-Dawley rats was generated by ligation of the left anterior descending coronary artery. Cardiomyocytes were isolated after sexteen weeks. This model of HF was previously validated (Lyon, et al., 2009) (see section 3.2.3 of Material and methods).

4.2.5 Cardiomyocytes plating and transduction with cAMP FRET biosensors

Cells isolated from atrial and ventricular cardiomyocytes of rat or mouse were plated on to laminin coated coverslips. In the case of rat cardiomyocytes, the cells were cultured for around 48 hours in the M199 (see general Materials and Methods, chapter 2) in the presence of an adenovirus, containing the FRET construct of interest. For the EPAC1-transgenic mice, they were used on the same day of isolation; they were just plated after isolation and used 1 hour later (time needed from the cells to attach to the bottom of the laminin coated coverslips).

4.2.6 Whole cell FRET imaging in cardiomyocytes

Atrial and ventricular EPAC1-TG mice cardiomyocytes were isolated and stored in a LowCa buffer until the beginning of the experiments. Otherwise, transfected rat atrial cells were taken from the plate in the incubator, they washed with FRET buffer and fastened into a coverslip holder. During the FRET experiments one of the protocols described in the next paragraphs was performed.

4.2.6.1 To determine anti-adrenergic effect of adenosine

When the coverslip was taken from the plate in the incubator it was washed with FRET buffer and fastened into a coverslip holder, which was placed onto the stage of an inverted microscope used for FRET measurements. Then cells were incubated with ICI118,551 (ICI, 100 nM) for 10 minutes in static conditions, to block β_2ARs activity. At beginning of the experiments, we recorded a couple of minutes to provide a good and stable baseline (figure 4.1). After this time, isoproterenol was applied to elicit the selective

response of β_1ARs. After the β_1ARs response had reached a plateau, adenosine was applied. After the achievement of a stable response to adenosine application, the inhibitor of the PDE (IBMX) was applied to elicit the total cAMP response.

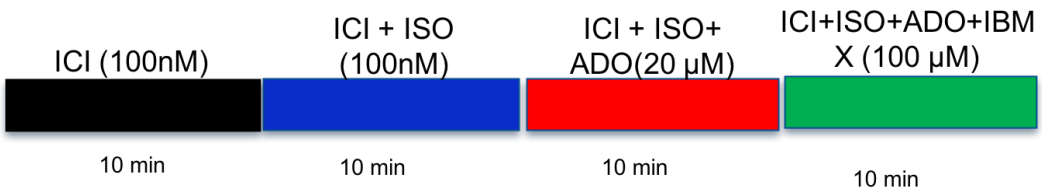

Figure 4.1: Schematic protocol to investigate anti-adrenergic effect of adenosine.

4.2.6.2 To determine selective anti-adrenergic effect of A1 adenosine receptors agonist after β_1 adrenergic stimulation

Similarly to the precedent protocol, a previous incubation with ICI was made (10 minutes) and the baseline was recorded. Then, isoproterenol was applied in the chamber, until the achievement of the plateau. In this protocol, we wanted to check, after the selective stimulation of the β_1AR, the specific anti-adrenergic effect given by A_1AR stimulation. For this purpose, we applied the 2-MeCCPA (A_1AR specific agonist). At the end, we also applied IBMX to elicit total cAMP response.

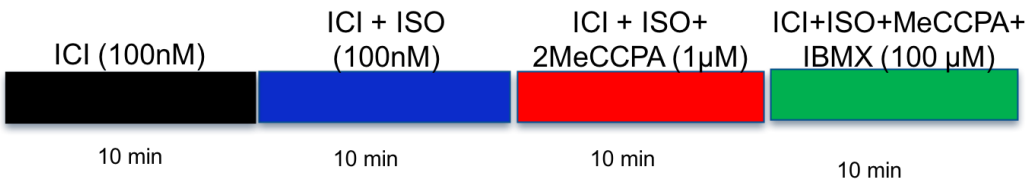

Figure 4.2: Schematic protocol to investigate anti-adrenergic effect of A_1 adenosine receptors agonist

4.2.6.3 To determine anti-adrenergic effect of A_1 adenosine receptors agonist after selective β_2 adrenergic receptors stimulation

In this protocol, we were looking for anti-adrenergic effect of A_1AR after a selective stimulation of β_2ARs. This time, an incubation with CGP (β_1ARs specific blocker) was made for 5 minutes, before starting experiments. At the beginning the baseline with CGP was recorded, after this time, isoproterenol was applied to elicit the selective response of β_2ARs. After the β_2ARs response had reached a plateau, A_1AR agonist was applied. After the achievement of a stable response to 2-MeCCPA application, the inhibitor of the PDE (IBMX) was applied to elicit the total cAMP response.

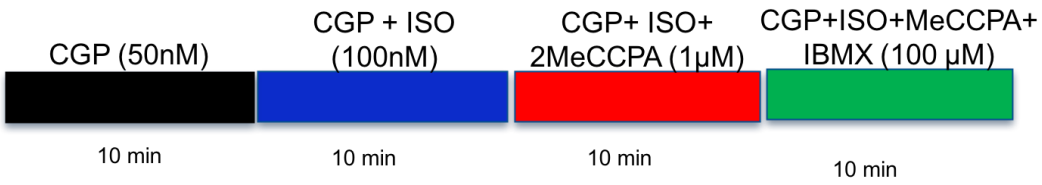

Figure 4.3 Schematic protocol to investigate anti-adrenergic effect of A_1 adenosine receptors agonist after the selective stimulation of β_2ARs.

4.2.6.4 To determine A1 adenosine response on whole-cell cAMP level

In this specific protocol, we wanted to investigate the possible direct effect of A_1AR activity at the cAMP level (without the previous beta-adrenergic stimulation). FRET buffer containing 2-MeCCPA (1 µm) was applied manually through pipette, to provide A_1AR activation. After the achievement of a plateau IBMX was administrated to check the total cAMP response.

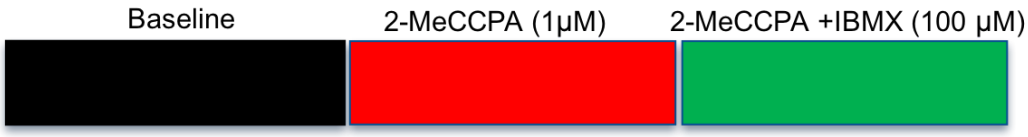

Figure 4.4 Schematic protocol to investigate effect of A_1 adenosine receptors activity

4.2.7 FRET analysis

FRET experiments and the analysis of the resulting FRET data was primarily performed by me. The FRET data was corrected for bleed through of CFP emission into the YFP spectrum and analysed as it was described previously (Nikolaev et al., 2010). Briefly, for the FRET data analysis Micro-Manager 1.4 with custom-written FRET analysis plugin was used. Sequential images were recorded every 5 seconds over the period of experiment for the CFP and the corresponding YFP channel, in each time-lapse image set a region of interest was selected, average pixel intensities for each channel were calculated and then YFP to CFP ratio was calculated and plotted over the recorded time. The obtained raw data was processed with the use of baseline correction functions using Graphpad prism 5.0 and recurring noise was reduced via 3 Median smoothing. For each part of every protocol, the FRET response was calculated by averaging the values of 10 frames, for example for protocol describe in section number 4.2.6.1, we did the average of 10 frames of the baseline signal and 10 frames of the response signal and by subtraction of the averaged response from the averaged baseline.

4.2.8 SICM/FRET with nanopipette agonist application

Atrial cardiomyocytes from the EPAC1-TG mice were scanned with the SICM nano-pipette to provide a 10μm x 10μm topography image of the

selected area of interest. After blocking β_2ARs, by incubation with with ICI118,551 (ICI, 100 nM) in the bath, we repeated the scanning at 5μm x 5μm, a resolution sufficient to elucidate the position of T-tubule openings and area free of T-tubules (crests). At this point using a command from the SICM software, the pipette was moved to coordinates that positioned the pipette 500nm above either a T-tubule opening or a crest area. At this moment of the experiment we started to record the FRET signal, as a baseline like in the whole-cell FRET experiments. Then, β_1ARs were stimulated with the application of the isoproterenol directly in the bath, using the normal pipette. The whole-cell FRET response was recorded with the Micro-Manager program until we see a plateau and a stable response. At this moment, we stimulated the A_1AR locally, via voltage application, by switching the relative electrical potential inside the scanning nano-pipette, containing inside 1 μM of 2-MeCCPA, from positive (+500 mV) to negative (-1,000 mV) value. Having stopped the local application of the 2-MeCCPA, by removing the nano-pipette from the area the FRET images were collected and the FRET ratio was calculated for the regions of interest, which were selected by splitting the cell into different sectors starting with region close to the site of application and the moving in to the direction of perfusion the perfusion, to account for the diffusion of the drug. The signal was analyzed as before by averaging the values of 10 frames for each step of the protocol.

4.3 Results

4.3.1 Influence of adenosine on the β1-AR-stimulated whole-cell cAMP level in EPAC-1 atrial cardiomyocytes.

The aim for this set of experiments was to dissect cellular mechanisms of the anti-adrenergic effect of adenosine. For that purpose we used the protocol described in Figure 4.1 (see section 4.2 Materials and Methods). After the incubation with ICI118,551 (ICI,100 nM) to elicit only β_1AR response, we applied isoproterenol. Figure 4.6 a) shows a representative curve in which we can observe the action of isoproterenol and adenosine on the cAMP level (FRET ratio %). After the application of the isoproterenol there was an increase of the cAMP level, visible in the curve with a reduction of the FRET signal; this because upon cAMP binding and the resulting conformational change, a reduction in FRET signal occurs, which indicates cAMP presence. Adenosine (20 μM) significantly decreased the whole-cell cAMP concentration following β_1AR stimulation (44.5 ± 15.7%). In order to determine what the maximal cAMP response detectable with our sensor, the phosphodiesterase inhibitor IBMX was used and a further decrease (84.1 ± 16.4%) was observed, indicating that β_1AR stimulation did not elicit the maximal cAMP possible response. Figure 4.6 b) represents the percentage change of the calculated FRET ratio averaged for the all the cells recorded with this protocol.

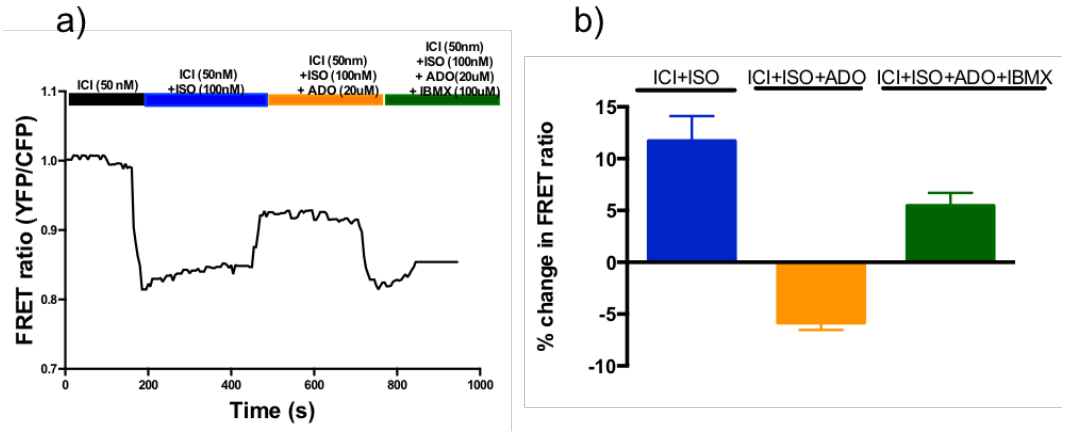

Figure 4.6 Adrenergic and adenosine modulation of the cAMP level (FRET ratio) in atrial cardiomyocytes. a). A representative example of a FRET ratio trace of one cell incubated with the compounds as indicated above the trace; b) Average % change in the FRET ratio following incubation with treatments as indicated in the figure 4.6 a) (N= 7 cells).

4.3.1 Influence of adenosine on the β1-AR-stimulated whole-cell cAMP level in EPAC1 ventricular cardiomyocytes.

The whole-cell cAMP level following adrenergic and adenosine stimulation was investigated also in ventricular cardiomyocytes, using the same protocol as in atrial cardiomyocytes (see Figure 4.1). The ventricular cardiomyocytes were also incubated with ICI (100 nM), to block the activation of the β_2ARs. Figure 4.7 a) shows a significant increase of whole-cell cAMP production after isoproterenol application. As before, adenosine lead to a significant decrease of whole-cell cAMP level following β_1ARs stimulation (39.4 ± 7.8%), however this effect was smaller compared to the atrial cardiomyocytes.

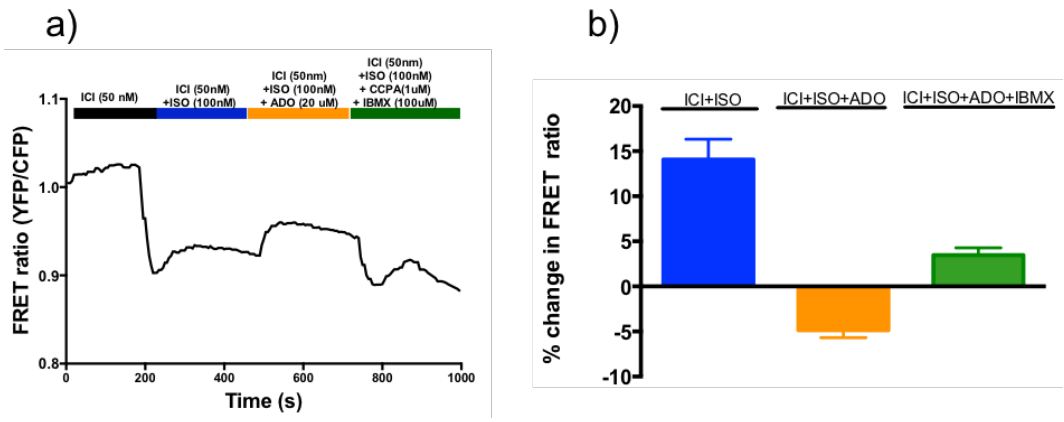

Figure 4.7: Adrenergic and adenosine modulation of the cAMP level (FRET ratio) in ventricular cardiomyocytes. a). A representative example of a FRET ratio trace of one cell incubated with the compounds as indicated above the trace; b) Average % change in the FRET ratio following incubation with treatments as indicated in the figure 4.7 a) (N= 7 cells).

4.3.2 Effect of A_1 Adenosine receptor agonist on whole-cell cAMP level after β1-AR stimulation in EPAC1-TG atrial cardiomyocytes.

After checking the anti-adrenergic effect given by adenosine administration, we focused our attention on the specific anti-adrenergic effect of a selective stimulation of A_1 adenosine receptors subtype. For these experiments, we tested atrial EPAC1-TG cardiomyocytes to a similar protocol we used for checking adenosine activity (Figure 4.1). In this case, we applied directly 2-MeCCPA, a selective agonist of A_1AR, in the bath rather than adenosine. Figure 4.8 shows that the administration of 2-MeCCPA lead to a significant decrease of the whole-cell cAMP level (43.4 ± 7.9%). The response elicited by A_1AR agonist seems to be quite comparable to the response given by adenosine.

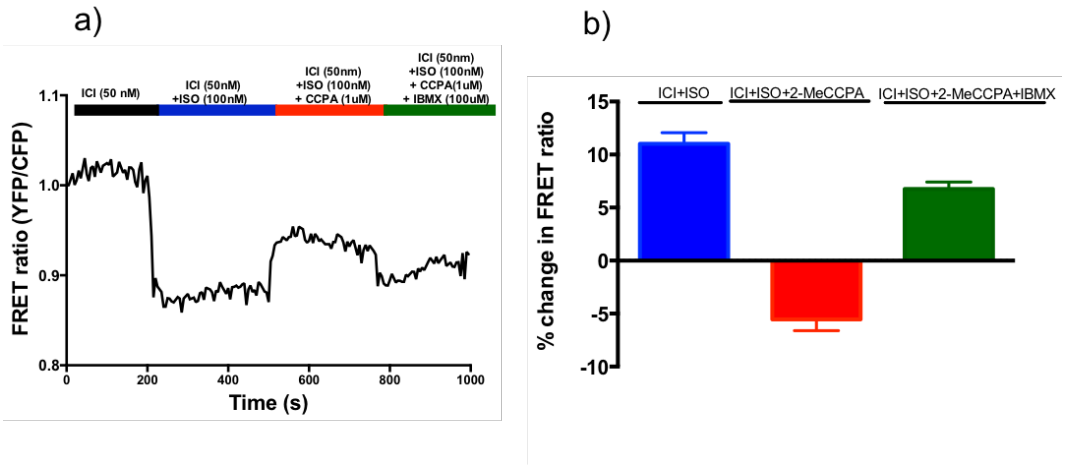

Figure 4.8 Adrenergic and adenosine modulation of the cAMP level (FRET ratio) in atrial cardiomyocytes. a). A representativen example of a FRET ratio trace of one cell incubated with the compounds as indicated above the trace; b) Average % change in the FRET ratio following incubation with treatments as indicated in the figure 4.8 a) N=7 cells.

4.3.2 Effect of A_1 Adenosine receptor agonist on whole-cell cAMP level after β1-AR stimulation in EPAC1-TG ventricular cardiomyocytes.

Ventricular cardiomyocytes were also tested to the same protocol used before (Figure 4.8), to check if there were differences between the anti-adrenergic effect given by adenosine and the other given by a selective stimulation of A_1ARs. In this case, as in atrial cardiomyocytes, the A_1AR agonist shows a similar response to the effect elicited by adenosine, leading to a significant decrease of whole-cell cAMP level (29.4 ± 4.6 %); the antiadrenergic effect in the ventricular cardiomyocytes was much less compared to the results obtained in atrial cardiomyocytes for both stimulations with adenosine and 2-MeCCPA.

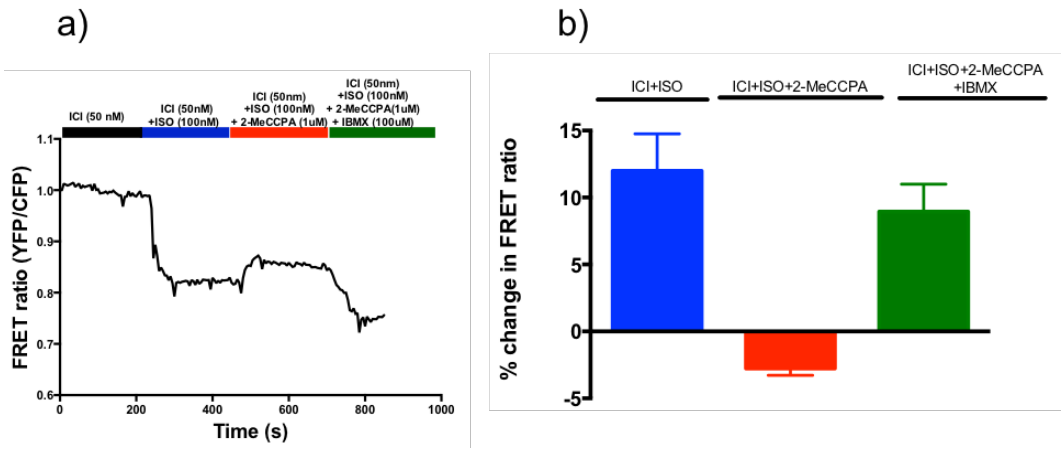

Figure 4.9: Adrenergic and adenosine modulation of the cAMP level (FRET ratio) in ventricular cardiomyocytes. a). A representativen example of a FRET ratio trace of one cell incubated with the compounds as indicated above the trace; b) Average % change in the FRET ratio following incubation with treatments as indicated in the figure 4.9 a) N=6 cells.

4.3.3. Direct effect of A1 adenosine receptor agonist on the whole-cell cAMP level in EPAC1-TG atrial cardiomyocytes.

With the previous results, we demonstrated that A_1AR led to significant response after β1-adrenergic stimulation, a process known as indirect effect. We now aimed to investigate if a selective stimulation of A_1ARs was able to generate a direct effect on the whole-cell cAMP level, without the previous adrenergic stimulation. For this aim, we used the simple FRET protocol described in section 4.2.3.2. Briefly we recorded a stable baseline and then we directly applied 2-MeCCPA in the bath to study the effect of A_1ARs activation. Figure 4.10 a) shows a representative curve in which it is possible to see the reduction of the whole-cell cAMP level after the application of A_1AR agonist (33.1 ± 11.4%). This whole-cell cAMP level reduction is much smaller than if the A_1AR agonist is applied after the previous stimulation of the adrenergic receptors.

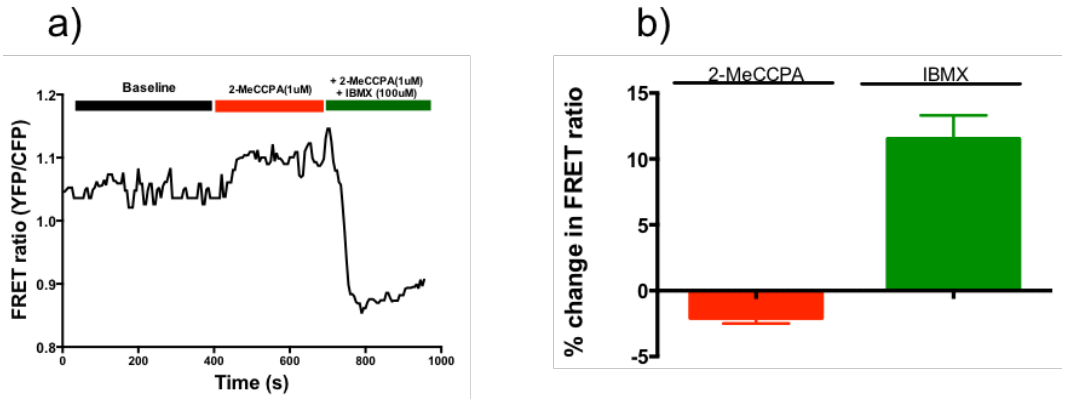

Figure 4.10: A1 adenosine receptor-mediated modulation of the baseline cAMP level (FRET ratio) in atrial cardiomyocytes. a). A representativen example of a FRET ratio trace of one cell incubated with the compounds as indicated above the trace; b) Average % change in the FRET ratio following incubation with treatments as indicated in the figure 4.10 a). N= 7 cells.

4.3.4. Direct effect of A1 adenosine receptor agonist on the whole-cell cAMP level in EPAC1-TG ventricular cardiomyocytes.

We repeated the same protocol used before (Figure 4.10) in ventricular cardiomyocytes. Figure 4.11 shows the direct effect of 2-MePPCA administration without any βARs blocker. This effect was much smaller as compared to that we observed in atrial cells; it was also much lower compared to the effect of A_1AR given after the previous βAR stimulation in ventricular cardiomyocytes.

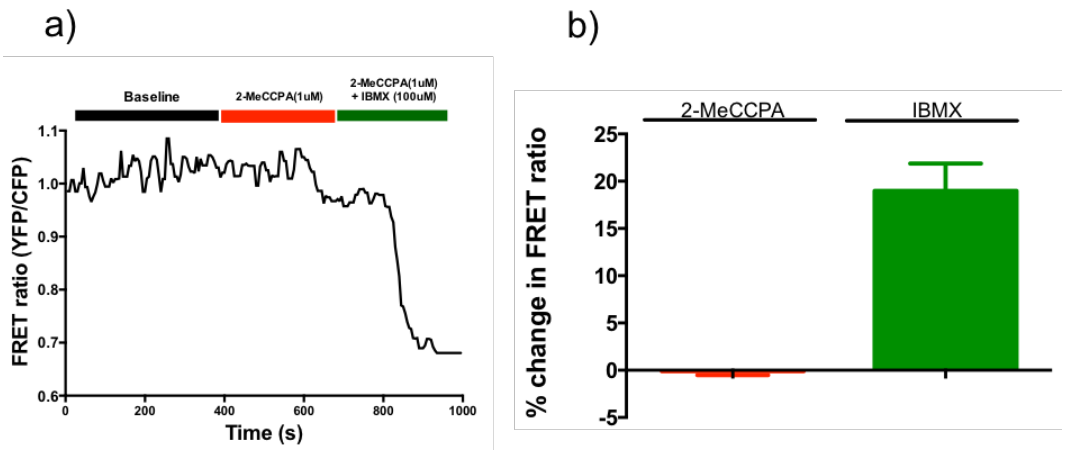

Figure 4.11: A1 adenosine receptor-mediated modulation of the baseline cAMP level (FRET ratio) in atrial cardiomyocytes. a). A representativen example of a FRET ratio trace of one cell incubated with the compounds as indicated above the trace; b) Average % change in the FRET ratio following incubation with treatments as indicated in the figure 4.11 a) N=7 cells.

4.3.5 A_1 adenosine receptor agonist has not effect on cAMP level after β_2ARs stimulation in both atrial and ventricular cells

The next logical experimental step was to investigate the antiadrenergic effect of A_1AR following the selective stimulation β_2ARs (Figure 4.3). Here, we incubated both atrial and ventricular cardiomyocytes with the CGP (specific β_1AR blocker) for 5 minutes. After the incubation, we recorded a stable baseline and then we applied isoproterenol to elicit only the response of β_2ARs. After this step, we applied 2-MeCCPA to elicit the anti-adrenergic effect of A_1ARs. We observed that stimulation of A_1 adenosine receptor agonist has not effect on whole-cell cAMP level after β_2AR stimulation in both atrial and ventricular cardiomyocytes (Figure 4.12 and Figure 4.13).

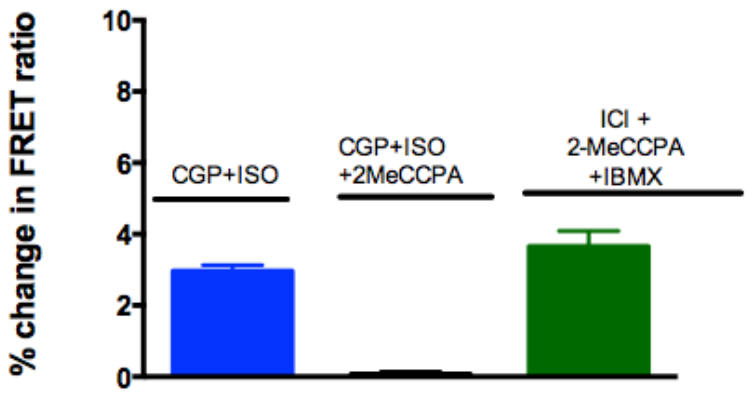

Figure 4.12: Lack of A_1 adenosine receptor-mediated modulation of the baseline cAMP level (FRET ratio) in atrial cardiomyocytes following β_2AR stimulation. a). A representativen example of a FRET ratio trace of one cell incubated with the compounds as indicated above the trace; b) Average % change in the FRET ratio following incubation with treatments as indicated in the figure 4.12 a) N=6 cells

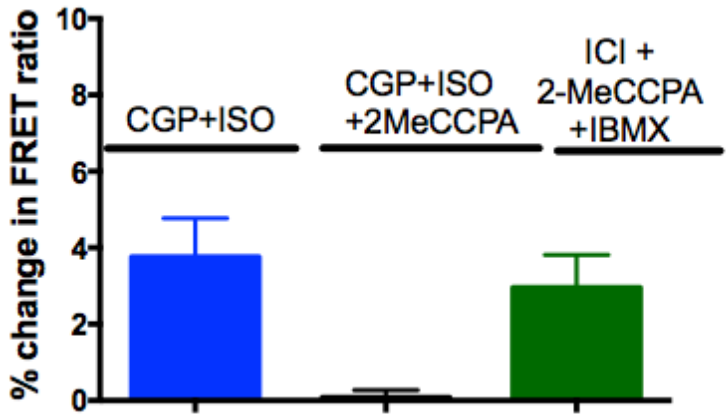

Figure 4.13: Lack of A1 adenosine receptor-mediated modulation of the baseline cAMP level (FRET ratio) in ventricular cardiomyocytes following β_2AR stimulation. a). A representativen example of a FRET ratio trace of one cell incubated with the compounds as indicated above the trace; b) Average % change in the FRET ratio following incubation with treatments as indicated in the figure 4.13 a) N=4 cells.

4.3.6 SICM/FRET microscopy study of atrial cardiomyocytes

Given that the antiadrenergic effect of adenosine at the whole-cell cAMP level was much more pronounced in atrial cardiomyocytes than ventricular, we decided to focus our attention only on the atrial cardiomyocytes for these experiments. SICM was utilized for the visualization of the three-dimensional surface topography of living cells of atrial EPAC1-camps cardiomyocytes. This technique allows resolution of the structural features of cardiomyocytes, such as Z-grooves, cell crests located between them, and T-tubule openings. Once these structures had been resolved both the T-tubular openings and areas without T-tubule openings were investigated to determine both position and function of endogenous β-adrenergic and adenosine receptors, with the use of the SICM nano-pipette for the precise delivery of drugs with the protocol described in section 4.3 of Materials and Methods (chapter 2). FRET ratio was first acquired to record a stable baseline and then isoproterenol was applied manually to the bath solution to elicit a whole-cell cAMP response. Then A_1AR agonist 2-MeCCPA was administered through the nano-pipette used for the scanning, resulting in a local release of 2-MeCCPA, Change in the cAMP level (FRET ratio) was measured in several regions of interest on the cell membranes (equal in size): at the site of the application, behind the area of application, and immediately next to the application zone in the path of the perfusion; multiple regions of interest (ROI) were selected depending on the size of the cell (Figure 4.13 b)). In this way, it was possible to estimate the relative diffusion of cAMP in differing cellular regions. This technique allows an investigation of cAMP signal compartmentation in atrial cardiomyocytes. Figure 4.14 a) shows the response of an area without T-tubule openings; no difference in the cAMP level was observed between an area close the site of the application and an area far from it. On the contrary, in an area full of T-tubule openings the application of the agonist gave rise to a localized cAMP response at the site of applicaton (Figure 4.14 b)), as the FRET ration changed more in the ROI close to the site of application than in the ROI far

from it.

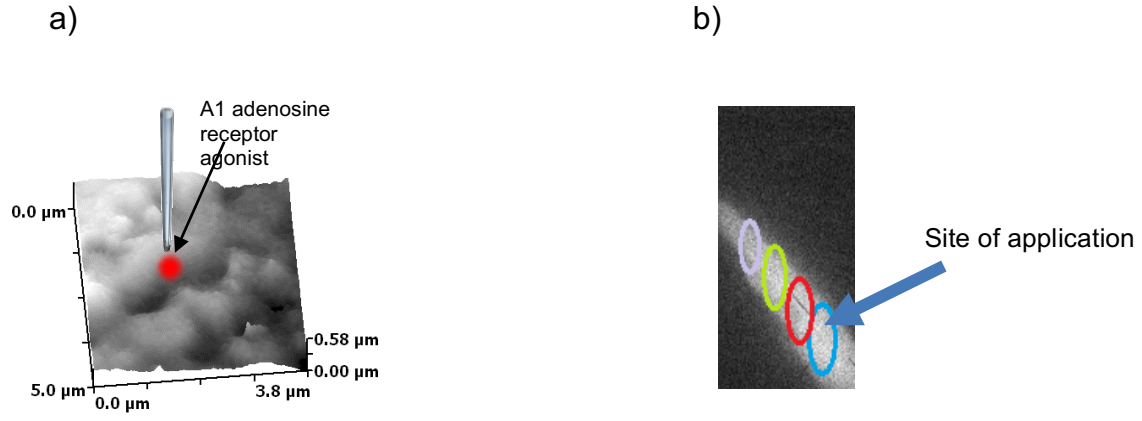

Figure 4.14: SICM/FRET analysis of epac-1 atrial cells. a) Representative 5x5µm.SICM surface scans of an atrial EPAC1-camps cardiomyocyte. b) representative fluorescent image of an EPAC1-camps cardiomyocyte. Regions of interest (colored ovals) situated at various distances from the point of application of the agonist (indicated by an arrow) where FRET was measured after local stimulation of A1ARs following whole-cell stimulation of βARs.

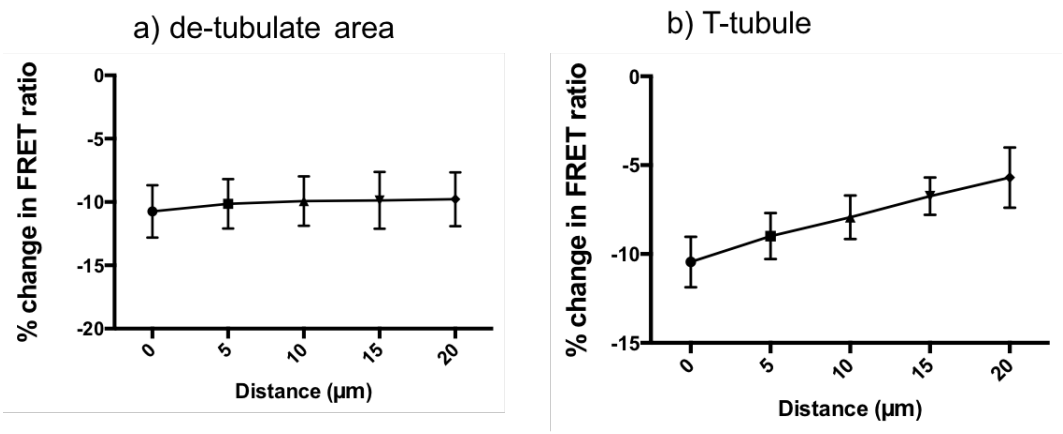

Figure 4.15 Diffusion of cAMP signal (FRET ratio change) in atrial cardiomyocytes in a plasma membrane area devoid of T-tubulesa) and in t-tubule-reach area b) as

function of the distance from the site of the local application of A1AR agonist 2-MePPCA following adrenergic stimulation.

4.3.7 Effect of A1 Adenosine receptors agonist on the FRET change following β1 adrenergic stimulation in rat atrial cardiomyocytes in HF.

One of the aim of this work was to prove that during HF, some remodelling occurs and the functionality of the adenosine and adrenergic receptors is altered. For this purpose, we used cardiomyocytes isolated from the atrial tissue of HF rats rather than from EPAC1-camps transgenic mice. When we decided to use atrial cardiomyocytes from rat atrial tissue, the first obstacle was the cardiomyocytes isolation, because we needed a massive number of cells in order to be able to transfect those with a virus bearing an EPAC2-camps cAMP sensor construct (necessary to visualize the FRET response). After the optimization of the rat atrial isolation protocol (see chapter 2 of the General Materials and Methods), we started trying to transfect the cardiomyocytes. This step was really complicated in atrial cardiomyocytes, due by the fact the initial number of the cardiomyocytes from atria is much less compared to the number obtained with the ventricular isolation. However, after atrial cardiomyocytes isolation we plated and transfected the cells with RII-epac sensor virus. RII-epac sensor is formed by the Epac cAMP binding domain fused to the regulatory subunit of the RII isoform of PKA and then sandwiched betwen CFP and YFP. For this reason, the sensor, once expressed, moves and localizes in the cellular mocro-domains associated with the particulate fraction of cellular PKA (see General Materials and Methods, chapter 2). After several tests, we were able to isolate a good number of rat atrial cardiomyocytes and to transfect them with the RII-epac sensor. The next experimental step was to check if A_1AR stimulation has an effect at the whole-cell cAMP level after β_1 adrenergic stimulation (indirect effect) in these normal rat atrial cardiomyocytes. For

this, we repeated the same protocol that has been used with the EPAC1-camps mouse cardiomyocytes (Figure 4.1). In order to check if a remodeling occured during HF disease, we also tested the same protocol in atrial cardiomyocytes isolated from HF rat model describe previously (see Materials and Methods section 4.2.4). Our results show that the application of 2-MeCCPA in the bath following β_1 adrenergic stimulation, leads to a significant reduction in the whole-cell cAMP level in both control and failing atrial cardiomyocytes (72.67 ±11.1 % for control and 15.1± 6.69% for HF) (Figure 4.16). In addition, this reduction was significantly lower in failing atrial cardiomyocytes compared to the control group (Figure 4.17 b)). In contrast the application of isoproterenol generated similar change in the cAMP level in both control and HF cells (Figure 4.17 a)).

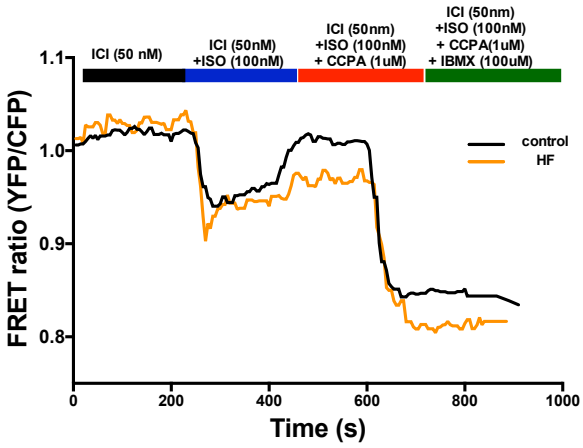

Figure 4.16: Rerpresentative trace of cAMP level (FRET ratio) in rat atrial control (black line) and failing (yellow line) cardiomyocytes following treatments as indicated in the panel above the graph. N= 10 cells for both control and HF groups.

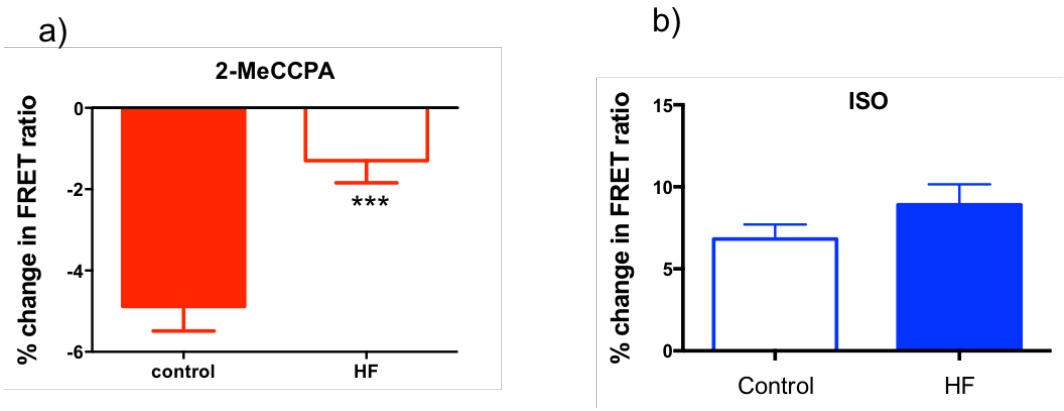

Figure 4.17: Influence of 2-MeCCPA administration (a) and isoproterenol administration (b) on the FRET ratio in normal and failing atrial rat cardiomyocytes.

4.3.8 Anti-adrenergic effect of A1 adenosine receptor agonist on rat atrial cardiomyocytes after cholesterol depletion

In the light of the results we obtained with contraction experiments (see chapter 3), when we proved that caveolae played a role in the localization, compartmentation and control of both β-adrenergic and adenosine receptors in cardiomyocytes, we wanted to test the A_1AR effect on cAMP release following adrenergic stimulation in rat atrial cardiomyocytes after the cholesterol depletion by the agent methyl-β-cyclodextrin (MβCD). As for contraction experiments, rat atrial cardiomyocytes transfected with EPAC2-camps sensor construct were incubated for an hour in the presence of MβCD, dissolved this time in M199 (see chapter 2 for detailed composition). Our results show that both control and cells treated with MβCD lead to a significant reduction of whole cell-cAMP level (21.9± 3.9%). This reduction, as we observed in atrial failing cardiomyocytes, was significantly lower in cells after the cholesterol depletion compared to control cells (Figure 4.18). Figure 4.18 also show that there is no difference in whole-cell cAMP level

production after the application of isoproterenol between control and MβCD treated cells.

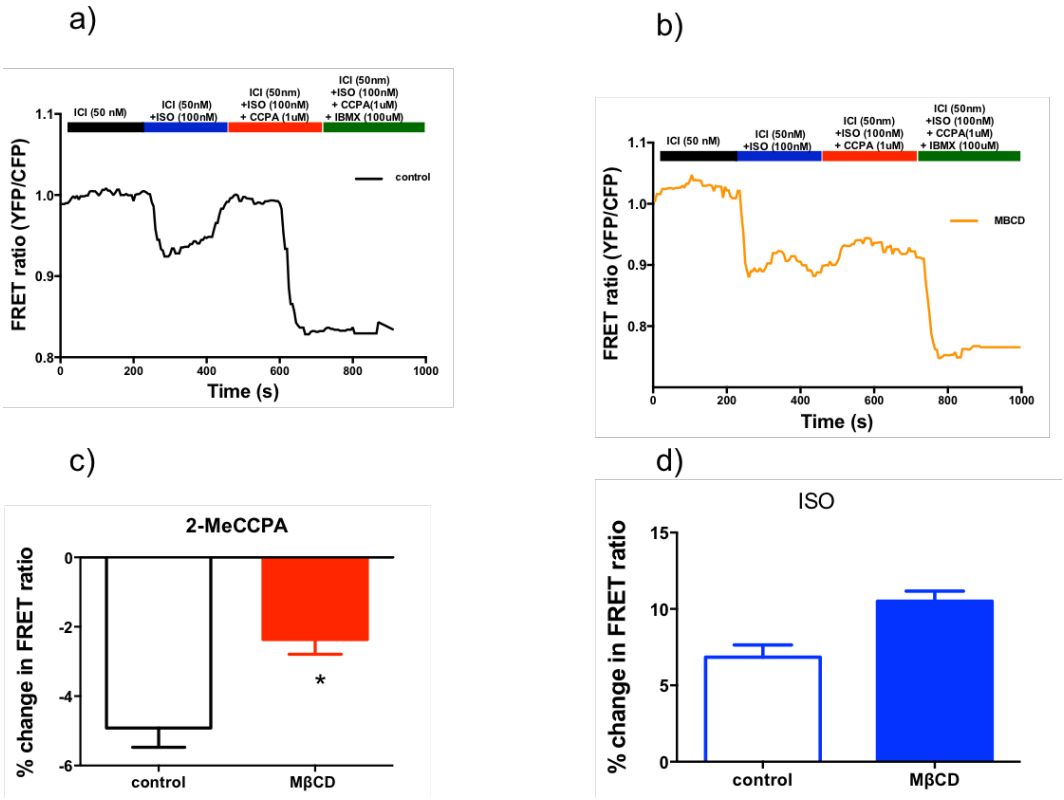

Figure 4. 18: A_1 adenosine receptor-mediated modulation of the cAMP level (FRET ratio) following adrenergic stimulation in rat atrial cardiomyocytes depleted of cholesterol with MβCD. A representative traces of FRET ratio of one cell incubated with the compounds as indicated above the trace for both control (a) and cells treated with MβCD (b); Average % change in the FRET ratio following incubation with A1AR agonist 2-MeCCPA (c) and βAR agonist isoproterenol (d) as indicated in the figure. N=10 cells

4.3.9 Direct effect A1 adenosine receptors on cAMP level in rat atrial cardiomyocytes following cholesterol depletion with MβCD

All of these results demonstrate that A_1AR stimulation leads to anti-adrenergic effect after β_1AR stimulation. Such effect was present in all experimental group we tested (rat atrial cardiomyocytes isolated from control/HF model/ MβCD treated). We also wanted to investigate if a selective stimulation of A_1AR was able to generate a direct effect on whole-cell cAMP level without previous adrenergic stimulation. For this, we used the same protocol tested on atrial cardiomyocytes from the EPAC1-camps transgenic mice (Figure 4.5). In control cells the application of A_1AR agonist lead to a redution of the whole-cell cAMP level (31.7 ± 7.8 %). Similar situation was found in cardiomyoctes treated with MβCD for cholesterol depletion (3.9 ± 1.6 %).

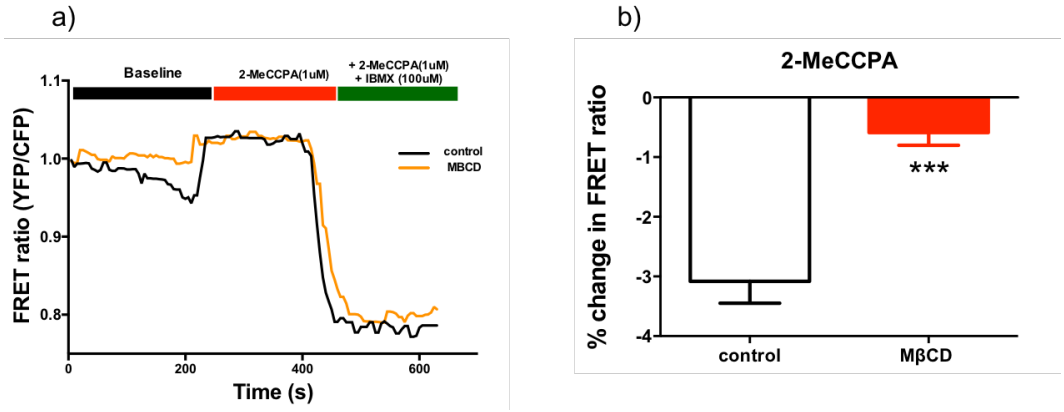

Figure 4. 19: Direct A1 adenosine receptor-mediated modulation of the cAMP level (FRET ratio) in rat atrial cardiomyocytes following cholesterol depletion with MβCD. a). A representative traces of FRET ratio of one cell incubated with the compounds as indicated above the trace; (b) Average % change in the FRET ratio following incubation with A_1AR agonist 2-MeCCPA. N=10 cells

4.4 Key concepts:

- In both mouse and rat atrial cardiomyocytes, both adenosine and A_1AR agonist stimulations have an anti-adrenergic effect on the cAMP production after selective β_1AR stimulation.

- The anti-adrenergic effect of adenosine and A_1AR agonist is present in ventricular cardiomyocytes while it is significantly lower compared to atrial cardiomyocytes.

- The anti-adrenergic effect A_1ARs is significantly lower in both MβCD and failing atrial cardiomyocytes.

- A_1AR does not influence cAMP production after the selective β_2AR stimulation in both atrial and ventricular cardiomyocytes.

- Without βAR pre-stimulation, A_1AR stimulation alone supresses cAMP production in rat control, failing and MβCD treated cardiomyocytes.

4.5 Discussion and Conclusions

The aim of this set of experiments was to dissect the cellular mechanisms of the anti-adrenergic effect of A_1AR agonist and adenosine by measuring cAMP level in both atrial and ventricular cardiomyocytes in three different conditions: control, HF model and MβCD treated cells.

The first part of our experiments was focused on investigating the anti-adrenergic effect after the application of both adenosine and selective A_1 adenosine receptors agonist at the whole-cell cAMP level, in both atrial and ventricular cardiomyocytes. For this experiments we used the EPAC1-camps transgenic mice that show a uniform distribution of the sensor in all cells of the heart. FRET shows a significant anti-adrenergic effect of A_1ARs

agonist 2-MeCCPA in both atrial and ventricular cells. Comparable anti-adrenergic effect was seen after adenosine application in both atrial and ventricular cells (44.5 ± 15.7% for adenosine and 43.4 ± 7.9% for 2-MeCCPA in atrial cells and 39.4 ± 7.8% for adenosine and 29.4 ± 4.6 % for 2-MeCCPA in ventricular cells). The fact that in both atrial and ventricular cardiomyocytes the effect of the two agonists was equivalent suggests that both responses may be mediated by the same A_1 adenosine receptors. In the following studies we focused our attention particularly on this specific subtype of adenosine receptor.

The next logical experiment was to check if there were any differences at the whole-cell cAMP level, between atrial and ventricular cardiomyocytes. For these experiments, we also used EPAC1-camps transgenic mice. Our previous contraction results (see chapter 3) showed that the anti-adrenergic effect of A_1AR agonist is present only in atrial but not in ventricular cardiomyocytes. In contrast, FRET experiments show a decrease of whole-cell cAMP level in both atrial and ventricular cardiomyocytes after the application of A_1AR agonist followed the β1-adrenergic receptors stimulation (43.4 ± 7.9% for 2-MeCCPA in atrial cells and 29.4 ± 4.6 % for 2-MeCCPA in ventricular cells). However, this effect is significantly lower in ventricular cardiomyocytes compared to the atrial cardiomyocytes. Our results are consistent with other reports where perfusion of hearts with 0.1 (μM) isoproterenol increased myocardial cAMP content 2.8-fold, but when perfused with the isoproterenol, 10 μM adenosine reduced the catecholamine-produced increase in cAMP (Dobson, 1983). Linden et al. also showed that the adenosine analogue PIA reduced atrial tissue contractility, cAMP content and adenylate cyclase activity (Linden et al., 1985). However, there are other studies that present different results. Bohm et al. showed that in atrial and ventricular muscle preparations from guinea-pig hearts, the force of contraction was attenuated after adenosine administration. Nevertheless, this effect was much smaller in ventricular muscle compared to the atrial muscle. They also investigated the cAMP content after the application of isoproterenol and adenosine. In both

preparations the isoprenaline-induced increase in cAMP content of the intact contracting preparations was not diminished by adenosine (Bohm et al., 1984). However, in these experiments the authors used the radioimmunoassay to measure the cAMP level. In contrast to traditional biochemical antibody-based techniques such as radioimmunoassay, which measure total cyclic nucleotide concentrations, including those molecules bound to proteins and sequestered in cells (Brookeret al., 1979 and Williams, 2004), in our experiments we used the FRET technique; FRET is able to report physiologically relevant free intracellular cAMP levels that are present in the cytosol and capable of activating effector proteins. In addition, FRET imaging technique can report rapid changes in cAMP at higher temporal resolution and spatially resolve intracellular signaling at the subcellular level. In this respect, by our results (both contractility and FRET results) we can hypothesize that the activation of A_1 adenosine receptors appears to be a primary pathway for antiadrenergic action of adenosine on cAMP level in both atrial and ventricular myocytes. However, in atria, but not in the ventricles, an additional effect of adenosine on transmembrane ion currents, such as $I_{Ca,L}$ and $I_{K,Ado}$, might be of a greater importance for modulation of cell contraction.

Another aim of this work was to check if the possible receptors remodelling occurs during heart failure conditions in atrial cardiomyocytes. We transfected rat atrial cardiomyocytes with RII-epac sensor. Our results showed that in rat atrial cardiomyocytes, in both control and failing condition, the administration of isoproterenol (100 nM) increased myocardial cAMP content 5.8-fold, but when 1 uM of A1 adenosine receptors agonist was applied into solution, it reduced the catecholamine-produced increase in cAMP level (2-5 fold) (Figure 4.12). Although the course of the response is the same, in the case of the failing cardiomyocytes, it is possible to observe that such effect of A_1AR agonist is significantly lower compared to the condition of control. Such differences in spatial cAMP level and dynamics might result from the differences in localization of these receptor subtypes, in particular with respect to the caveolae micro-domains. In ventricular

cardiomyocytes β_1ARs have been found in both caveolar and non-caveolar membrane fractions, whereas β_2ARs have been shown to exclusively localize in caveolae (Nikolaev et al., 2009). There are studies that report the localization of A_1AR in caveolae microdomains in ventricular cardiomyocytes. To study the possible localization of these recepetors, in relationship with this specific micro-domain, we used transfected atrial cardiomyocytes treated with the MβCD to remove the cholesterol. Our results suggest that A_1AR stimulation leads to a reduction of the whole-cell cAMP level in both control and treated cells. We reported this trend for both direct effect, while applying 2-MeCCPA directly in the bath, or indirect effect, while applying 2-MeCCPA following the previous β_1AR stimulation. (Figure 4.5 and Figure 4.6). Despite that the trend was similar, the effect of 2-MeCCPA in the cells treated with MβCD was significantly diminished compared to control. Our data shows that there is a reduction of the effect of this particular adenosine receptors for both failing and treated cardiomyocytes, suggesting a possible localization between caveolae micro-domain and A_1AR and also a possible remodelling of this micro-domain during heart failure condition. Our results are consistent with the increasing evidence that caveolae play a key role in compartmentalization of the receptors and second messengers in close proximity with the plasma membrane. Several studies show that some GPCRs are able to redistribute to caveolae after the binding with the specific agonist. In addition, Lasley et al., reported that adenosine A1 receptors translocate out to caveolae in the presence of agonist 2-chlorocyclopentyladenosine (CCPA) in ventricular cardiomyocytes (Lasley et al., 1999). The authors showed that the incubation with the adenosine A1 receptor agonist CCPA induced the rapid translocation of the receptors from caveolae into non-caveolae micro-domain. This effect was blocked with the application of the adenosine A1 receptor antagonist, 8-cyclopentyl-1,3-dipropylxanthine. Another report (Yang et al., 2009) demonstrated a colocalization of caveolin 3 and the PKCε or PKCδ isoforms at the cell peripheral region and T-tubular like structures in response to adenosine A1 receptor activation. Their results

suggest the idea that adenosine A1 receptors promote the selective translocation of PKCε and PKCδ to the caveolin-3 plasma membrane microdomains in cardiac myocytes. The authors also demonstrated that the activation of A1ARs promotes the translocation to caveola microdomail only for PKCε and PKCδ but not PKCα, PKCβ and PKCζ isoforms.

CHAPTER 5 Molecular investigation of β-adrenergic and andosine receptors.

5. Molecular investigation of β-adrenergic and andosine receptors.

5.1 Introduction

β-adrenergic and adenosine receptors are critical regulators of cardiac function in both normal and pathophysiological conditions. Under normal conditions, β-ARs modulate both the heart rate and the force of contraction and relaxation of the heart, allowing the appropriate response of the individuals to physiological stress or exercise. However, in chronic heart failure, sustained activation of the βARs signaling could have negative consequences (Port and Bristow, 2001; Vatner et al., 1985). Indeed, numerous clinical trials demonstrate the usefulness of beta-blocker therapy in chronic congestive heart failure patients (Barrese and Taglialatela, 2013). The beneficial effects of adenosine receptors are well known and render them an attractive target for clinical manipulations. At the same time, their function could be modified during disease pathology, contributing to the potential disease pathogenesis. Indeed, adenosine receptors may play a crucial role in several diseases such as cardiac hypertrophy, arrhythmogenesis and heart failure. Several studies show a relationship between adenosine handling and the remodelling of adenosine receptors and heart failure (Headrick et al., 2013; Funakoshi et al., 2007 and Funaya et al., 1997). In cardiovascular disease including hypertension and heart failure, plasma adenosine levels are elevated possibly to serve as an endogenous antimyocardial remodeling factor. (Gan et al., 2004 and Ohnishi et al., 1988). Adenosine levels have been reported to be increased in patients with heart failure (Funaya et al., 1997). In rats with hypertrophy, the adenosine uptake blocker dipyridamole reduced the abnormal left ventricular filling and preserved adrenergic responsiveness in pressure overload-induced hypertrophy (Chung et al., 1998). However, whether the possible changes occurred during HF conditions reflect the molecular mechanistic involvement remain unclear.

To investigate the possible reasons for the reduced activity of A_1 adenosine receptors during heart failure, we extracted the mRNA and proteins from both rat atrial control and failing tissues to perform the qRT-PCR and the western blot. We decided to focus our attention only in atrial tissue, since we did not see a significant effect of adenosine A_1 receptors in ventricular cardiomyocytes on both the contractility and the cAMP level. This difference between atrial and ventricular tissue could be explained by the greater density of A_1 adenosine receptors in the atrium, as reported by Linded J et al (Linded et al., 1985). Indeed, they observed in rat myocardium differences in density between the two parts of the heart, reporting a density of 30 fmol/mg protein and 23 fmol/mg protein in atria and ventricles, respectively (Linded et al., 1985).

In this thesis we investigated the mRNA expression and the protein levels of both adrenergic and adenosine receptors. In addition, since we found a relationship between the function of the adenosine receptors and the presence of the caveolae domains, we also studied cav3 expression.

This chapter aims to explore the molecular mechanisms of the anti-adrenergic effect of adenosine and its possible remodelling occurring during failing conditions.

The main objectives of this chapter are:

1. To characterise molecular remodelling occurring in rat atrial tissue model of HF of both adrenergic and adenosine receptors

2. To explore the possible remodelling of cav3 expression, occurring during failing conditions.

5.2 Materials and methods:

5.2.1 Animals

In these experiments both male and female Sprague Dawley Rats were used (8-10 weeks old, weight ~250 g).

5.2.2 Rat atrial tissue storing

Left and right atria were placed either together or separately in eppendorf tubes immediately after the excision of the heart. Then the tissues were snap-frozen in liquid nitrogen and kept in -80°C.

5.2.3 Rat Post-Infarction HF Model

To study heart function during HF conditions a model of chronic myocardial infarction in adult Sprague-Dawley rats was generated. The rat model of HF was generated by ligation of the left anterior descending coronary artery. Cardiomyocytes were isolated after sixteen weeks post-MI. This model of heart failure was validated from our group on 2009 (Lyon et al., 2009). (see Chapter3 for more details).

5.2.4 Solutions

All solutions used during real-time PCR and western blot experiments are:
ß-mercaptoethanol (Sigma-Aldirich #63689)
Proteinase K (Quiagen #19131)
peqGOLD total RNA kit (Peqlab #12-6634)
peqGOLD total DNAse digestion kit (Peqlab #12-1091)

RIPA Buffer composition: 150mM NaCl, 10mM TrisHCl pH7.2 0.1%, SDS 1%, Triton X-100, 5mM EDTA, 100uM Sodium Orthovanadate, 10mM P-nitrophenylphosphate,1 µl Dnase.

5.2.5 Total RNA extraction and quantification

Each sample was placed in an Eppendorf tube containing 1 stainell-steel bead, 400 µl of lysis buffer form the peqGOLD total RNA kit and 4 µl of ß-mercaptoethanol (10 µl of ß-mercaptoethanol per 1 ml of lysis buffer). Samples were disrupted for 2 minutes at 50Hz frequency in the TissueLyser II (Qiagen), and then were transfered in a new Eppendorf tube, adding 590 µl of RNAse- free water and 10 µl of proteinase K. This mixture was incubated and shacked for 10 minutes at the temperature of 55°C. The resulting solution was transfer into the green column of the kit and the procedure was made according to manufacturer's instruction.

At the end of the extraction procedure, 30µl of RNase-free water was used for RNA elution. Subsequently the RNA concentration was determined using a Thermo Scientific NanoDrop 1000 spectrophotometer. The purity of RNA was quantified with Nanodrop and the A260/A280 absorbance ratio = 2.00±0.10 represented an acceptable purity.

PCR analysis was performed using SYBR Green JumpStart taq ReadyMix (Sigma) in an Eppendorf Mastercycle EP Realplex machine (Mauritz et al., 2008). SYBR-Green is a dye able to emits bright fluorescence when it is bound to the DNA amplified from the corresponding cDNA template. The fluorescence emission is related to the amount of starting cDNA material in the reaction. With this method the cycle threshold (Ct) value was measured; this value is representative of the number of PCR cycles required to be able to generate fluorescence with enough intensity that it reaches the threshold within the linear phase of the reaction. Ct value is correlated to the starting quantity of target mRNA.

For each sample relative expression levels were calculated after normalization against the housekeeping gene, that was validated to ensure

that the different groups had similar gene expression values. Relative mRNA expression levels were analysed using comparative Ct methods (the 2-ΔΔCt method) with a normalization to the housekeeping gene Rpl32 (Table 1).

Table I. Oligonucleotides used for real-time PCR for rats genes

Target gene		Primer sequence
β_1*AR* (**NM_012701.1**)	Fw	5´- CTGGACTTCGGTAGACGTGC -3´
	Rv	5´- CACTTGGGGTCGTTGTAGCA -3´
β_2*AR* (**NM_012492.2**)	Fw	5´- TGGTGCGAGTTCTGGACTTC -3´
	Rv	5´- TAAGGCCCGACACAATCCAC -3´
A_1*AR* (**NM_017155.2**)	Fw	5´- GAGCTGAAGATCGCCAAGTCG-3´
	Rv	5´- TGGGAGGTCTTCATCGATGGG-3´
A_{2a}*AR* (**NM_001357942.1**)	Fw	5´- CCATGCTGGGCTGGAACA -3´
	Rv	5´- GAAGGGGCAGTAACACGAACG -3´
A_3*AR* (**NM_001302755.1**)	Fw	5´- TCTTCACCCACGCTTCCATC -3´
	Rv	5´- GGTCAGTCCCACCAGAAAGG -3´
Rpl32 (**NM_013226.2**)	Fw	5´- TCTGGTCCACAATGTCAAGG-3´
	Rv	5´- TGTGCTGCTCTTTCTACGATG-3´

5.2.7 Protein extraction and quantification

The tissue (around 30 mg) was cut in small pieces and placed in an Eppendorf tube containing RIPA buffer, protease inhibitor and DTT (around 500 ul for each samples). The tissue was disrupted for 3 minutes at 50Hz using the TissueLyser II (Qiagen). After the disruption, the sample was transfer in a new tube, placed on ice and shacked for 15 minutes. Later was centrifuge at 14000 g for 15 minutes, the resulting pellet was discarded and the supernatant was kept for the quantification of the protein. A volume between 2-5 µl was kept for the quantification and the rest of the supernatant was stored at -80°C for the future western blot analysis. The quantification of the proteins levels was made using BioRad DCk+ kit. Serial dilutions of a bovine serum albumin (BSA) protein standardwere prepared

in several tubes and used to calibrate with dilutions of 1 µl tissue lysates in 9 µl ddH2O. Standards and samples were placed into a 96 well plate in duplicate along with 25 µl of solution A+S and 200 µl of working solutions B given by the kit, then the plate was incubated for 30 minutes at room temperature. The absorbance at 550 nm was read in a plate reader (ChemiDoc XRS+, BioRad).

5.2.8 Western blot protocol

5.2.8.1 Polyacrylamide gel and protein transfer

After the quantification, the results given by the protein assay, were used to calculate the volumes of sample for loading to have 40 µg of protein for tissue lysates. Loading buffer was used to prepare the sample that was then heated at the temperature of 95°C for 5 minutes, centrifuged and finally loaded onto 14-18% polyacrylamide gel and run at 120 V for approximately 2 hours. The protein ladder (Thermo Fisher #26620) was loaded into the first lane to have an indication about the molecular weight of our molecular protein of interest. After the run finished the proteins were transferred to nitrocellulose membranes (Pall Corporation) using the Trans-Blot Turbo Transfer System (Bio-rad Laboratories, UK) at for 10 minutes. When this process was finished to check the real transfer of the protein to the nitrocellulose membranes, they were stained with Ponceau S solution (Sigma Aldirich # P7170). This step was also important to check the equal loading of transfer proteins. The membranes were then washed with phosphate-buffered saline (PBS) and Tween 0.1% for 10 minutes (this step was repeated 3 times) (Granata et al., 2014).

5.2.8.2 Membrane incubation and Development

After the transfer, the nitrocellulose membrane was blocked in 5% of milk dissolved in PBS-Tween for 1 hour. Then the membrane was incubated with primary antibody solution (Table 2) at the temperature of 4°C overnight. The day after the membrane was washed in PBS-Tween for 10 minutes; this process was repeated 3 times. When the washing process was done, the membrane was incubated with the appropriate secondary antibody (Table 2) for 1 hour. After 1 hour of incubation, the membrane was washed again for 3 times, 10 minutes each in PBS-Tween, then the membrane was covered with ECL Western blotting detection solution (BioRad). The membrane was develop using the ChemiDoc XRS+ Imaging System (Bio Rad).

Table 2: antibody used for western blot

Primary antibody (dilution)	**Secondary antibody (dilution)**	**Catalog number**	**Source**
A1 adenosine receptor (1:200)	Goat anti rabbit (1:10000)	#AAR-006	Alomone Lab
Cav3 (1:1000)	Goat anti-mouse(1:10000)	#610421	BD
GAPDH (1:1000)	Goat anti rabbit (1:1000)	#2118	Cell signalling

5.2.9 Statistical analysis

Data obtained from these experiments were expressed as mean ± standard error of the mean (SEM). All statistical analysis was performed using Excel and Graphpad prism 6.0 software. The statistical differences of measurements made between two groups were analysed using a paired T-test, whereas multiple comparisons between groups were analysed using a

one-way or two ways analysis of variance (ANOVA). A P value of less than 0.05 was considered statistically significant.

5.3 Results

5.3.1 Messenger RNA expression profiles of adrenergic and adenosine receptors: no differences between control and failing conditions

To clearly understand the possible reasons for the reduction of the adenosine effect in both basal condition and after the previous β_1-adrenergic stimulation in failing cardiomyocytes, we wanted to investigate mRNA expression level of both β-adrenergic and adenosine receptors, in control and failing conditions by qRT-PCR. In this set of experiments, we extracted the mRNA from atrial tissue of both healthy and heart failure model rats. We did not separate the right atrium from the left but as we extracted the mRNA from both parts separately we mixed them together for qRT-PCR analysis. Figures 5.1 a) and b) show the mRNA expression profile for the β_1 and β_2-adrenergic receptors, respectively. No statistical significance was recorded between the levels of mRNA expression of β-adrenergic receptors in control and failing conditions. The same situation was observed in the mRNA expression profile for A_1, A_{2a} and A_3 adenosine receptors. Figure 5.2 shows the comparison between all adenosine receptor subtype expression in both control and failing conditions; as before no statistical significance was recorded.

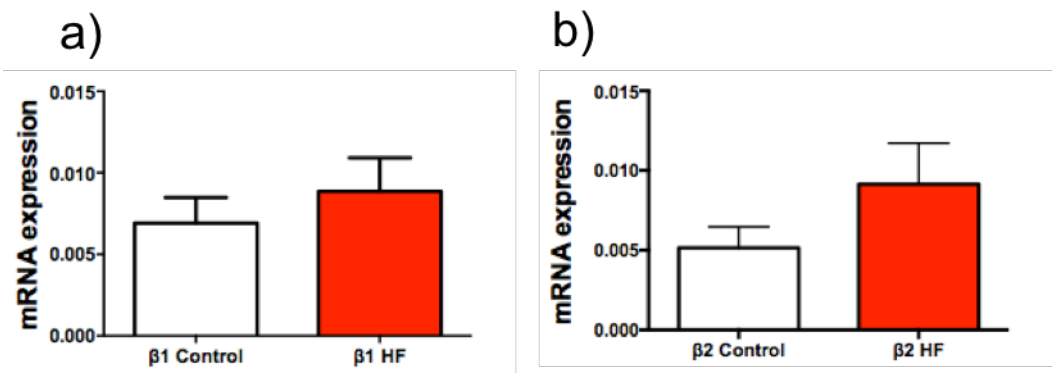

Figure 5.1: Relative quantification of mRNA expression of β_1ARs and β_2ARs in normal and failing rat hearts. Control rats n=4, Myocardial infarction rats n= 6.

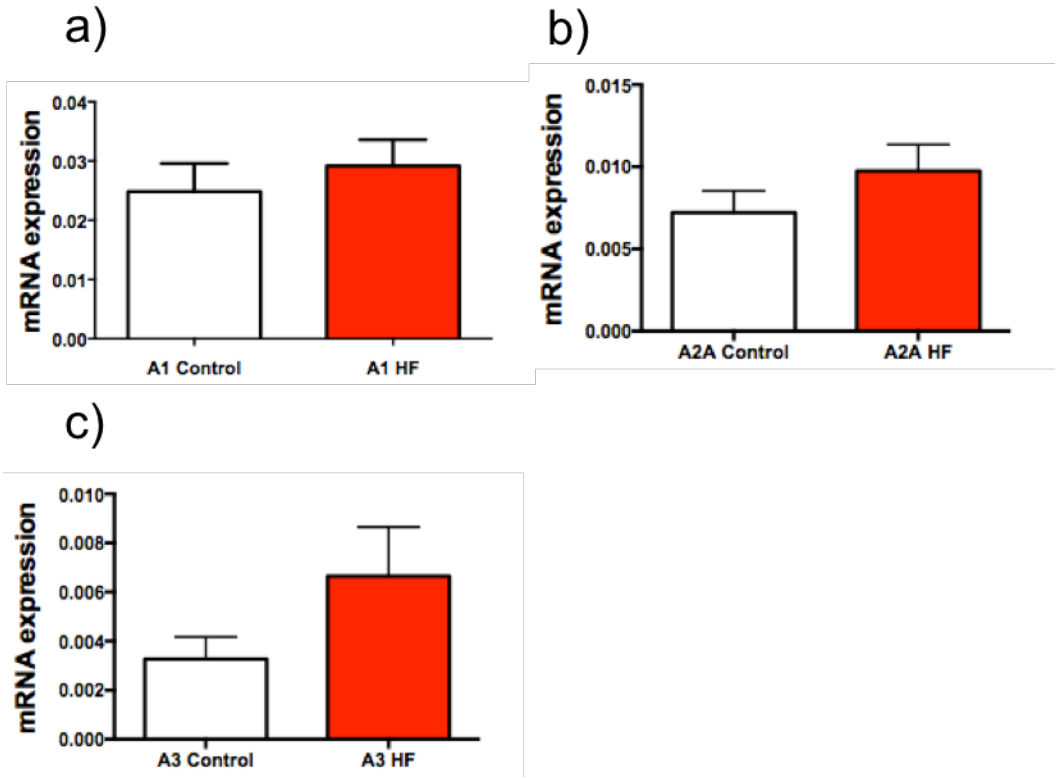

Figure 5.2: Relative quantification of mRNA expression of adenosine A_1, A_{2a} and A_3 receptors in normal and failing rat hearts. Control rats n=4, Myocardial infarction rats n= 6.

5.3.2 No differences in mRNA expression level between left and right atrial tissue in normal heart.

The previuos results showed that there are no differences in both β-adrenergic and adenosine receptor mRNA expression between control and failing rat hearts when the mRNA was extracted from the whole atrial tissue. To check if there are differences in the expression level between left and right atria, in the next set of experiments, we repeated the mRNA extraxtion separating the two part of the atria. Figure 5.3 a) and b) shows the

expression of β_1 and β_2 adrenergic receptors in control atrial tissue of both right and left atrium. In control atrial tissue, no statistical significance was recorded between the levels in the two different part of atrial tissue. Figure 5.4 shows the expression profile of adenosine receptors in right and left atrium of control rats. As for the adrenergic receptors, no differences were observed between the two parts.

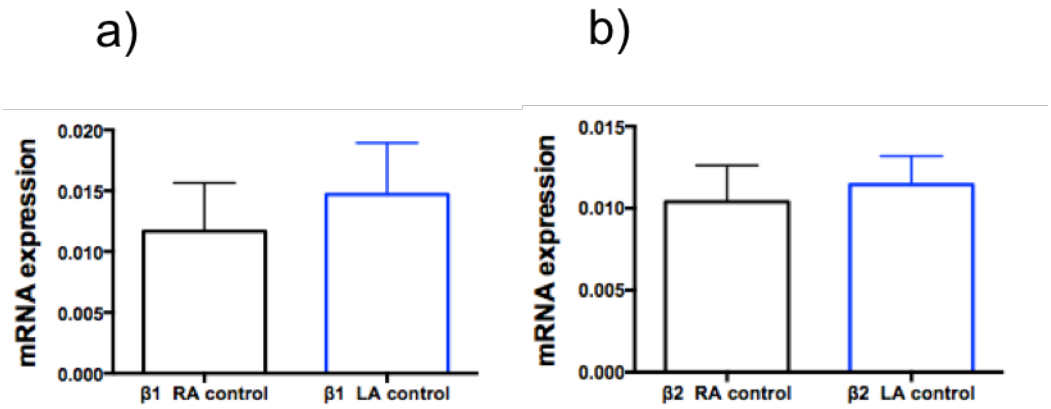

Figure 5.3: Relative quantification of mRNA expression of (a) β_1AR and b) β_2ARs in the left atrium (LA) and the right atrium (RA) of the normal rat heart. Right atrium n=5 animals, Left atrium n=5 animals.

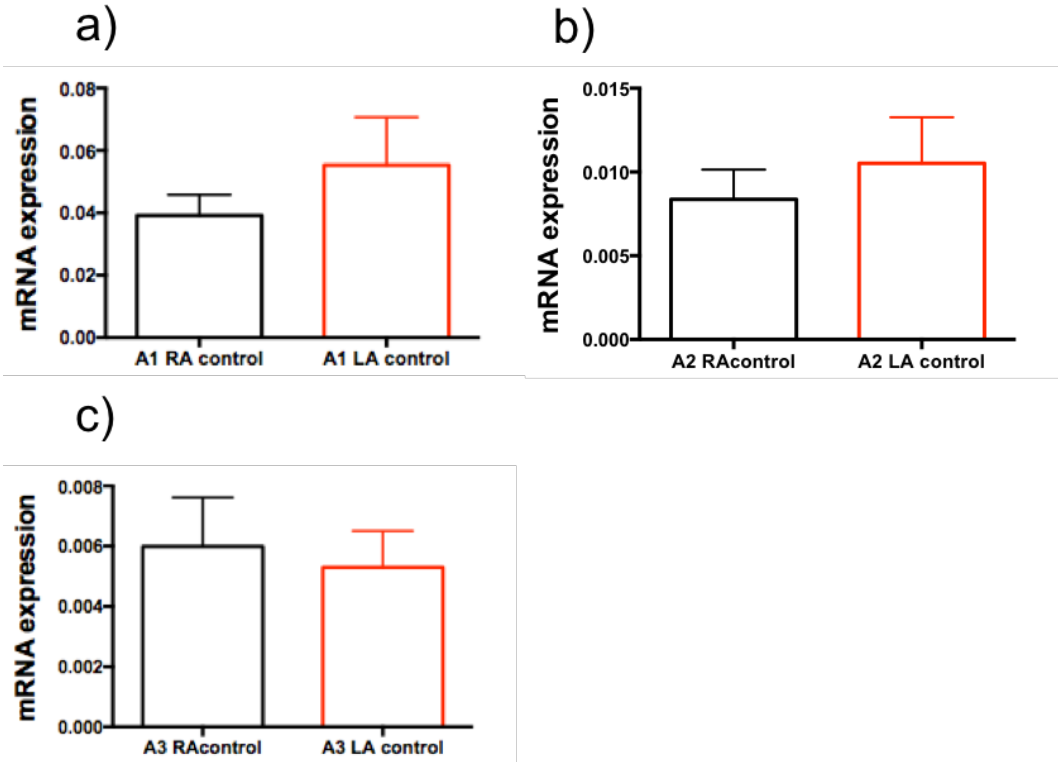

Figure 5.4: Relative quantification of mRNA expression of adenosine A1, A2a and A3 receptors in the left atrium (LA) and the right atrium (RA) of the normal rat heart. Right atrium n=5 animals, Left atrium n=5 animals.

5.3.3 Adrenergic and adenosine receptor mRNAs are more expressed in left atrium than in right atrium in the rat failing hearts.

The next logical step was to check if there were any differences in the expression of adenosine and beta adrenergic receptors in the atria during the heart failure. For this reasons we extracted the mRNA in rat model of HF, separating the left from the right atrium.

Interestingly, the comparison of the expression level between left and right, showed several differences.

Figure 5.5 a) and b) shows that both β_1 and β_2 adrenergic receptors are more expressed in the left atrium compared to the right; there is 48% more of the β_1AR mRNA and 53% more of the β_2AR mRNA in left atrium than in the right. A similar situation was recorded for all adenosine receptors we investigated. Indeed, all subtypes appear to be more expressed in left atria: 49 % higher expression of the A_1ARs, 39% higer expression of the A_2aARs ~ and 54% higher expression of the A_3ARs ~ (Figure 5.6 a) b) and c)).

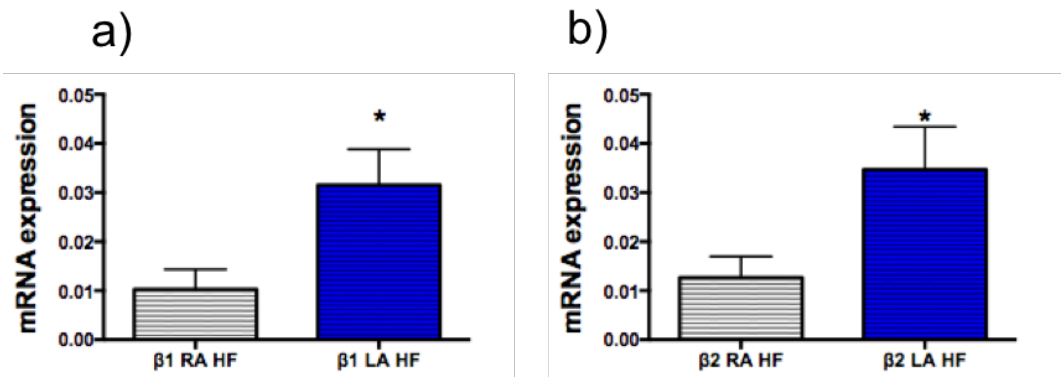

Figure 5.5: Relative quantification of mRNA expression of (a) β_1ARs and b) β_2ARs in in the right atria (RA) and left atria (LA) in failing rat hearts. *P<0.05; HF right atria n=5 animals, HF left atria n=5 animals.

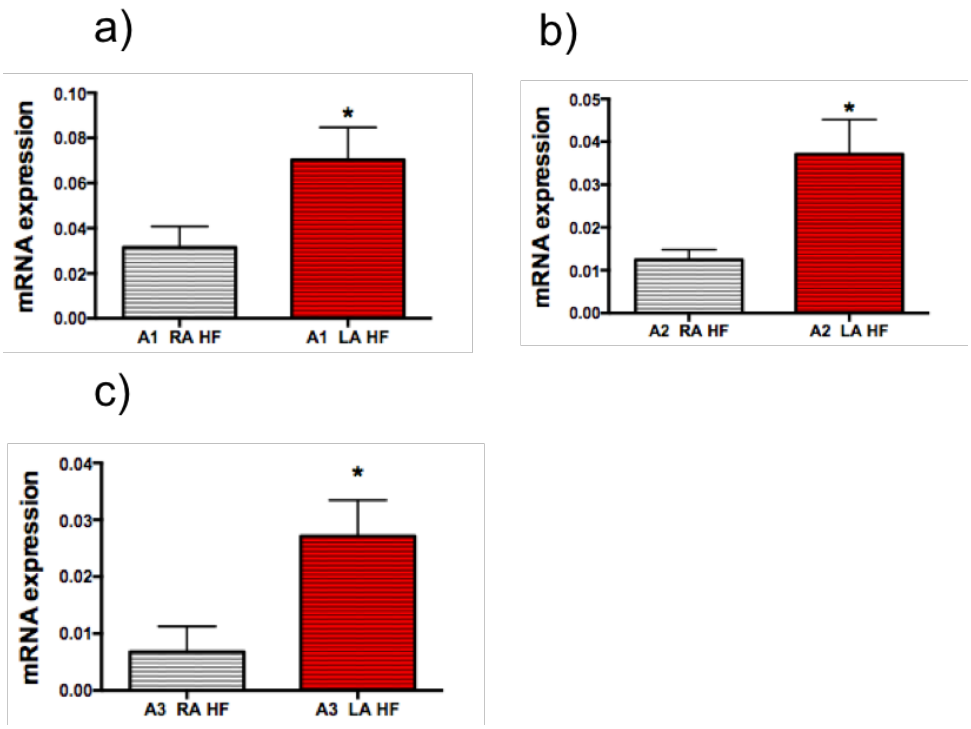

Figure 5.6: Relative quantification of mRNA expression of adenosine A1, A2a and A3 receptors in in the right atria (RA) and left atria (LA) in failing rat hearts. *P,0.05; ;HF right atria n=5 animals, HF left atria n=5 animals

5.3.4 Expression of β_1 and β_2 adrenergic and A_1, A_{2a} and A_3 adenosine receptors in normal and failing hearts: differences between left and right atrial tissue.

To conclude our investigation, we also compared the mRNA expression profiles found in right and left atria during failing conditions with the mRNA expressions profiles obtained in control samples. Figures 5.7 a) and b) represent the mRNA expression for both β_1 and β_2 adrenergic receptors. No statistical significance was recorded between control failing right atrium (0.97±0.1 NS for βAR and 1.16 ± 0.12 NS for β2 AR). Figures 5.8 a), b) and c) show the mRNA expression for adenosine receptors (A_1, A_{2a} and A_3). As

before, no significant changes were observed (0.76± 0.06 NS for A_1, 1.68 ± 0.02 NS for A_{2a} and 0.86 ±0.17 NS for A_3).

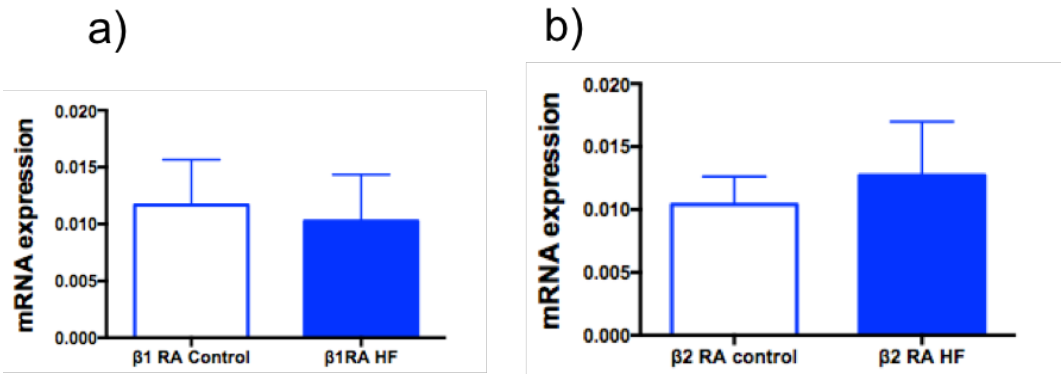

Figure 5.7: Relative quantification of mRNA expression of adrenergic (a) β_1ARs and b) β_2ARs in the right atria (RA) in control and failing samples. Control rats n=5, Myocardial infarction rats n= 5

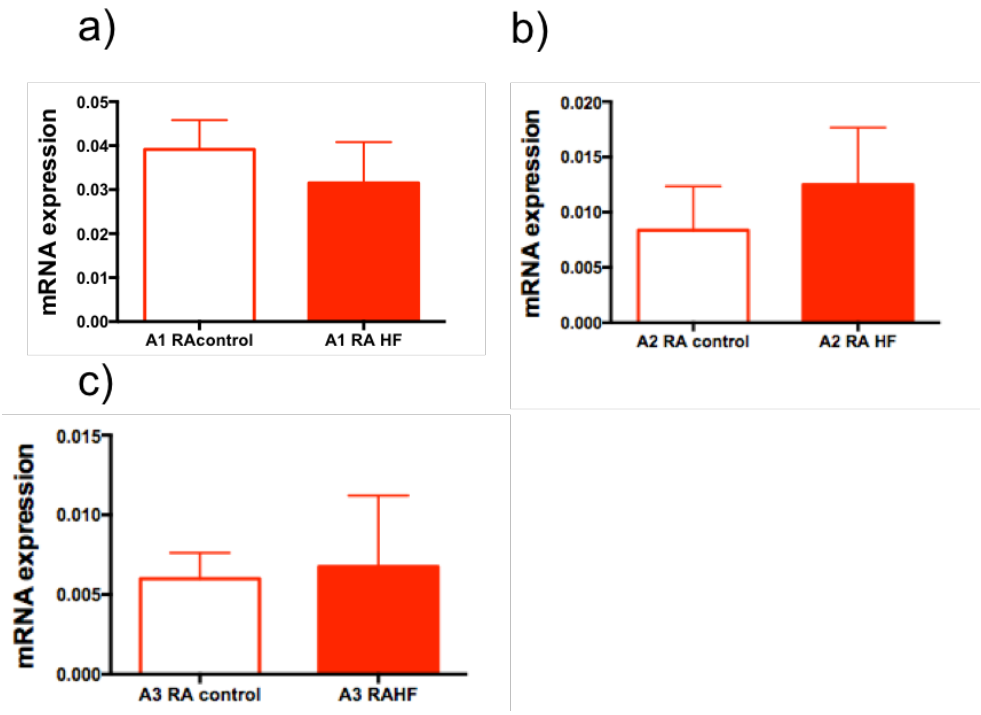

Figure 5.8: Relative quantification of mRNA expression of adenosine (a) A_1,(b) A_{2a} and (c) A_3 receptors in the right atria (RA) in control and failing samples.Control rats n=5, Myocardial infarction rats n= 5.

However, when we compared the mRNA expression of adenosine and β-adrenergic receptors in left atrial tissue of control and failing samples, higher expression was noted for some of the proteins. Expression of β_1AR in failing left atrium seems to be greater compared to the normal left atrium, while this difference is not statistically significant (2.5± 0.3 NS P=0.08) (figure 5.9 a)) On the other hand, expression of β_2AR mRNA is significantly higher in the failing left atrium compared to normal left atrium (2.9 ±0.02 P<0.05) (figure 5.9 b)).

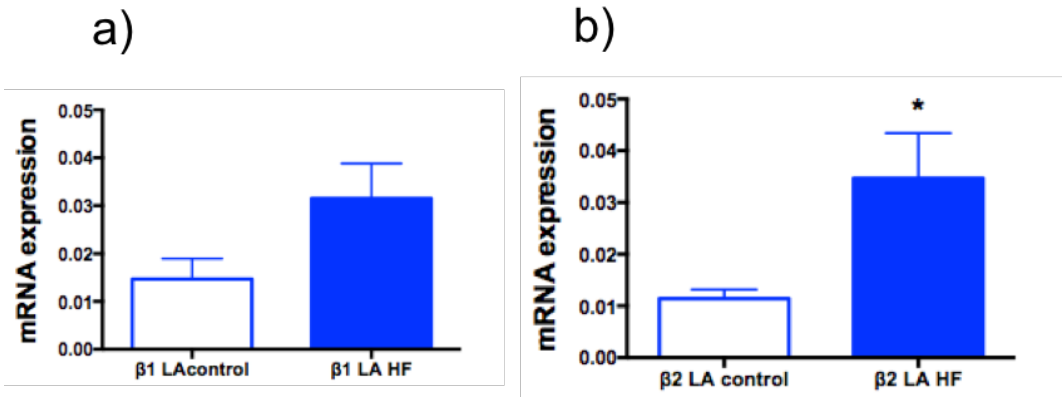

Figure 5.9: Relative quantification of mRNA expression of adrenergic (a) β_1ARs and b) β_2ARs in the normal and failing left atrial (LA) samples. P<0.05 Control rats n=5, Myocardial infarction rats n= 5.

Similarly, between the adenosine subtype receptors, A_1AR expression seems to be higher in failing samples, but this difference is not significant (1.6±0.03 NS) (figure 5.10 a)); on the other hand, a significant increase of both A_{2a}AR and A_3AR expression is found in the left atrium in failing

conditions compared to control (6.3 ±2.3 P<0.05 and 8.6 ±3.01 P<0.05) (Figure 5.10b) and c)).

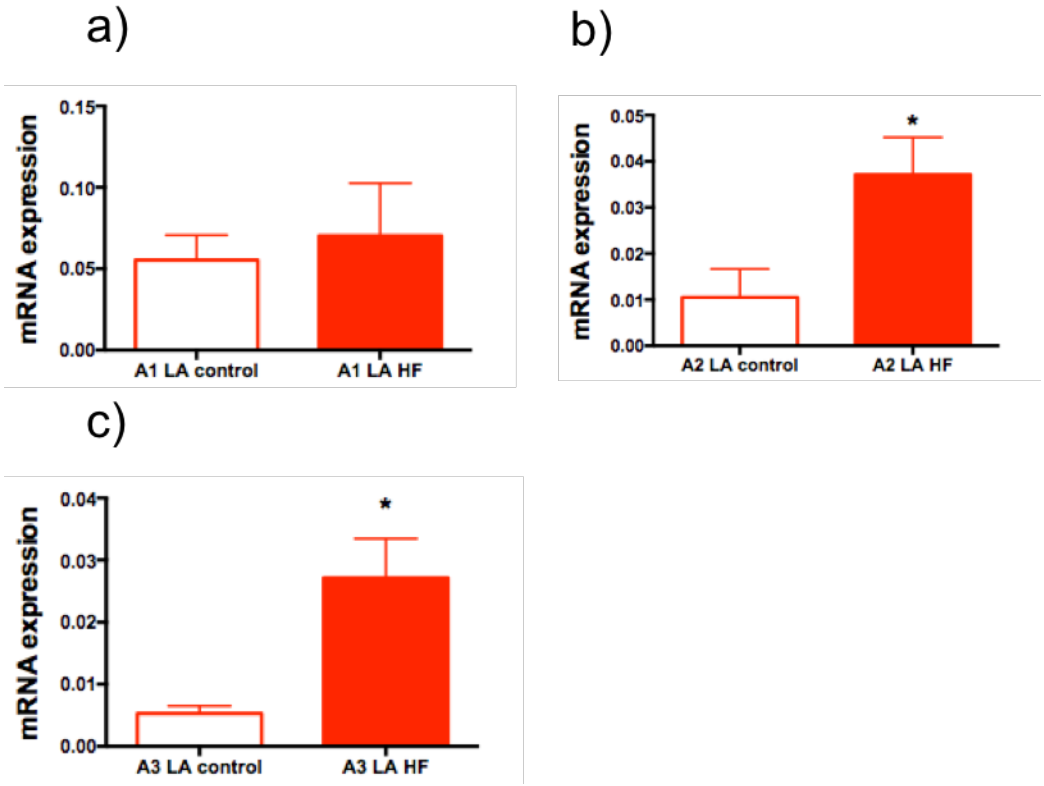

Figure 5.10: Relative quantification of mRNA expression of adenosine (a) A_1, (b) A_{2a} and (c) A_3 receptors in the normal and failing left atrial samples. P<0.05 Control rats n=5, Myocardial infarction rats n= 5.

5.3.4 Expression of caveolin-3 mRNA is decreased in failing atrium.

After checking the mRNA expression profile of adenosine and adrenergic receptors we moved to investigate the distribution of cav3 expression in

both right and left atrium in order to monitor possible remodelling occurring in failing atrium versus normal. Figure 5.11 shows cav3 mRNA expression comparison of right atrium in control and HF samples. In failing heart samples cav3 expression has a tendency to be lower both in the right and in the left atrium (0.38±0.06 NS P<0.09 for RA and P=0.) but this difference was not statistically significant.

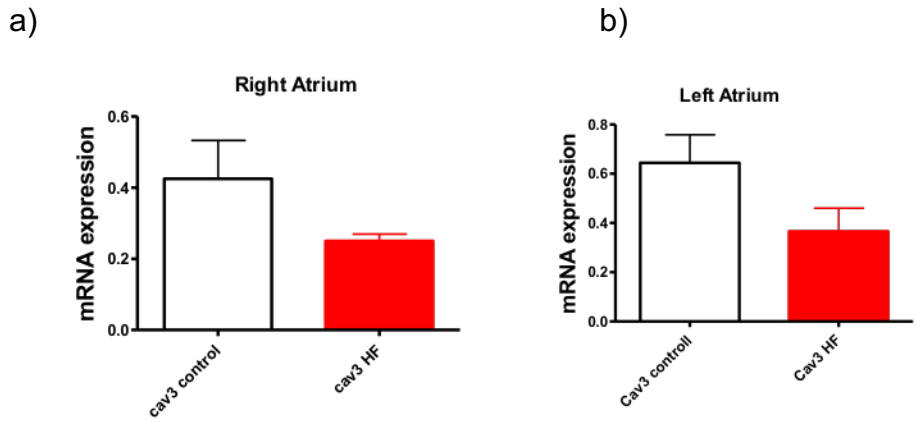

Figure 5.11: Relative quantification of mRNA expression of cav3 in the normal and failing right (a) and left (b) atrial samples. Control rats n=5, Myocardial infarction rats n= 5.

5.3.5 Protein level of A1 adenosine receptors in the right atrium does not change in failing hearts, but is higher in the left atrium.

Given the observation of the increase in mRNA levels of A_1ARs we moved assess protein expression by western blot on atrial frozen tissue from both control and HF model rats. We extracted the protein separately from right and left atria. Figure 5.12 shows the difference of the protein levels between left and right during control and HF model. As we can see from the figure, no difference in A_1ARs protein levels were observed in the right atria in both

condition examinated. In contrast, in the left atrium a significant increase of the A_1 AR protein level was observed.

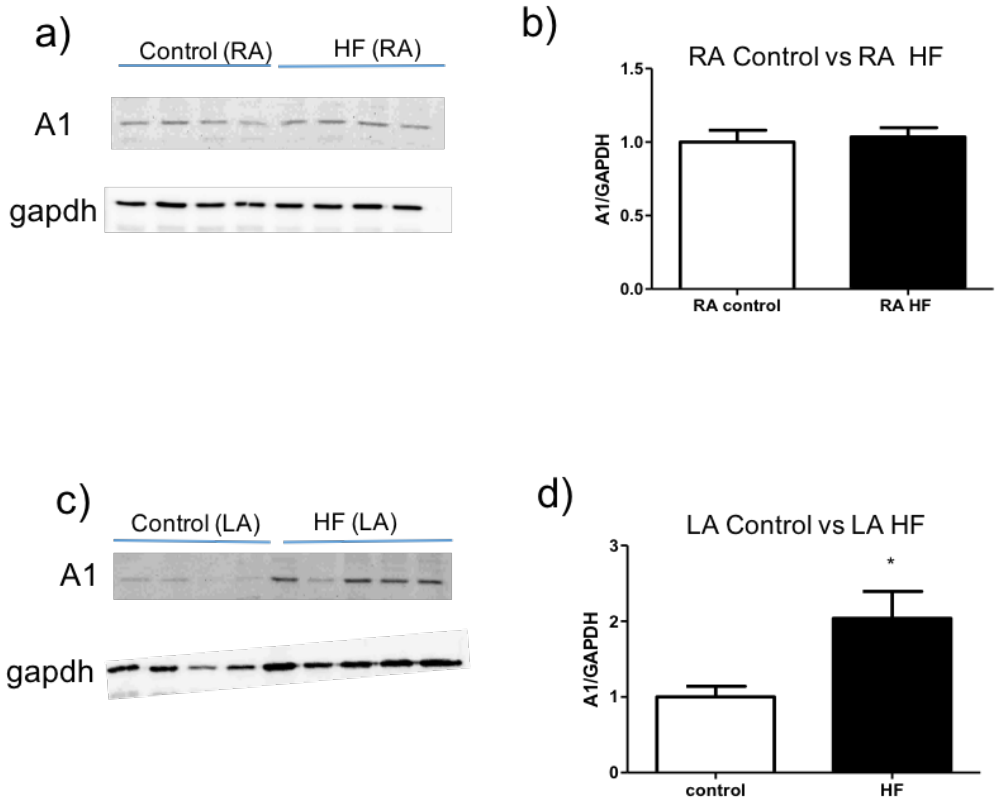

Figure 5.13 Relative protein expression of A1ARs in right and left atria in normal and failing hearts. a) A representative blot showing A1ARs expression in the right atrial tissue in control and failing hearts. b) Relative average density of the A1AR band in a) normalized to the GAPDH 'housekeeping' gene band c) A representative blot showing A1ARs expression in the left atrial tissue in control and failing hearts d) Relative average density of the A1AR band in a) normalized to the GAPDH band. n=4 control n=5 HF

5.3.5 Protein level of caveolin-3 does not change in failing hearts.

Cav3 is the main component forming caveolae and a decrease of these molecules should lead to a remodeling of the caveolae stability and possible decrease in the caveolar number. Given the difference in the functionality of A_1ARs during both failing conditions and during caveolae disruption, it was questioned whether there were differences in cellular levels of cav3. To explore the role that cav3 could play, atrial tissue of both control and heart failure model rats were processed and Cav3 levels were quantified by western blot.

Figure 5.14 shows cav3 levels (normalized to the level of GAPDH) in both left and right atrium of normal and failing hears. As we observed before for mRNA, neither in the left, nor in the right atria any statistically significant differences were observed.

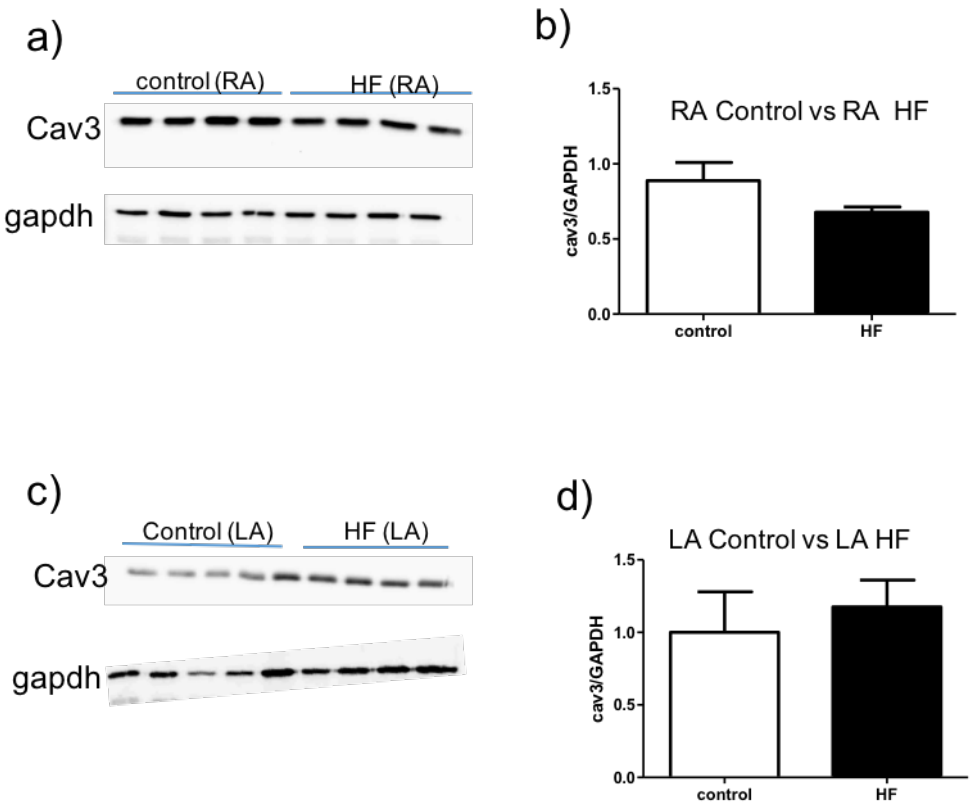

Figure 5.13 Relative protein expression of cav3 in right and left atria in normal and failing hearts. a) A representative blot showing cav3 expression in the right atrial tissue in control and failing hearts. b) Relative average density of the cav3 band in a) normalized to the GAPDH 'housekeeping' gene band c) A representative blot showing cav3 expression in the left atrial tissue in control and failing hearts d) Relative average density of the A1AR band in a) normalized to the GAPDH band. n=4 control n=5 HF

5.4 Discussion and Conclusions

The aim of this chapter was to study, in atrial tissue, the molecular mechanism of the interaction occurring between adenosine and beta-adrenergic receptors in heart failure. Indeed, atrial chambers can be equally affected by the pathological remodelling even if the heart disease originates in the ventricles (Schotten et al., 2011).

Initially, we used both atria for the extraction and the consequent quantification, without taking into account the possible difference in the expression levels between the left and the right atria and our results did not show any difference in the mRNA expression levels of adrenergic and adenosine receptors in both control and HF atrial tissue (Figure 5.1). Then, we repeated the experiments, extracting the mRNA separately from the left and the right atria. Interestingly, in control tissue we did not observe any statistical difference between the left and the right atrial tissue (Figure 5.3). Consequently, no change was found in the amount of mRNA expressed in the right atrium in failing conditions compared to control. In contrast, in the failing hearts, an upregulation of both adenosine and adrenergic receptors was observed in the left atrium (Figure 5.5). A statistically significant upregulation in failing model was found in the left atrium for β_2ARs and both A_{2a} and A_3 ARs. For β_1ARs and A_1ARs, an upregulation was observed, however not statistically significant (P=0.08 for β1ARs and P=0.192 for A_1ARs). This could be explained by the low number of samples used for the extraction (n= 5 for both control and HF samples). Nevertheless, we

conclude that these receptors are also upregulated, as western blot confirmed the higher presence of A_1ARs in left failing atrium compared to the left atrium control (P= <0.05). Our results are consistent with other studies that reported high levels of expression of adenosine receptors in heart with left ventricular systolic dysfunction (Funakoshi et al., 2007 and Gauthier et al., 1998). Funakoshi and collegues assessed adenosine levels and adenosine receptors expression in control and transgenic mice with left ventricular systolic dysfunction secondary to overexpression of tumor necrosis factor (TNF1.6). They demonstrated that the ventricular levels of adenosine are significantly decreased in mice with diminished left ventricular performance. This decrease was accompanied by a marked increase in the levels of the A_1AR and a small but significant decrease in the number of A_{2a}AR. Consistent with these results, Meyer and collegues showed that adenosine production was initially increased during the compensated phase of pressure-overloaded rat heart but it was decreased during cardiac decompensation (Meyer et al., 2001). Regarding βARs, Bristow et al. found a decrease of the βARs in the left ventricle during HF. (Bristow et al., 1982). The density of β-adrenergic receptors was found to be decreased by 29%, whereas the β_1/β_2-adrenergic receptor density remained unchanged.

The studies mentioned above, involved principally the remodeling occurring in the left ventricle, however, heart failure is reported to be associated with atrial dysfunction (Schotten et al., 2011). Yeh et al. showed, in a reproducible dog model of HF that the changes occurred in ventricles led to increased LA and RA intracavitary pressures causing pathological atrial cardiomyocyte remodeling. They reported that, in contrast to the characteristic intracellular Ca^{2+} transient amplitude depression in failing ventricular cardiomyocytes, atrial cardiomyocytes from the same hearts showed abnormally increased intracellular Ca^{2+} concentrations in diastole. Such effect is consistent with Ca^{2+} overload leading to depressed cell shortening (Yeh et al., 2008).

The left atrium modulates left ventricular filling by acting as an elastic reservoir (Braunwald et al., 1961). LA dysfunction and the consequent remodeling are commonly observed in patients with HF. Growing body of evidence suggests that LA dysfunction is an active contributor to symptoms and to the progression of disease (Donal et al., 2008; Melenovsky et al., 2006; Welles et al., 2012 and Hoit, 2014). However, HF-related LA remodeling is poorly understood. These evidences could also explain the reasons why in our results we observed, during failing conditions, differences in the expression of the receptors only in LA rather than in the RA.

Our results show that there are no differences in Cav3 mRNA expression in both normal and failing conditions for both the right and the left atrium. However a slight downregulation of cav3 mRNA was observed in failing conditions ($P< 0.08$ for RA and $P= 0.111$ for LA); in contrast, western blot did not show any difference for Cav3 protein levels in failing hearts in both chambers. These results may suggest that the differences of adenosine receptors activity related to the caveolae microdomain (see chapter 2 and 3) are not a result of an increase or a decrease in Cav3 expression. It is possible that the differences that we observed are not related to the differences in the gene expression but for example related to a possible dynamics physical effect occurring during the structural changes present in HF conditions. On the other hand, the increase of A_1ARs density that we observed during failing conditions appears to follow the loss of the adenosine effects, suggesting the establishment of a potential compensatory mechanism that could be a driving factor of the failing phenotype.

CHAPTER 6 Functional and molecular remodelling in human atrial cardiomyocytes isolated from different groups of patients.

6 Functional and molecular remodeling in human atrial cardiomyocytes isolated from different groups of patients.

6.1 Introduction

Congestive heart failure (CHF) is the global term used to describe the condition when cardiac function is not sufficient to cover the demands of the body and the lungs. The failing conditions are associated with several alterations of both structural and functional properties, resulting in a non-sufficient cardiac function (Lloyd-Jones et al., 2002). HF is the endpoint for several cardiovascular diseases including coronary artery disease, myocardial infarction, hypertension, cardiomyopathy, congenital heart defects, myocarditis. Compensatory and adaptive changes occur in the heart to preserve cardiac output. Some of these adaptive changes are mediated by enhanced sympathetic nervous system activity (Leimbach et al., 1986)

Atrial fibrillation (AF) is the most common type of arrhythmia that leads to an abnormal heart rhythm characterized by rapid and irregular beating of the atria (Khairy and Nattel, 2002). Although it is often associated with others cardiac diseases, AF could occur in many patients with no detectable disease state (Fuster et al., 2001). AF is a supraventricular tachyarrhythmia characterized by uncoordinated atrial activation with consequent deterioration of the mechanical functionality of the tissue (Bellet, 1971). The ventricular response to AF depends on several factors such as the electrophysiological properties of the AV node, the level of vagal and sympathetic tone, and the action of drugs used for the treatment (Prystowsky et al., 1998). AF condition could be isolated or associated with other arrhythmias, often atrial flutter or atrial tachycardia. AF is associated with increased morbidity and mortality due to increased risk for congestive

heart failure and cerebral infarction (stroke) (Khairy and Nattel, 2002; Van Gelder et al., 2002). Indeed, there is a complex links between the onset of CHF and AF, although the exact mechanism of this association has not been fully understood. Different studies showed that the occurrence of AF increases 6 times when CHF is present and enhancement seems to follow the increasing severity of CHF (Iwasaki et al., 2011). The occurrence of AF also increases with age and others several cardiac disorders predispose to AF, including coronary artery disease, pericarditis, mitral valve disease, congenital heart disease, thyrotoxic heart disease and hypertension (Nattel et al., 2002). Many of these are thought to promote the onset AF via a mechanism that include the increase of the atrial pressure and/or via atrial dilation; however, the precise relationship is not completely defined.

Adenosine is an endogenous nucleoside commonly used in both diagnosis and treatment of superventricular tachyarrhythmias (Camm et al., 1991, Rankin et al., 1992 and Datino et al., 2010). Adenosine can influence myocardial function in humans, and has been successfully used in the treatment of different type of tachyarrhythmias, suggesting a physiologically important role played by adenosine in human heart (Dimarco et al., 1983, Belhassen and Pelleg, 1984). Several studies, however, indicate that intravenous adenosine administration can cause spontaneous or pacing-induced atrial fibrillation in patients (Tebbenjohanns et al., 1997 and Strickberger et al., 1997). In both clinical and animal model investigations, adenosine was reported to shorten atrial action potential duration (APD) and refractoriness that could play a role in the AF initiation (Lou et al., 2014; Kabell et al., 1994; Tebbenjohanns et al., 1997 and Strickberger et al., 1997).

The exact molecular and functional mechanism of adenosine-induced AF and occurring during HF, remain unclear. Adenosine is released mainly during myocardial ischaemia and reperfusion, and is produced not only by cardiomyocytes but also in endothelial cells (Li et al., 2016).

The cardio-protective action of adenosine is well known. Adenosine receptors A_1 are known to attenuate the release of catecholamines which is β-adrenorecepetors-mediated. On the other hand, adenosine receptors A_2 are known to increase coronary blood flow and inhibit platelet and leukocytes activation (Masufami and Masatsugu, 2000). These effects may synergistically inhibit and delay the deleterious effects present in both ischemic and non-ischemic heart disease and consequently adenosine may trigger and mediate cardio-protection; at the same time can also attenuate the severity of the heart failure conditions. Indeed, considering that adenosine actions seems to be involved in the attenuation of the deleterious neurohumoral factors in the pathophysiology of heart failure, it may become interesting clearly understand the action mechanism occurring during failing condition for a future treatment of the disease. As mentioned before, adenosine could be implicated in the onset of AF (Tebbenjohanns et al., 1997 and Strickberger et al., 1997). Recently, Fedorov et al. demonstrated that sustained adenosine-induced AF may be driven by different localized reentry circuits in right atrium areas in close relationship with highest expression of adenosine A_1 receptors (Fedorov et al., 20016).
In this chapter we wanted to compare our finding in rat and mice heart failure models with samples collected from human patients. We decided to divide the patient samples in different groups, taking into account the possible relationship between HF and AF diseases.

The aims of this chapter are the following:

1. To explore the functional interaction between beta-adrenergic and adenosine receptors in the human atrial cardiomyocytes

2. To dissect cellular mechanisms of the anti-adrenergic effect of adenosine by measureing cAMP level into human atrial cardiomyocytes transfected with a cAMP FRET sensor

3. To study molecular mechanisms of the anti-adrenergic effect of adenosine in human atrial tissue

6.2 Materials and methods

6.2.1 Patients screening

Patients examined in this study were enrolled from routine cardiac surgery at both Hammersmith Hospital, Imperial College London, UK and Ospedale Civile Maggiore di Verona, Italy. The permission to obtain heart tissue biopsy was received from the respective patients.

6.2.2 Patients groups

Human tissues were obtained from both left and right atrium during cardiac surgery (n= 6 patients for contraction study n=5 patients for FRET experiments n=11 patients for PCR and western blot). Human biopsies were collected either during mitral valve (MV) surgery or during bypass surgery as well as from dilated (DCM) and ischemic cardiomyopathy (ICM) heart transplant with and without LVADs (Figure 6.1). In our study we considered both males and females (M= ~11% and F=~ 8%) with an average age of 66.20 ± 13.00 (Table 6.1).

We divided all patients in 4 different groups, considering the heart rhythm and the ejection fraction. According to the heart rhythm we can divide the patients into two groups: Synus rhythm (SR) and Atrial fibrillation (AF) patients. Ejection fraction also allowed us to divide the patients into two groups: heart failure (HF) patiens (EF < 40 %) and not heart failure (nHF) patients (EF > 40%).

Table 6.1: Basic patient's characteristics.

Age (mean ± SD)	66.20 ± 13.00
Gender	M (11%), F (8%)
BMI (mean ± SD)	27.65 ± 4.55
BSA (mean ± SD)	1.87 ± 0.23
Previous MI	31.58%
Previous Cardiac Intervention	21.05%
Previous Cardiac surgery	5.26%

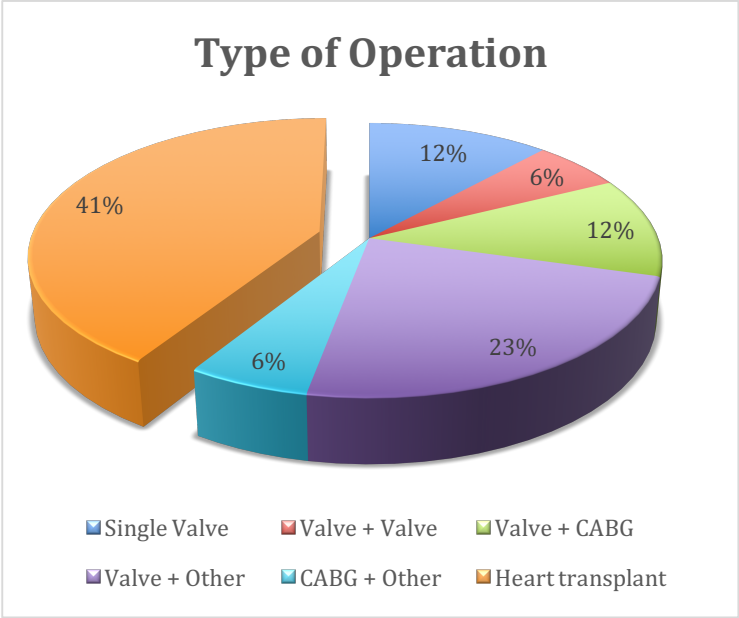

Figure 6.1: Percentage of type operations in which biopsies were collected and used during this work

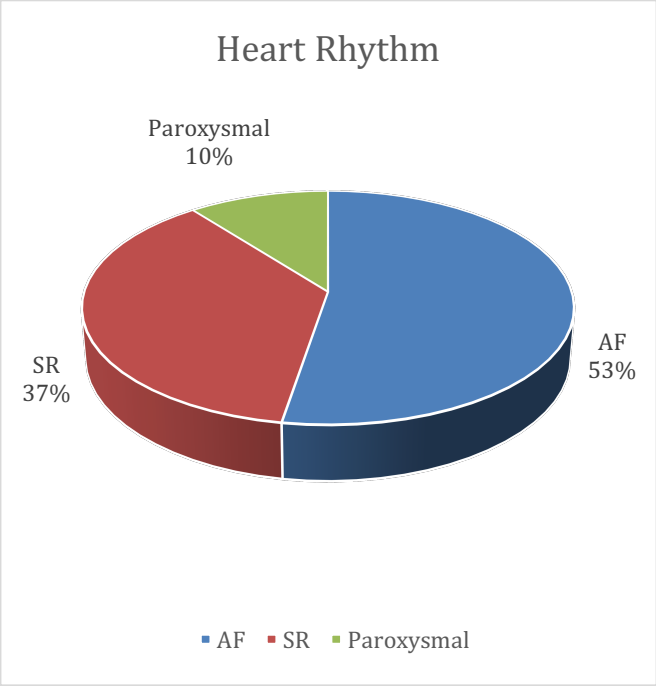

Figure 6.2: Heart rhythm populations of the enrolled patients.

6.2.3 Human atrial cardiomyocyte isolation

Tissue collected during the surgery operation was placed in cold $LoCa^{2+}$ solution (4-7°C) specific for human tissue storing (see section 2.3.4 for the details for composition), until it is transported to the laboratory. Atrial cardiomyocytes were isolated by enzymatic dissociation and mechanical disaggregation using modification of Harding's isolation protocol (Workman et al., 2001). Briefly, tissue was washed in the cold human $LoCa^{2+}$ solution and minced in small pieces of around the size of 1-2 mm.

Once cut into small pieces, tissues were quickly transferred into a new falcon tube, containing 10ml of oxygenating $LoCa^{2+}$ solution. The tube containing tissue, was manually shaken for 3 minutes to permit the cleaning of the sample from the blood; this step was repeated three times.

After this cleaning process, tissue was placed into a new tube with Enz buffer (see Material and Methods) plus protease (Type XXIV, Sigma, 0.36mg/ml) and collagenase (type V Sigma, 0.5mg/ml). The solution was bubbled with oxygen and mechanically shaken for at least 10-15 minutes, until tissue started to look digested. The buffer containing protease was then exchanged with another one, containing collagenase (1mg/ml) for further digestion of tissue. After 2 or 3 step of 10 minutes each, the tissue was filtered and the all solution was centrifuge at 600 Rpm for 3 minutes. After the centrifuge, the supernatant was removed, leaving the pallet containing the cells in the bottom. At this time a fresh Enz solution was transfer in the falcon and the cells were leaved in the tube until the onset of the experiments (see chapter two Materials and methods for more details). Human experiments and the analysis of the resulting data was primarily performed by me with the contribution of some data by Carla Lucarelli.

6.2.4 Human Cardiomyocytes plating and transfection with cAMP FRET biosensors

Human cardiomyocytes isolated from atrial tissue were plated onto laminin coated coverslips in recovery medium (M199 with the addition of fetal bovine serum 10ml/L). After 1 hour of plating the cells that did not attach to the coverslips were removed and the others were left in the modified M199 medium in the incubator with CO2. In the case of FRET experiments, an additional step was done: the adenovirus containing an expression vector for a FRET biosensor was added to the medium for 48h. The FRET biosensor used in human cells was the same that we used in rat atrial cardiomyocytes (RII-epac2, see chapter 4).

6.2.5 Functional investigation of cardiomyocytes contractility using IonOptix system

Atrial human cardiomyocytes were isolated and stored in a low calcium buffer until the onset of the experiments. The specific chamber described before in chapter 3, was used and the cells were placed into. The chamber was been filled with KH buffer (see Meterial and Methods) and the solution was perfused through a pump inside the apparatus. All solutions used during these experiments were bubbled with the oxygen/CO2 mixture and the temperature in the chamber was kept at 37 degrees. The cells were left on the coverslip for around 5-10 minutes, time needed for the cardiomyocytes to attach to the bottom of the glass. After this time, the perfusion was turned on again. Once a cell was selected, the simulator was switched on at the rate of 0,5 Hz (voltage of 50V, 20 msec duration). Baseline was usually recorded for at least 10 minutes and then, different agonist/antagonist were applied to provide data concerning different aspects of the adenosine and adrenergic receptors effect on the contractility of atrial cardiomyocytes.

6.2.6 Investigation of contractile responsiveness to adenosine and adrenergic stimulation in human atrial cardiomyocytes

To investigate the contractility of human atrial cardiomyocytes and to study the activity of the adenosine receptors after β_1 adrenergic stimulation we performed the same protocol used for experiments in rat atrial and ventricular cardiomyocytes (see chapter 2 and 3 for more details). Briefly we perfused the cells with a specific β_2 adrenergic receptors blocker, ICI 118, 551 (ICI,100 nm) for at least 10 minutes. After the blocking of β2 adrenergic receptors, we added Isoproterenol (100 nm) in the bath for the selective stimulation of the β_1ARs. At the end 2-MeCCPA (1 μm), the specific agonist of the A_1 adenosine receptors, was applied in the solution (Figure 6.3).

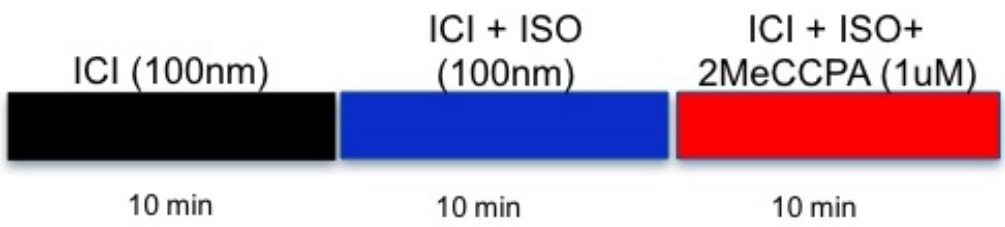

Figure 6.3 Protocol of whole-cell β_1-adrenergic stimulation of rat atrial cardiomyocytes**.**

6.2.7 Functional investigation of cAMP level: FRET

To measure the cAMP level produced during adenosine and β-adrenergic stimulation in human atrial cardiomyocytes, FRET technique was used (see chapter 2 Materials and Methods).

Atrial and ventricular human cardiomyocytes were isolated and plated in the medium. After 1 hour of the plating the cells were transfected with the RII-epac sensor (same used in rat atrial experiments in chapter 4). After 48

hours, transfected cells were taken from the plate in the incubator and they were washed with FRET buffer and fastened into a coverslip holder. During the FRET experiments the following protocols was performed (Figure 6.2). Briefly, the cells were incubated with ICI and baseline was recorded. After this time Isoproterenol was applied to the cells and finally we applied the 2-MeCCPA to see only the activation of the A_1Rs subtypes. At the end, we also applied IBMX to elicit total cAMP response.

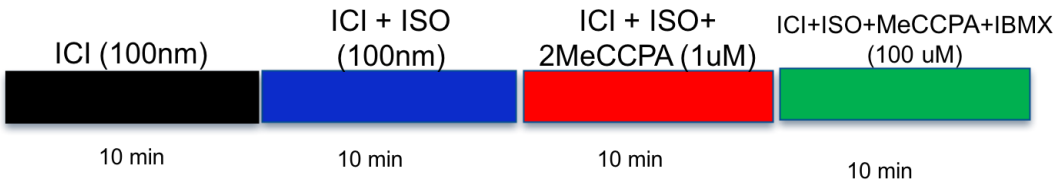

Figure 6.2: Protocol to investigate anti-adrenergic effect of A1 adenosine receptors agonist

6.2.8 Total RNA extraction and quantification

Total RNA was extracted from 30mg of atrial tissue for all human tissue we collected in the hospital during the surgery. Each sample was placed in an ependorff tube containing 1 stainless steel bead, 400 µl of lysis buffer given by peqGOLD total RNA kit (Peqlab #12-6634) and 4 µl of ß-mercaptoethanol (10 µl of ß-mercaptoethanol per 1 ml of lysis buffer). After the disruption of the sample (see chapter 5 for more details), the extraction was made according to manufacturer's instruction. 30µl of RNase-free water was used for RNA elution and RNA concentration was determined using a Thermo Scientific NanoDrop 1000 spectrophotometer. The purity of RNA was quantified with Nanodrop and the A260/A280 absorbance ratio = 2.00±0.10 represented an acceptable purity. PCR analysis was performed using SYBR Green JumpStart taq ReadyMix (Sigma) in an Eppendorf Mastercycle EP Realplex machine (Mauritz et al., 2008). SYBR-Green is a dye able to emits bright fluorescence when it is bound to the DNA amplified

from the corresponding cDNA template. The presence of the fluorescence is related to the amount of starting cDNA material in the reaction. With this method the cycle threshold (Ct) value was measured; this value is representative of the number of PCR cycles required to be able to generate fluorescence with enough intensity that it reaches the threshold within the linear phase of the reaction. Ct value is correlated to the starting quantity of target mRNA. For each sample relative expression levels were calculated after normalization against the housekeeping gene, that was validated to ensure that the different groups had similar gene expression values. Relative mRNA expression levels were analysed using comparative Ct methods (the 2-ΔΔCt method) with a normalization to the housekeeping gene Rpl32 (Table 6.2).

Table 6.2. Oligonucleotides used for real-time PCR for human genes

Target gene		Primer sequence
B_1ADR (NM_000684.2)	Fw	5'-GACGCTCACCAACCTCTTCA-3´
	Rv	5'-CACAGCTCGCAGAAGAAGGA-3´
B_2ADR (NM_000024.5)	Fw	5'-TTGCCTCTTCCATCGTGTCC-3´
	Rv	5'-CCACCTGGCTAAGGTTCTGG-3´
ADORA $_1$(NM_000674.2)	Fw	5'-CTTTGGTGACCTTGGGTGCT-3´
	Rv	5'-CACCTCGATGCCGATGTAGG-3´
ADORA$_{2a}$ (NM_000675.5)	Fw	5'-CATTGACCGCTACATTGCCA-3´
	Rv	5'-GTGGTTCTTGCCCTCCTTTG-3´
ADORA$_3$(NM_000677.3)	Fw	5'-AGGACCCATTGAGCAGAAGG-3´
	Rv	5'-CCACATGACTGGAAGGAAGCA-3´
RPL32(NM_000994.3)	Fw	5´- CATCTCCTTCTCGGCATCA-3´
	Rv	5´-AACCCTGTTGTCAATGCCTC -3´

6.2.9 Protein extraction and quantification

The tissue (around 30 mg) was cut in small pieces and placed in an ependorff containing RIPA buffer, ptotease inhibitor and DTT (around 500 ul for each samples, as describe before for rat atrial tissue (see chapter 5

for details). After isolation of protein, a volume between 2-5 ul was kept for the quantification and the rest of the supernatant was stored at -80°C.

6.2.10 Western blot protocol

After the quantification, the results given by the protein assay, were used to calculate the volumes of sample for loading to have 40 µg of protein for tissue lysates. The protocol of the western blot was the same used for rat atrial samples, as describe before in chapter 5.

6.2.9.1 Membrane incubation and development

After the transfer of the protein in the nitrocellulose membrane, it was blocked in 5% of milk dissolved in PBS-Tween (see chapter 5) for 1 hour. Then the membrane was incubated with primary antibody solution (Table 1) at the temperature of 4°C overnight. Next day, the membrane was washed in PBS-Tween for 10 minutes; this process was repeated 3 times. When the washing was done the membrane was incubated with the appropriate secondary antibody (Table 2.1) for 1 hour. Then the membrane was washed again 3 times, for 10 minutes each in PBS-Tween. When the washing finished, the membrane was covered with ECL Western blotting detection solution (Bio RAD). The membrane was develop using The ChemiDoc XRS+ system BIORAD, and analyzed using imaj, Version 5.

6.2.11 Statistical analysis

Data obtained from these experiments were expressed as mean ± standard error of the mean (SEM). All statistical analysis was performed using Excel and Graphpad prism 6.0 software. The statistical differences of measurements made between two groups were analysed using a paired T-test, whereas multiple comparisons between groups were analysed using a one-way or two ways analysis of variance (ANOVA). A P value of less than 0.05 was considered statistically significant.

6.3 Results

6.3.1 Human cardiomyocytes contractility after adrenergic and adenosine stimulation: differences between patient groups.

Functionality investigation of cardiomyocytes performed using IonOptix, clearly showed a strong heterogeneity in the response among the different patient groups considered. For these reasons we decided to analyze all the patients and dived them into several groups, considering two principal parameters: heart rhythm and ejection fraction.

6.3.1.2 Contraction of myocytes from patients with SR and without HF versus patients with SR and with HF.

The first group was formed of all patients in sinus rhythm (SR). The subgroups were made according with the ejection fraction: patients in SR without heart failure (nHF) (EF > 40%), and patients in SR with heart failure (HF) (EF < 40%). All cells used in these experiments were isolated from the left atrium. After isolations the cells were placed on the ionOptix chamber and the perfusion started. To check the anti-adrenergic effect of A_1 adenosine receptors after the selective stimulation of β_1ARs, we decided to use the same protocol that has been extensively tested in both rat atrial and ventricular cardiomyocytes (see chapter 3).

Figure 6.5 shows the cellular shortening of human atrial cardiomyocytes of patients in sinus rhythm and without heart failure (number of cells = 2). An increase in contraction after the application of isoproterenol (34.3 ± 3.08% NS) and a decrease in contraction after the application of 2-MeCCPA (61.2 ± 6.7 NS) are seen.

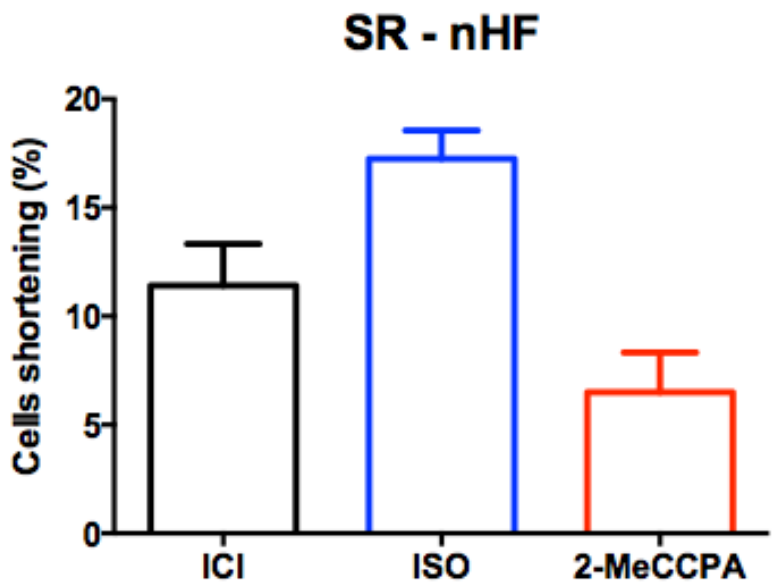

Figure 6.5: Human cardiomyocytes from patients with sinus rhythm and without heart failure: atrial shortening: at baseline (ICI) and after selective β1AR stimulation (ICI 50nM +ISO 1μM) as well as after the specific stimulation of the A1ARs (ICI+ISO+2-MeCCPA) (n=2 cells from 1 patient).

The second group was formed by patients in SR and with HF (number of patients= 2 number of cells=4). The cells used in these experiments were isolated from left atrium. A significant increase (85.7 ± 0.6 $P<0.05$) was observed after the administration of isoproterenol and a significant decrease after the administration of 2-MeCCPA was also recorded (67.8 ± 6.7 $P< 0.05$).

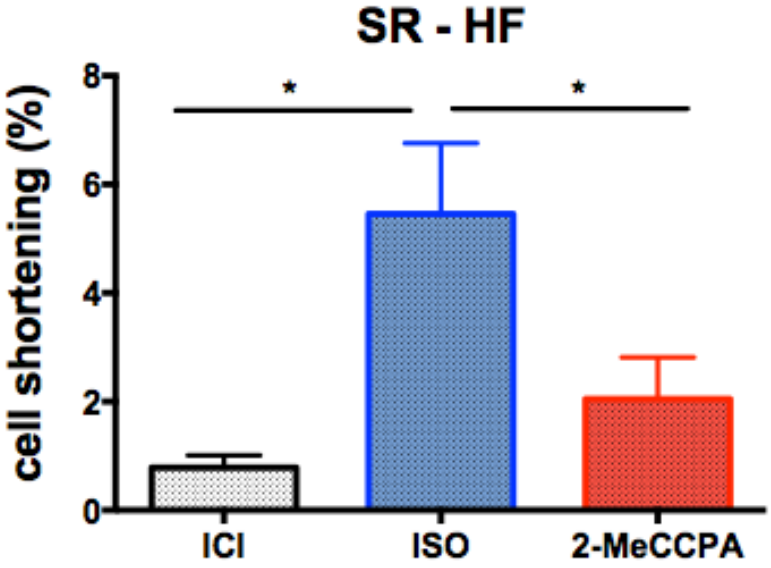

Figure 6.6: Human cardiomyocytes from patients with sinus rhythm and with heart failure: atrial shortening at baseline (ICI) and after selective β1AR stimulation (ICI 50nM +ISO 1μM) as well as after the specific stimulation of the A1Rs (ICI+ISO+2-MeCCPA) (n=4 cells from 2 patients).

The statistical comparison between this two groups, SR nHF vs SR HF, cannot be reported due to the low number of cells used in the experiments.

6.3.1.2 Contraction of myocytes from patients with AF and without HF versus patients with AF and with HF

In this set of experiments, all patients we analyzed were in atrial fibrillation and the cells used were isolated from both left and right atrium. As for SR patients, we also dived AF patients in two groups, according with ejection fraction: AF nHF patients and AF HF patients. Figure 6.6 shows the cell shortening of the patients with AF and without HF (n= 7 cells from 3 patients). After the application of isoproterenol a significant increase (77.9 ± 2.2 P <0.01) was found. Equally, a significant reduction occurred after the application of 2-MeCCPA (79.8 ± 5.3 P<0.05).

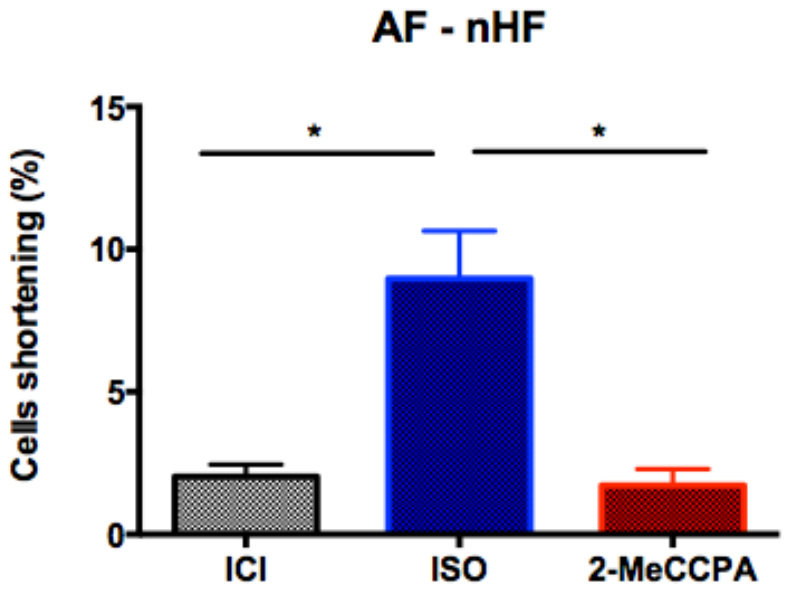

Figure 6.7: Human cardiomyocytes from patients with atrial fibrillation and without heart failure: atrial shortening at baseline (ICI) and after selective β1AR stimulation (ICI 50nM +ISO 1μM) as well as after the specific stimulation of the A1Rs (ICI+ISO+2-MeCCPA) (n=7 cells from 3 patients)

We analyzed also a patient with AF and HF, although we recorded a very low number of cells (n= 2 cells).

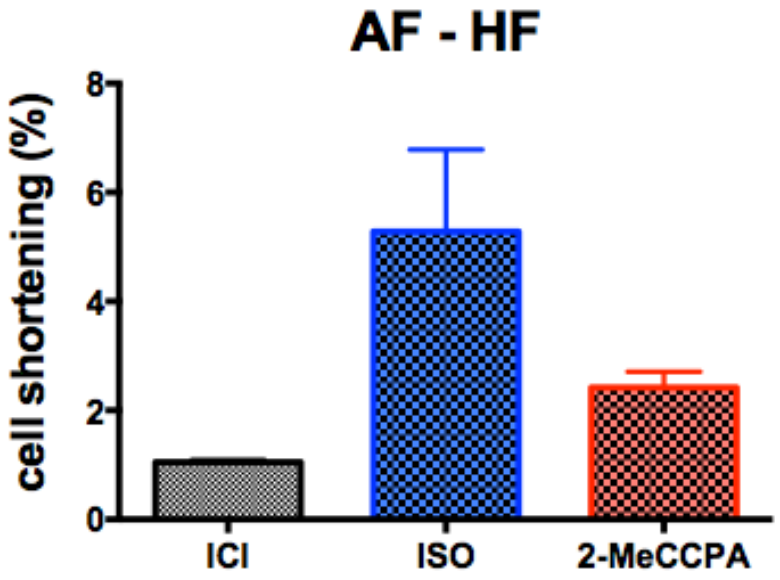

Figure 6.8 Human cardiomyocytes from a patient with atrial fibrillation and with heart failure: atrial shortening at baseline (ICI) and after selective β1AR stimulation (ICI 50nM +ISO 1μM) (n=2 cells from 1 patients) as well as after the specific stimulation of the A1ARs (ICI+ISO+2-MeCCPA)

An increase after β1ARs stimulation was recorded (78.5 ± 3.2 NS); also after the application of A1ARs agonist a reduction was observed (49.3±9.6 NS)

6.3.1.3 Comparison of contraction of myocytes from patients without HF: SR versus AF

The results presented before, showed a similar trend for all group we studied, however the low number patients and cells used during the experiments, did not allow us to make proper comparison. In the next step we investigated the possible differences occurring in patients in SR versus patients in AF. All the patients we examined were with a preserved EF (>40%). Unfortunately, also in this case it was not possible to calculate any statistical difference since the group SR nHF contained only two cells. The trend after the application of the various agonists/antagonists was similar, but, as shown on Figure 6.9, cells from patients in AF started with a smaller contraction at the baseline.

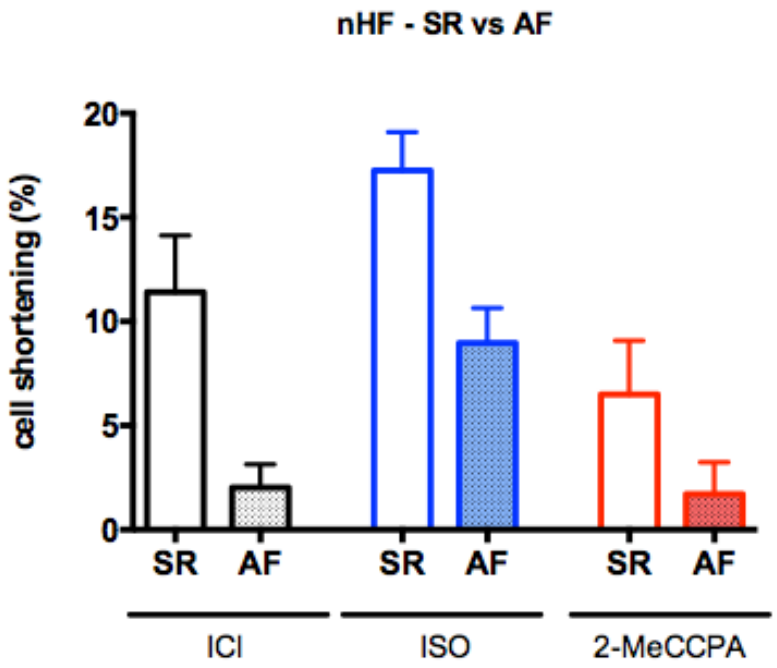

Figure 6.9: Human atrial cardiomyocyte shortening: baseline (ICI) and after selective β1AR stimulation (ICI 50nM +ISO 1μM) as well as after the specific stimulation of the A1ARs (ICI+ISO+2-MeCCPA) (N= 2 cells for SR and N= 6 cells for AF; number of patients=4).

6.3.1.4 Comparison of contraction of myocytes from patients with HF: SR versus AF

Figure 6.10 shows the comparison between SR and AF patients both with heart failure (EF<40%). In this case, as before, the data lack of the statistical power.

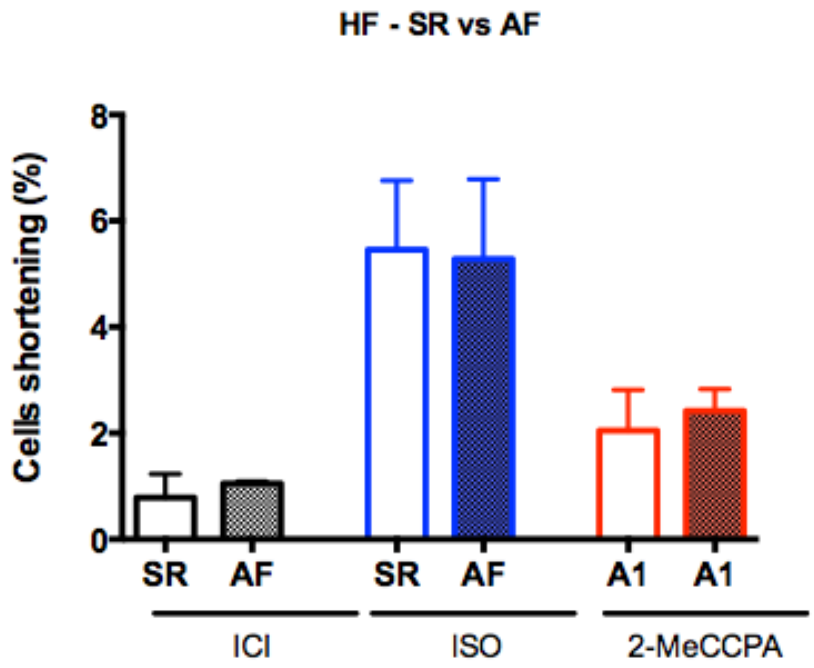

Figure 6.10: Human atrial cardiomyocyte shortening: baseline (ICI) and after selective β_1AR stimulation (ICI 50nM +ISO 1μM) as well as after the specific stimulation of the A_1ARs (ICI+ISO+2-MeCCPA) (N= 4 cells for SR and N= 2 cells for AF; number of patients=3).

6.3.1.5 Comparison of contraction of myocytes from patients with HF versus patients without HF

Lastly, we compared all patients without HF (n= 9 cells) versus patients with HF (n=6 cells), not taking into account atrial rhythm. Figure 6.11 shows the comparison of the cell shortening between the goups. No significant change was observed in the baseline of both groups. After the application of isoproterenol a significant increase was recorded in both groups (83.2± 2 % for nHF patients and 67.5±7.6 % for HF patients). After the application of the agonist for A1ARs a significant reduction was observed for both groups, as before (75.4 6.3% for nHF patients and 61.6 7.5 % for HF patients).

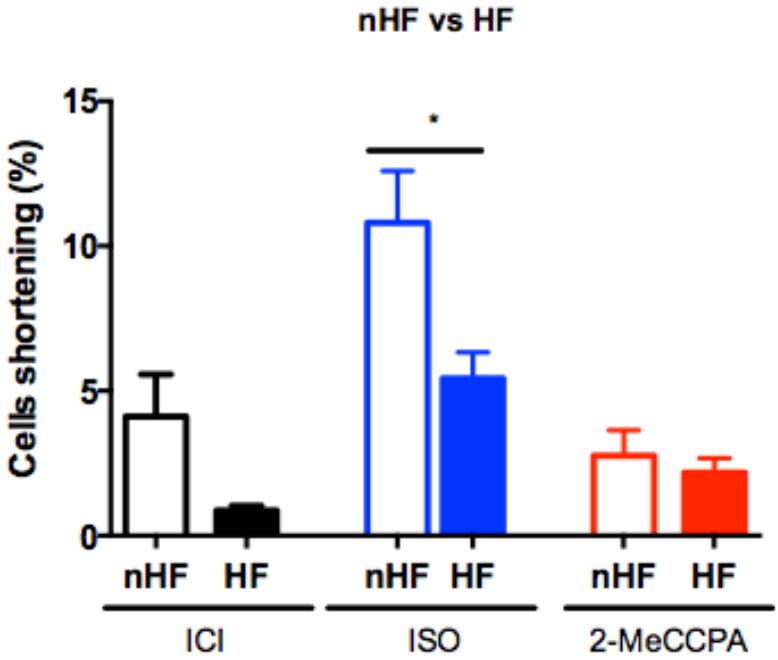

Figure 6.11: human atrial cardiomyocyte shortening: baseline (ICI) and after selective β1AR stimulation (ICI 50nM +ISO 1μM) as well as after the specific stimulation of the A1Rs (ICI+ISO+2-MeCCPA) N= 9 cells for nHF and N= 6 cells for HF.

As it has been done for rat atrial cardiomyocytes, we calculated how big was the reduction occurring after the administration of A_1AR agonist and if there were differences between the all patients. Figure 6.12 shows the reduction in shortening given by the application of 2-MeCCPA in both groups. The reduction is significantly lower ($P<0.05$) in patients with HF compared to the patients without HF.

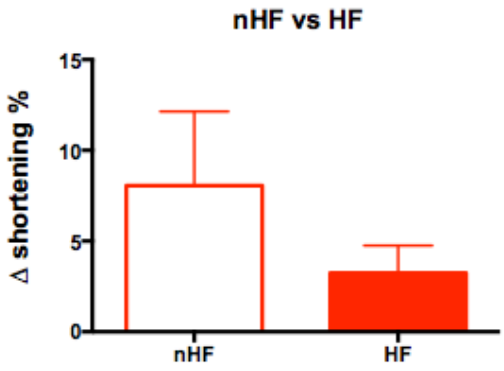

Figure 6.12: Human atrial cardiomyocyte delta shortening.

6.3.2 Whole cell cAMP level analysis in human atrial cardiomyocytes from different patients

As for rat atrial cardiomyocytes, the human cells needed to be transfected before using for the FRET experiments. After the optimization of human atrial isolation protocol (see chapter 2 of General materials and methods) we started to try to transfect the cardiomyocytes. When the atrial cardiomyocytes were isolated, they were plated and transfected with RII-epac sensor, the same sensor used for the transfection of rat atrial cardiomyoctes. RII-epac sensor is formed by the Epac cAMP binding domain fused to the regulatory subunit of PKA-RII and placed in between two fluorescent proteins: CFP and YFP (Zaccolo ans Pozzan 2002). For this reason, the sensor is localized in the cellular components associated with the particulate fraction of cellular PKA (chapter 2, Materials and Methods). After 48 hours, time needed for the full transfection of the cardiomyocytes; we checked if the transfection has occurred, and started FRET experiments, using the same protocol as was used for both EPAC1-camps TG mice and rat transfected cardiomyocytes (see figure 6.3 in Materials and Methods).
With these set of results we are able to show only very preliminary results, due to the low number of cells and patients used in the experiments; indeed, we miss the statistical power and the possibility to make real and strong

conclusions. Figure 6.13 a) shows a representative curve of the FRET response. In this case atrial cardiomyocyte was isolated from the left atrium of a patient with a preserved EF (>40 %). As we can observe from the figure, FRET shows in human cardiomyocytes a response similar to both mice and rats (see Chapter 4).

Figure 6.13 b) shows average FRET ratio change calculated for all the cells used for this set of experiments (n= 6 cells from 3 different patients, type of sample: LA from patients in AF and not HF, collected during MVrepair surgery).

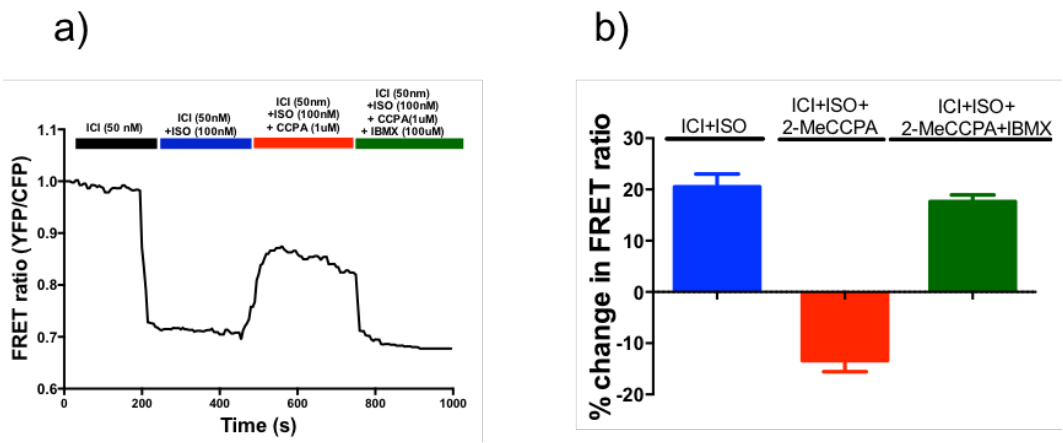

Figure 6.13 Production of cAMP following adrenergic and adenosine stimulation in human. a) A representative traces of FRET ratio of one cell incubated with the compounds as indicated above the trace; (b) Average % change in the FRET ratio following incubation with A_1AR agonist 2-MeCCPA. N= 6 cells from 3 different patients

We also transfected atrial cardiomyocytes from patients with heart failure. This samples were collected during the heart transplant procedure. (n= 3 cells from 2 different patients in AF, HT).

Figure 6.14 shows a representative curve of FRET response obtained from these patients. Interestingly, after the application of isoprotenerol, no

response at the cAMP level was recorded (arrows in the figure indicate the moment of isoproterenol application). Indeed, we can observe the baseline, no response after the adrenergic stimulation and no response after the stimulation of the A_1AR. lack of an anti-adrenergic effect given by A_1ARs agonist application could be explained by the fact that no previous adrenergic response was present either.

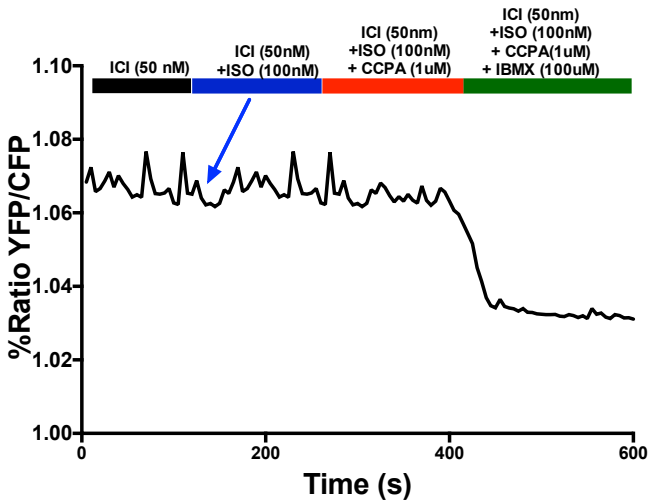

Figure 6.14: An example of one cell from a HF patient showing FRET ratio change following adenosine and β-adrenergic stimulation.

6.3.3 Adrenergic and adenosine receptors expression profile of human atrial cardiac myocytes: comparison between different patient groups

The results of the previous chapter suggested a different adenosine response between patients with HF compared to patients with no HF, although the small number of patients studied and the heterogeneity of the experimental groups, did not allow us to conclude on the possible mechanism of this difference. In order to understand better the possible

change occurred, we performed qRT-PCR to check if there were differences in the expression of the adenosine and adrenergic receptors in different patient groups examined.

6.3.3.1 Expression of mRNA e of β-adrenergic and adenosine receptors in different groups of human patients

In these set of experiments, we performed the RT-PCR in different group of patients. Fugures 15 to 18 show the mRNA expression profile of adenosine and adrenergic receptors in different groups. As we can observe, no significant changes between the groups were observed in both types of receptors.

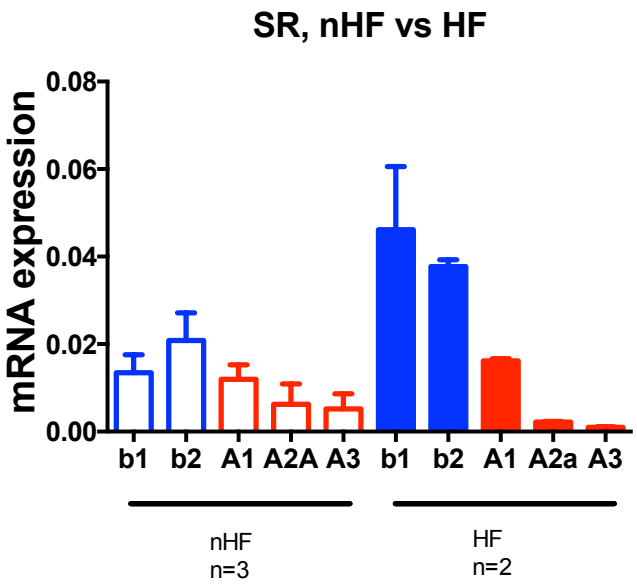

Figure 6.15: Expression of mRNA of adenosine and β-adrenergic receptorsin the myocytes from the patients with sinus rhythm with and without HF nHF n=3 patients SR HF n= 2 patients

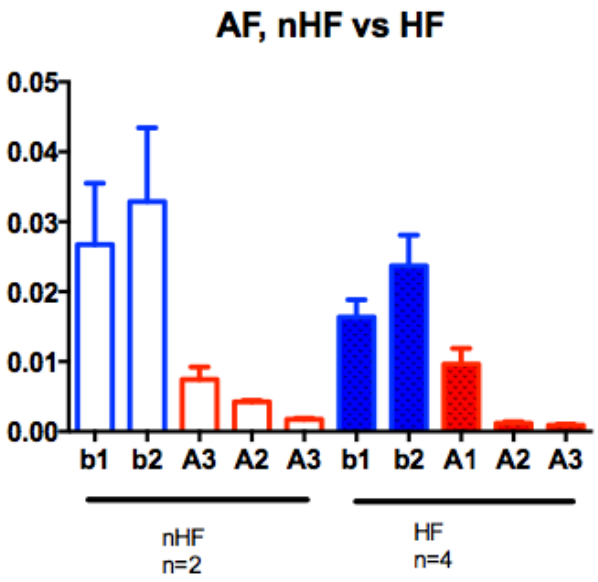

Figure 6.16: Expression of mRNA of adenosine and β-adrenergic receptorsin the myocytes from the patients with atrial fibrillation with and without HF: AF nHF n=2 patients AF HF n= 4 patients

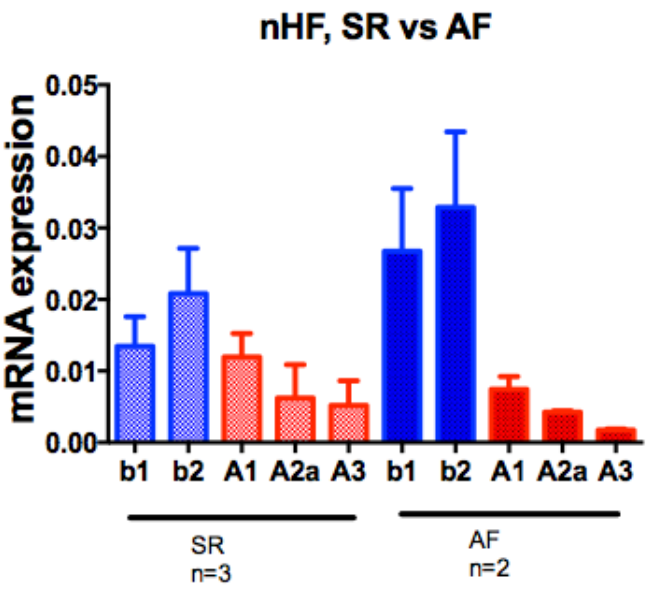

Figure 6.17: Expression of mRNA of adenosine and β-adrenergic receptorsin the myocytes from the patients without HF: comparison between SR and AF: SR n=3 patients AF n= 2 patients

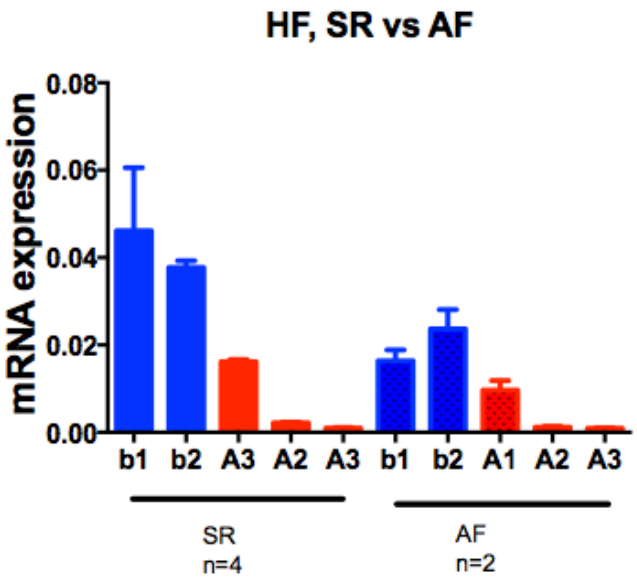

Figure 6.18 Expression of mRNA of adenosine and β-adrenergic receptorsin the myocytes from the patients with HF: comparison of SR versus AF. SR HF n=4 patients AF HF n= 2 patients.

6.3.4 Protein expression of A1 adenosine receptors in normal versus failing human atrial myocytes.

Protein expression level was assessed by western blot on atrial frozen tissue from different patients. We extracted protein from tissue of patients without and with HF. Figure 6.19 shows the protein levels normalized with the GAPDH and the respective quantification. No differences, in the levels of A_1ARs were observed between the patients with HF and patients without HF.

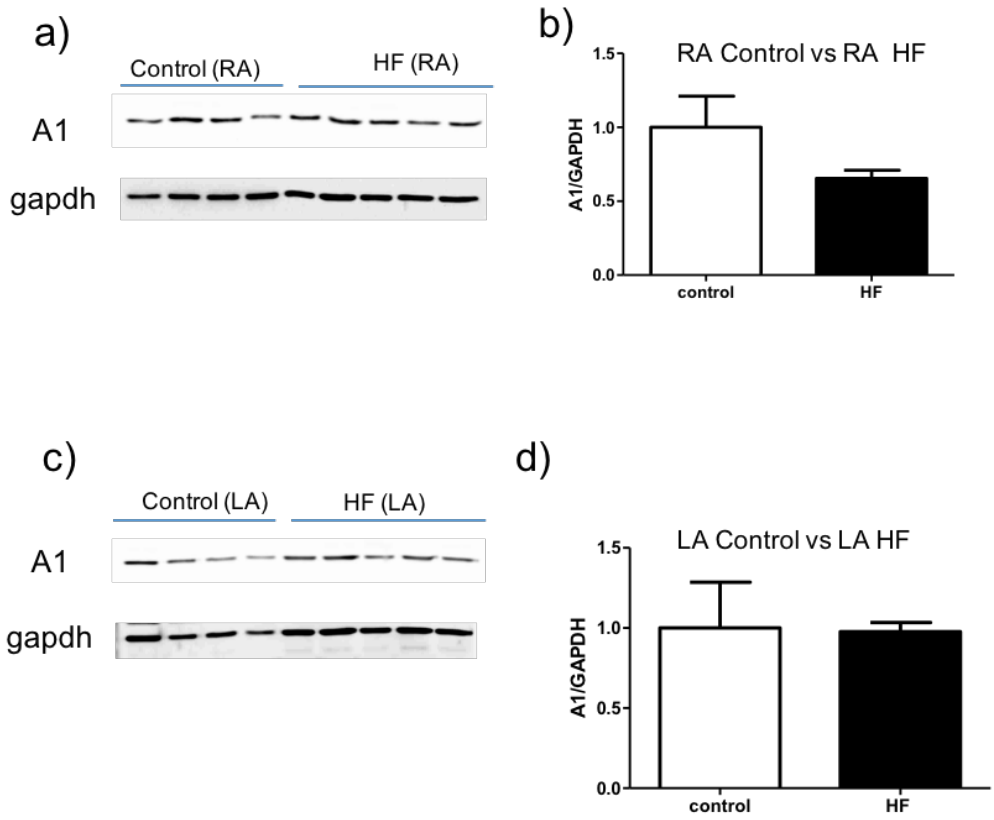

Figure 6.19: Relative protein expression of A1ARs in the human atria of patients with or without HF. a) A representative blot showing A1ARs expression in the human right atrial tissue in control and failing hearts. b) Relative average density of the A1AR band in a) normalized to the GAPDH 'housekeeping' gene band c) A representative blot showing A1ARs expression in the left atrial tissue in control and failing hearts d) Relative average density of the A1AR band in b) normalized to the GAPDH band. n=4 control n=5 HF.
A1 adenosine receptors protein levels visualization using western blot technique. Histogram shows the quantification normalized with the GAPDH

6.3.4 Protein expression of caveolin-3 in normal versus failing human atrial myocytes.

Protein expression level of cav3 was assessed by western blot using the same samples used to measure A1Ars levels. Figure 6.20 shows the protein

levels normalized with the GAPDH and the respective quantification. No differences were observed between patients with or without HF.

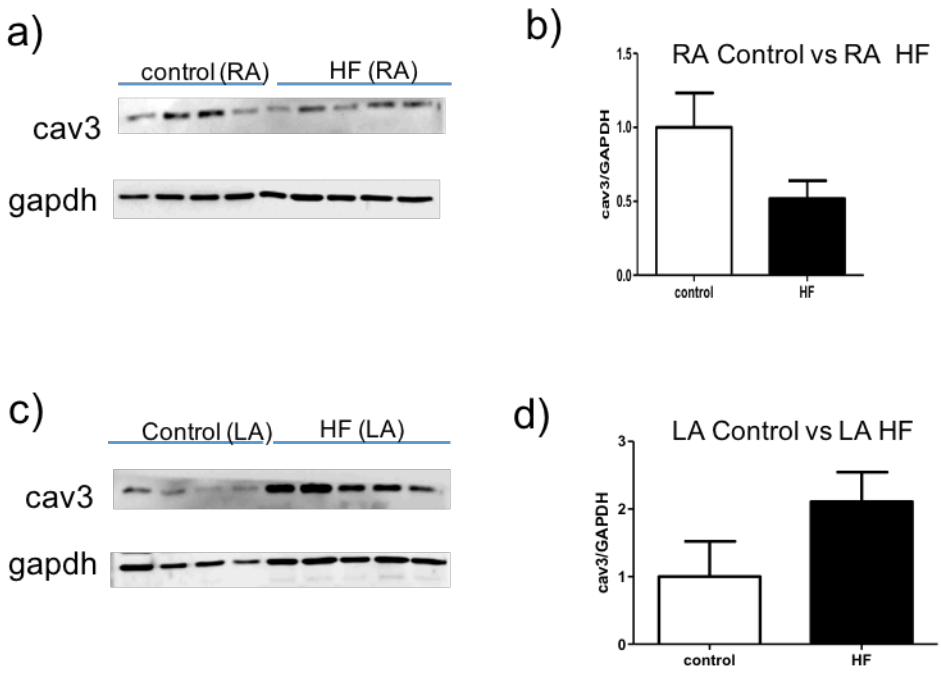

Figure 6.20: Relative protein expression of cav3 in the human atria of patients with or without HF. a) A representative blot showing cav3 expression in the human atrial tissue in control and failing hearts. b) Relative average density of the cav3 band in a) normalized to the GAPDH 'housekeeping' gene band c) A representative blot showing cav3 expression in the atrial tissue in control and failing hearts d) Relative average density of the cav3 band in b) normalized to the GAPDH band. cav3 protein levels visualization using western blot technique. Histogram shows the quantification normalized with the GAPDH.

6.4 Discussion and conclusions

The aim of this chapter was to investigate, in human atrial tissue, both functional and molecular mechanisms of the interaction between beta-adrenergic and adenosine receptors, occurring during heart failure and atrial fibrillation disorder. Predictably, the contractility at the baseline and after the application of isoproterenol is significantly lower in patients with HF. Indeed, in individuals with HF, the biology of the βARs signalling is altered drammatically as a response to the high level of endogeneous catecholamines and others factors (Bristow et al., 1990). In patients with chronic HF, the positive inotropic effects given by βARs agonists are greatly reduced (Port et al., 2001). This reduction occurring as a result of two alterations of cardiac βARs: loss of their function and possible reduction of their number (Ungerer et al., 1993). This could also explain the reason why in FRET experiments we didn' not see any response after βARs stimulation in failing atrial cardiomyocytes.

In patients in AF we observed less contractility compared to the patients in SR, however, since we collected very few cells, we were not able to make statistical analysis. Previously it has been already known that in AF patients the contractile function of the atria is temporarily impared (Schotten et al., 2001 and Logan et al., 1965). Some studies revealed that this atrial contractile dysfunction, correlated with the duration of AF, could take months before the atrial transport function was fully recovered (Manning et al., 1994 and Manning et al., 1995). Schotten et al, showed that the baseline contractility in the atrial myocardium of AF patients, was reduced by 75% (Schotten et al., 2001). This data was also confirmed by studies performed in a dog model of tachycardia-induced atrial contractile dysfunction, in which the systolic shorthening present in the atrial cardiomyocytes was drastically reduced (Sun et al., 1998).

In our contraction experiments the number of patients and cells analyzed was very small for a statistical test; meanwhile we did not see any difference in contraction in atrial myocytes from the patients with synus rhythm or atrial

fibrillation. A different situation was found when we compared all the patients without HF with all the patients with HF, not considering the rhythm. Indeed, we observed a significant reduction of the anti-adrenergic effect of A_1AR agonist after β_1ARs stimulation in failing patients compared to not failing patients. Such reduction mediated by A_1AR, suggests a crucial role of LVEF on atrial functional remodelling occurring during HF conditions. This result is also in accordance with our previous results, obtained in rat atrial cardiomyocytes, where a reduction of the anti-adrenergic effect of A_1ARs was recorded.

Our molecular analysis of gene expression of adenosine receptors did not show any statistical difference between all groups of patients, possibly due to the low number of patients used for each group. However, despite the inability to make strong statistical conclusions, a trend to an upregulation of A_1ARs was observed in patients with HF compared to patients without HF. This result is also in according with reports that showed an increase of the A_1ARs expression in mouse model of HF (Funakoshi et al., 2007; Funaya et al., 1997 and Hettinger-Smith et al., 1996). Funakoshi et al showed that cardiac adenosine levels was reduced by 70% in mouse model of HF. This reduction was accompanied by a 4-fold increase in levels of A_1ARs and a 50% reduction in the levels of A_{2a}ARs (Funakoshi et al., 2007). Perlini et al., also showed an overexpression of adenosine recptors in rat model of hypertrophy and HF (2007). Heart failure is also associated with several alterations in the βARs populations in human ventricular myocardium. Failing human left ventricles has a dcreased of the total population of βARs (Bristow et al., 1986). A reduction of the β_1AR levels of up to 50% was reported since interestingly levels of β_2AR remain constant (Freedman et al., 2004). In this chapter we found several limitations due to the fact that this is a study involving human patients and the opportunity to collect a human atrial biopsy did not come as often as for the animal studies. Indeed, the low number of patients and cells used in the experiments, was a major limitation for my project. In addition, the lack of a control human sample did

not allow us to make a comparison between the different pathologies and healthy condition.

However, in my oppinion, these results obtained in several groups of patients, may safely suggest that a remodeling of both β-adrenergic and adenosine receptors is occurring during failing conditions, since in patients with HF we did not observe any response to adrenergic stimulation at cAMP level. This also warrants for the need to perform further studies that could be very useful for getting a better view of the functional and molecular mechanisms occurring during the development of cardiac disease, especially during failing condition in atrial tissue.

CHAPTER 7. General discussion

7.1 General discussion

The research on the function and molecular mechanisms of the G-protein coupled receptors, such as beta- adrenergic and adenosine receptors plays an important role for the investigation of the physiology in the human heart and for the study of new therapeutic approaches for the patients with heart failure and atrial fibrillation. This thesis investigated the sub-cellular distribution of the A_1 adenosine receptors subtypes in atrial cardiomyocytes, suggesting a possible molecular coss-talk with the other essential receptors: β_1ARs. On the other hand, we found a close relationship between the A_1ARs and the cholesterol-rich domains, known as caveolae. Indeed, when we removed the caveolae from atrial cardiomyocytes a reduction of the A_1ARs activity was observed, suggesting also in this case a cross-talk between these two domains. A reduction of the A_1ARs activity was also reported in atrial cardiomyocytes of rat model of HF and possibly in human patients with HF, indicating the possible remodeling occurring during failing conditions of these receptors. At the same time, during failing condition an increase of A_1ARs density was shown. Such increase of A_1ARs density during failing conditions appears to follow the loss of the adenosine effects, suggesting the establishment of a potential compensatory mechanism that could be a driving factor of the failing phenotype.

7.2 Prospective

During this thesis we focused our attention mostly on the interaction occurring between A_1ARs and β_1ARs. However, in chapter 4 we also investigated the relationship between A_1ARs and β_2ARs, however we did not see any effect of A_1ARs after the selective stimulation of β_2ARs. The investigation of A1ARs signaling following both β1 and β2 ARs stimulation in rat model of HF could be useful for a better understanding of the adenosine signaling pathway occurring during HF. Both receptors are found

in T-tubule structure in ventricular cardiomyocytes; also there is evidence that they have a relationship with cav-3 proteins that also are resident on Cav-3-containing structures, caveolae.. Further experiments with SICM technique in combination with FRET, could be very helpful for the investigation of the spatial compartmentation of the resulting downstream cAMP signal. In addition, increasing the number of samples for both rats/mice and human samples and performing more RT-PCR could be very important to achieve an increase of the statistical powder and also to provide a stronger link between structural and functional remodeling occurring during heart failure.

7.3 Clinical implications

As described in chapter 6, congestive heart failure and atrial fibrillation are the major causes of morbidity and mortality in the world. The consequent number of deaths is also expected to rise in the next years. Several studies in the research are involved in the understanding that is around of the complex mechanism responsible for the heart failure condition and the related diseases, such as atrial fibrillation. In the treatment of early congestive heart failure, atrial fibrillation, hypertension, myocardial infarction and others cardiac disorders, β-blockers (antagonist of natural catecholamines) are largely prescribed to ease increased pressure on heart function by decreasing the heart rate (Prtichett et al., 2002). Also adenosine is commonly used in the diagnosis and treatment of supraventricular tachyarrhythmias. However, the administration of adenosine may be the cause of spontaneous or pacing induced atrial fibrillation. Indeed, such therapeutic approach in general are sometimes associated with severe side effects, such as problem in renal functionality (Kotecha et al., 2013). These therapeutic approaches are also limited in number due to the fact that the disease mechanisms such as heart failure and atrial fibrillationare not clearly understood. The results described in this thesis suggests possible remodeling of both β-adrenergic and adenosine receptors during failing

conditions. This work also build the foundation of further studies that could be very useful for a better view of the functional and molecular mechanisms occurring during the development of cardiac disease, especially during failing condition in atrial tissue. In addition, our results could be helpful for future studies aimed at the identification of new therapeutic approaches based around the dual modulation of both β-adrenergic and adenosine receptors signaling.

7.4 General Limitations and critical analysis

7.4.1 Differences between human and rodent cardiomyocytes.

The use of animal models of HF was for sure a good starting point, however it is important to keep in mind that there are strong species-dependent differences in the structure and in the signaling cascades of cardiomyocytes between humans and rodents. For these reasons the findings in animal models cannot be translated directly into clinical practice without taking into account the species differences.

7.4.2 Differences between right and left atrium

The results from experiments performed in chapter 3 and 4, demonstrated that the isolation of atrial cardiomyocytes from the whole atria, without a separation of the left and the right part, showed only a general picture of the receptors distribution and functionality in rat and mice atrial cardiomyocytes. Earlier reports (Kirk et al., 2003) demonstrated evidence of differences in the tissue between the left and the right atria, in particular in the cell size and the t-tubular organization. Indeed, in chapter 5 seethe evidence is presented on the differences between left and right atrium, mostly during failing conditions; both the RT-PCR and the western blot analysis clearly

showed these differences. Our results reinforce the idea the all experiments done in chapter 2 and 3, ideally should be done separately, for cardiomyocytes isolated from the left and the right atrium.

7.4.3 Human patients group

In chapter 6 we examined the possibility to do a clinical translation into human patients. As preliminary results, our finding seems good to make some suggestion about the possible mechanism occurring in several pathologies.
However, we have several study limitations:

- We miss the statistical powder due to low number of patients and cells we examined;

- We miss control human samples to make a comparison. Indeed, the only occasion when we may obtain a human control heart was when there was a rejection during the heart transplantation, which does not occur very often.

- Lack of homogeneity between groups was observed throughout the research.

7.4.4 Western blot experiments

Time did not permit to perform Western blot analysis for all β-adrenergic and adenosine receptors.
Indeed, as we can observe in chapter 5 and 6 we only performed the western blot analysis for A1 adenosine receptors and Cav3.
The choice not to perform the anlaysis of the proteins levels for all β-adrenergic receptors was due in part for low expression levels of β-

adrenergic receptors and furthermore due to the fact the antibodies we could get were considered to be not reliable. The antibodies that we found were poor and mostly they are not well cited in the literature.

7.5 Conclusions

Adenosine plays a crucial role in the heart and can elicit a variety of physiological effects in different tissues, acting through the interaction with the specific receptor subtypes: A_1ARs, A_{2a}AR and A_3AR.

Adenosine exerts a wide range of beneficial effect in the heart and is also released from metabolically compromised cells to mediate responses directed ti optimizing the balance between energy utilization and generation (Headrick et al., 2011; Olsson et al., 1990 and Shryock et al., 1997). For example, several studies have shown that myocardial levels of adenosine increase during even brief periods of ischemia and mediate the phenomenon of ischemia preconditioning (Ely and Berne, 1992; Newby et al., 1990 and Heyndrickx et al., 1975).

Far less is known about the role of adenosine receptors in the failing heart. Previous studies suggest that circulating levels of adenosine are elevated in patients with heart failure (Funaya et al., 1997); however, the consequences that the left ventricular dysfunction can have on the atrial myocardium levels remain unknown. Some studies in transgenic mice suggest that overexpression of selective adenosine receptor subtypes can actually be associated with compromised left ventricular dysfunction (Ashton et al., 2007; Matherne et al., 1997 and Gauthier, 1998).

In the present thesis, we demonstrate that adenosine A_1 receptors activity is significantly decreased in failing atrial cardiomyocytes and in cardiomyocytes with caveolae depletion, suggesting a possible cross-talk between these two components. The changes we observed are most likely associated with alterations in the levels of the adenosine receptor subtypes. Indeed, we observed an uperegulation of A_1AR subtype in failing left atria as compared to control. This increase appears to follow the loss of the

A_1ARs effects, suggesting the establishment of a potential compensatory mechanism that could be a driving factor of the failing phenotype. Although the findings of this thesis provide important information about the biology of the receptor signaling of adenosine receptors in the heart, they also have important therapeutic implications. For example, based on the premise that adenosine levels are alterated in the failing heart, the clinical trials could evaluate the role of using receptor-specific adenosine agonists and antagonists in the treatment of patients with heart failure.

The results obtained during this thesis suggest the need to learn more about the biological effects of the activity of adenosine receptors to safely and effectively develop new drugs for the treatment of different cardiovascular disorders.

CHAPTER 8

References:

Ahmad F, Shen W, Vandeput F, Szabo-Fresnais N, Krall J, Degerman E, Goetz F, Klussmann E, Movsesian M, Manganiello V. (2015) Regulation of sarcoplasmic reticulum Ca^{2+}ATPase 2 (SERCA2) activity by phosphodiesterase 3A (PDE3A) in human myocardium: phosphorylation-dependent interaction of PDE3A1 with SERCA2. *J Biol Chem*. 290(11):6763- 76

Amin, P., Singh, M. & Singh, K., 2011. β-Adrenergic Receptor-Stimulated Cardiac Myocyte Apoptosis: Role of β1 Integrins. Journal of signal transduction, 2011, p.179057.

Amy Cavalli, Mansoureh Eghbali, Tamara Y Minosyan, Enrico Stefani, Kenneth D. Philipson. Localization of sarcolemmal proteins to lipid rafts in the myocardium Cell Calcium 42 (2007) 313–322

Ansari H, Teng B, Nadeem A, Schnermann J, Mustafa S. A1 adenosine receptor-activated protein kinase C signaling in A1 knock-out mice coronary artery smooth muscle cells. FASEB J. 2008;22:1152.11.

Anumonwo, J. M., Y. N. Tallini, et al. (2001). "Action potential characteristics and arrhythmogenic properties of the cardiac conduction system of the murine heart." Circ Res **89**(4): 329-335.

Ashton KJ, Peart JN, Morrison RR, Matherne GP, Blackburn MR, and Headrick JP (2007) Genetic modulation of adenosine receptor function and adenosine handling in murine hearts: insights and issues. J Mol Cell Cardiol 42:693–705

Audet M and Bouvier. Restructuring G-Protein- Coupled Receptor Activation. 28 2012. Cell 151. Pages 14-23

Barrese V, Taglialatela M. New advances in beta-blocker therapy in heart failure. Front Physiol. 2013;4:323. doi: 10.3389/fphys.2013.00323.

Belhassen B, Pelleg A (1984) Acute management of paroxysmal supraventricular tachycardia: Verapamil, adenosine triphos- phate or adenosine? Am J Cardiol 54: 225-227

Bellet S. Clinical Disorders of the Heart Beat. 3rd ed. Philadelphia: Lea & Febiger, 1971

Benjamin E J, Wolf PA, D'Agostino RB, Silbershatz H, Kannel WB, Levy D. Impact of atrial fibrillation on the risk of death: the Framingham Heart Study. Circulation 1998;98:946-952

Benjamin EJ, Levy D, Vaziri SM, D'Agostino RB, Belanger AJ, Wolf PA. Independent risk factors for atrial fibrillation in a population-based cohort: the Framingham Heart Study. *JAMA*. 1994;271:840–844.

Bers, D. M. (2002). Cardiac excitation-contraction coupling. Nature 415, 198–205. doi: 10.1038/415198a

Bers, D. M. *Excitation–Contraction Coupling and Cardiac Contractile Force* edn 2 (Kluwer Academic, Dordrecht, Netherlands, 2001).

Black, R. G., Jr., Guo, Y., Ge, Z. D., Murphree, S. S., Prabhu, S. D., Jones, W. K., et al. (2002). Gene dosage-dependent effects of cardiac-specific overexpression of the A3 aden- osine receptor. Circ Res 91, 165–172.

Boateng SY, Lateef SS, Mosley W, Hartman TJ, Hanley L, Russell B. RGD and YIGSR synthetic peptides facilitate cellular adhesion identical to that of laminin and fibronectin but alter the physiology of neonatal cardiac myocytes. Am J Physiol Cell Physiol. 2005;288:C30–C38.

Böhm, M., Pieske, B., Ungerer, M., & Erdmann, E. (1989). Characterization of A1 adeno- sine receptors in atrial and ventricular myocardium from diseased human hearts. Circ Res 65, 1201–1211.

Bootman, M. D., I. Smyrnias, et al. (2011). "Atrial cardiomyocyte calcium signalling." Biochim Biophys Acta **1813**(5): 922-934.

Borst M.M., Schrader J. Adenine nucleotide release from isolated perfused guinea pig hearts and extracellular formation of adenosine. Circ Res. 1991 Mar;68(3):797-806.

Brandenburg S, Arakel EC, Schwappach B, Lehnart SE. The molecular and functional identities of atrial cardiomyocytes in health and disease. Biochim Biophys Acta. 2016;1863(7 Pt B):1882–1893.

Braunwald E, Frahm CJ. Studies on starling's law of the heart: IV. Observations on the hemodynamic functions of the left atrium in man. *Circulation*. 1961;**24**:633–642

Brette F, Despa S, Bers DM, Orchard CH (2005) Spatiotemporal characteristics of SR Ca(2+) uptake and release in detubulated rat ventricular myocytes. *J Mol Cell Cardiol* 39:804–812.

Brette F, Salle L, Orchard CH (2004) Differential modulation of L-type Ca2+ current by SR Ca2+ release at the T-tubules and surface membrane of rat ventricular myocytes. *Circ Res* 95:1–7.

Brette, F., K. Komukai, et al. (2002). "Validation of formamide as a detubulation agent in isolated rat cardiac cells." Am J Physiol Heart Circ Physiol **283**(4): H1720- 1728.

Bristow M.R., Ginsburg R, Minobe W, Cubiciotti R.S, Safeman W.S., Lurie K, Bellingham M.E, Harrison DC and Stinson B. Decreased catecholamine sensitivity and beta- adrenergic receptor density in failing human heart. *N. Engl. J. Med.* 307: 205–211, 1982.

Brodde OE, Michel MC. Adrenergic and muscarinic receptors in the human heart. *Pharmacol Rev*. 1999;51:651–690

Brodde OE. Adrenoceptors in cardiac disease. *Pharmacol Ther*. 1993; 60:405– 430.

Brooker, G., Harper, J.F., Terasaki, W.L. & Moylan, R.D. Radioimmunoassay of cyclic AMP and cyclic GMP. *Adv. Cyclic. Nucleotide Res.* **10**, 1–33 (1979).

Calaghan, S. and E. White (2006). "Caveolae modulate excitation-contraction coupling and beta2-adrenergic signalling in adult rat ventricular myocytes." Cardiovasc Res **69**(4): 816-824.

Camm AJ, Garratt CJ. Adenosine and supraventricular tachy- cardia. *N Engl J Med*. 1991;325:1621–1629. doi: 10.1056/ NEJM199112053252306.

Carafoli, E., L. Santella, et al. (2001). "Generation, control, and processing of cellular calcium signals." Crit Rev Biochem Mol Biol 36(2): 107-260.

Carmeliet and Vereecke, Cardiac cellular electrophysiology. Chapter V-IV. 2002

Cavalli A*, Eghbali M, Minosyan TY, Stefani E, Philipson KD* Caveolin-3 null mice show a loss of caveolae, changes in the microdomain distribution of the dystrophin-glycoprotein complex, and t-tubule abnormalities.
Cell Calcium. 2007 Sep; 42(3):313-22.

Chandrasekera, P.C. et al., 2013. Adenosine A1 receptors heterodimerize with β1- and β2-adrenergic receptors creating novel receptor complexes with altered G protein coupling and signalling. Cellular signalling, 25(4), pp.736–42.

Chang WJ, Rothberg KG, Kamen BA, Anderson RG Lowering the

cholesterol content of MA104 cells inhibits receptor-mediated transport of folate. 1992 10.1083/jcb.118.1.63

Chien KR, Knowlton KU, Zhu H, and Chien S. Regulation of cardiac gene expression during myocardial growth and hypertrophy: molecular studies of an adaptive physiologic response. FASEB J 5: 3037–3046, 1991

Chung ES, Perlini S, Aurigemma GP, Fenton RA, Dobson JG Jr, and Meyer TE (1998) Effects of chronic adenosine uptake blockade on adrenergic responsiveness and left ventricular chamber function in pressure overload hypertrophy in the rat. *J Hypertens* **16**:1813–1822.

Ciruela F, Casadó V, Rodrigues RJ, Luján R, Burgueño J, Canals M, Borycz J, Rebola N, Goldberg SR, Mallol J, Cortes A, Canela EI, Loepz-Gimenez JF, Milligan G, Lluis C, Cunha RA, Ferre S, Franco R. The Journal of Neuroscience. 2006; 26:2080.

Communal, C. et al., 1999. Opposing Effects of 1- and 2-Adrenergic Receptors on Cardiac Myocyte Apoptosis : Role of a Pertussis Toxin-Sensitive G Protein. Circulation, 100(22), pp.2210–2212.

Conti M, Beavo J. (2007) Biochemistry and physiology of cyclic nucleotide phosphodiesterases: essential components in cyclic nucleotide signaling. *Annu. Rev. Biochem*. 76:481-511.

Cordeiro, J. M., K. W. Spitzer, et al. (2001). "Location of the initiation site of calcium transients and sparks in rabbit heart Purkinje cells." J Physiol **531**(Pt 2): 301-

Correll, R. N., C. Pang, et al. (2007). "Plasma membrane targeting is essential for Rem-mediated Ca2+ channel inhibition." J Biol Chem **282**(39): 28431-28440.

Cranefield PF,Aronson RS: inCardiac Arrhythmias. TheRole of Triggered Activity and Other Mechanisms. Mt Kisco,NY,Futura Publishing Co, 1988

Datino T, Macle L, Qi XY, Maguy A, Comtois P, Chartier D, Guerra PG, Arenal A, Fernández-Avilés F, Nattel S. Mechanisms by which adenosine restores conduction in dormant canine pulmonary veins. *Circulation*. 2010;121:963–972. doi: 10.1161/CIRCULA- TIONAHA.109.893107.

Deussen A., H.G. Lloyd, J. Schrader Contribution of S-adenosylhomocysteine to cardiac adenosine formation J. Mol. Cell. Cardiol., 21 (1989), pp. 773–782

Di Marco JP, Sellers TD, Berne RM, West GA, Belardinelli L (1983) Adenosine: Electrophysiologic effects and therapeutic use for terminating paroxysmal supraventricular tachycardia. Circula- tion 6: 1254-1263.

Dobrev, D., Teos, L.Y. & Lederer, W.J., 2009. Unique atrial myocyte Ca2+ signalling. Journal of molecular and cellular cardiology, 46(4), pp.448–51.

Dobson, J.G., 1983. Mechanism of adenosine inhibition of catecholamine-induced responses in heart. Circulation Research, 52(2), pp.151–160.

Donal E, Raud-Raynier P, De Place C, Gervais R, Rosier A, Roulaud M, Ingels A, Carre F, Daubert JC, Denjean A. Resting echocardiographic assessments of left atrial function and filling pressure interest in the understanding of exercise capacity in patients with chronic congestive heart failure. *J Am Soc Echocardiogr*. 2008;**21**:703–710. doi: 10.1016/j.echo.2007.10.002

Dusan B. Velimirovic. Ventricular myocardial band concept and ventricular resynchronization device therapy: crossing the roads? European Journal of Cardio-Thoracic Surgery, Volume 30, Issue 5, 1 November 2006, Pages 816–817,

Ehrlich JR, Nattel S., Honloser SH. Atrial Fibrillation and Congestive Heart Failure: Specific Considerations at the Intersection of Two Common and Important Cardiac Disease Sets. J Cardiovasc Electrophysiol. 2002;13:399-405

Ely S.W., Berne R.M..Protective effects of adenosine in myocardial ischemia Circulation, 85 (1992), pp. 893-904

Endoh M & Yamashita S. Adenosine antagonizes the positive inotropic action mediated via β-, but not α-adrenoceptors in the rabbit papillary muscle. European Journal of Pharmacology. 1980.445-448

Engelhardt S, Bohm M, Erdmann E, Lohse MJ. Analysis of -adrenergic receptor mRNA levels in human ventricular biopsy specimens by quantitative polymerase chain reactions. *J Am Coll Cardiol*. 1996;27:146–154.

Esler M, Kaye D, Lambert G, et al. Adrenergic nervous system in heart failure. Am J Cardiol. 1997;80:7L–14L

Fabiato, A. and F. Fabiato (1979). "Calcium and cardiac excitation-contraction coupling." Annu Rev Physiol **41**: 473-484.

Feldman AM, Koch WJ, Force TL. Developing strategies to link basic cardiovascular sciences with clinical drug development: another opportunity for translational sci- ences. Clin Pharmacol Ther. 2007;81(6):887–92.

Fenton, R. A & Dobson, J.G., 1987. Measurement by fluorescence of interstitial adenosine levels in normoxic, hypoxic, and ischemic perfused rat hearts. Circulation Research, 60(2), pp.177–184.

Fenton, R. A. & Dobson, J.G., 1993. Hypoxia enhances isoproterenol-induced increase in heart interstitial adenosine, depressing beta-adrenergic contractile responses. Circulation Research, 72(3), pp.571–578.

Fenton, R.A, Moore E. D, Fay F. S., Dobson J. G. Adenosine reduces the Ca2+ transients of isoproterenol-stimulated rat ventricular myocytes. The

American journal of physiology, 1991. 261(6 Pt 1), pp.C1107–14.
Fischmeister, R., Castro, L. R., Abi-Gerges, A., Rochais, F., Jurevicius, J., Leroy, J., et al. (2006). Compartmentation of cyclic nucleotide signaling in the heart: the role of cyclic nucleotide phosphodiesterases. Circ. Res. 99, 816–828. doi: 10.1161/01.RES.0000246118.98832.04

Forbes M.S., Van Neil E.E., Membrane systems of guinea pig myocardium: ultra- structure and morphometric studies, Anat. Rec. 222 (1988) 362–379.

Fredholm, B. B., Arslan, G., Halldner, L., Kull, B., Schulte, G., & Wasserman, W. (2000). Structure and function of adenosine receptors and their genes. Naunyn Schmiedebergs Arch Pharmacol 362, 364–374.

Fredriksson R, Lagerström M. C., Lundin Lars-Gustav and. Schiöth H. B The G-Protein-Coupled Receptors in the Human Genome Form Five Main Families. Phylogenetic Analysis, Paralogon Groups, and Fingerprints. Molecular Pharmacology June 2003, 63 (6) 1256-1272

Freedman NJ, Lefkowitz RJ. Anti-beta(1)-adrenergic receptor antibodies and heart failure: causation, not just correlation. J Clin Invest. 2004;113:1379–82.

Frisk, M., J. T. Koivumaki, et al. (2014). "Variable t-tubule organization and Ca2+ homeostasis across the atria." Am J Physiol Heart Circ Physiol **307**(4): H609- 620.

Funakoshi H., Zacharia L C., Tang z, Zhang J, Ling L. Lee, Good JC,. Herrmann DE, Higuchi Y, J. Koch W, Jackson E, Tung O. Chan, Feldman AM. A1 Adenosine Receptor Upregulation Accompanies Decreasing Myocardial Adenosine Levels in Mice With Left Ventricular Dysfunctio. Circulation. 2007;115:2307-2315

Funaya H, Kitakaze M, Node K, Minamino T, Komamura K, and Hori M (1997). Plasma adenosine levels increase in patients with chronic heart failure. Circulation 95:1363–1365.

G. Isenberg. Cardiac Purkinje fibers: Cesium as a tool to block inward rectifying potassium currents.1976. Pflügers Archiv 365: 99.

Galbiati F, Engelman JA, Volonte D, Zhang XL, Minetti C, Li M, Hou H Jr, Kneitz B, Edelmann W, Lisanti MP J Biol Chem. 2001 Jun 15; 276(24):21425-33

Gan XT, Rajapurohitam V, Haist JV, Chidiac P, Cook MA, and Karmazyn M. Inhibition of Phenylephrine-Induced Cardiomyocyte Hypertrophy by Activation of Multiple Adenosine Receptor Subtypes. JPET 312:27–34, 2005

Gauthier NS, Headrick JP, Matherne GP. Myocardial function in the working mouse heart overexpressing cardiac A1 adenosine receptors. *J Mol Cell Cardiol*. 1998;30:187–193.

Germack R, Dickenson JMBr .Characterization of ERK1/2 signalling pathways induced by adenosine receptor subtypes in newborn rat cardiomyocytes. J Pharmacol. 2004 Jan; 141(2):329-39

Ginés S, Hillion J, Torvinen M, Le Crom S, Casadó V, Canela EI, Rondin S, Lew JY, Watson S, Zoli M, Agnati LF, Verniera P, Lluis C, Ferre S, Fuxe K, Franco R. Proceedings of the National Academy of Sciences. 2000; 97:8606.

Glukhov AV, Balycheva M, Sanchez-Alonso JL, Ilkan Z, Alvarez-Laviada A, Bhogal N, Diakonov I, Schobesberger S, Sikkel MB, Bhargava A, Faggian G, Punjabi PP, Houser SR, Gorelik J. Direct Evidence for Microdomain–Specific Localization and Remodeling of Functional L-Type Calcium Channels in Rat and Human Atrial Myocytes. Circulation. 2015 Dec 22;132(25):2372-84.

Gorelik, J. Wright P, Lyon AR, Harding SE. Spatial control of the βAR system in heart failure: the transverse tubule and beyond. 2013.Cardiovascular research, 98(2), pp.216–24.

Gossop, M. R. and P. H. Connell. Attitudes of oral and intravenous multiple Drug Users toward Drugs of Abuse. 1975 Int J Addict 10: 459-472.

Granata R, Settanni F, Trovato L, et al. RFamide peptides 43RFa and 26RFa both promote survival of pancreatic cells and human pancreatic islets but exert opposite effects on insulin secretion. *Di- abetes.* 2014;63:2380–2393.

Gray H (1918) The heart In Lewis W H Anatomy of the human body (20th ed.) New York: Bartleby.com.

Haft, J. I. Cardiovascular injury induced by sympathetic catecholamines. 1974 Prog Cardiovasc Dis **17**(1): 73-86.

Han J., Wu H, Wang Q, Wang S. (2013) Morphogenesis of T-tubules in heart cells: The role of junctophilin-2 *Science China Life Sciences*. 56, 647-652

Hansma P.K., Drake B., Marti O., Gould S.A., Prater C.B. (1989) The scanning ion- conductance microscope. *Science*. 243(4891):641-3.

Head, B. P., H. H. Patel, et al. (2005). "G-protein-coupled receptor signaling components localize in both sarcolemmal and intracellular caveolin-3-associated microdomains in adult cardiac myocytes." J Biol Chem 280(35): 31036-31044.

Headrick J.P,. Matherne G.P, Berne R.M. Myocardial adenosine formation during hypoxia: effects of ecto-5-nucleotidase inhibition J. Mol. Cell. Cardiol., 24 (1992), pp. 295–304

Headrick J.P., Pearta JN, Reicheltb ME, Haselera LJ. Adenosine and its receptors in the heart: Regulation, retaliation and adaptation. Biochimica et Biophysica Acta 1808 (2011) 1413–1428

Hein, T. W., Belardinelli, L., & Kuo, L. (1999). Adenosine A_{2A} receptors mediate coronary microvascular dilation to adenosine: role of nitric oxide and ATP-sensitive potassium channels. J Pharmacol Exp Ther 291, 655–664.

Hettinger-Smith BD, Leid M, Murray TF. Chronic exposure to adenosine receptor agonists and antagonists reciprocally regulates the A1 adenosine receptor-adenylyl cyclase system in cerebellar granule cells. *J Neurochem*. 1996;67:1921–1930.

Hill S. (2006) G-protein-coupled receptors: past, present and future. *Brit. J. Pharmac.* 147 S27-37

Hinschen, A. K., Rose'Meyer, R. B., & Headrick, J. P. (2003). Adenosine receptor subtypes mediating coronary vasodilation in rat hearts. J Cardiovasc Pharmacol 41, 73–80.

Hisatome I Adenosine and cardioprotection in chronic heart failure: genes and protein expression. Hypertens Res. 2007 Sep;30(9):757-8.

Heyndrickx GR, Millard RW, McRitchie RJ, Maroko PR, Vatner SF: Regional myocardial function and electrophysiological alter- ations after brief coronary artery occlusion in conscious dogs. J Clin Invest 1975;56:978-985

Hoit BD. Left atrial size and function: role in prognosis. *J Am Coll Cardiol*. 2014;**63**:493–505. doi: 10.1016/j.jacc.2013.10.055.

Hong T.T., Smyth J.W., Gao D., Chu K.Y., Vogan J.M., Fong T.S., Jensen B.C., Colecraft H.M., Shaw R.M. (2010) BIN1 localizes the L-type calcium channel to cardiac T-tubules. *PLoS Biol.* 8(2):e1000312

Hopkins PM, Skeletal muscle physiology. Continuing Education in Anaesthesia Critical Care & Pain, Volume 6, Issue 1, 1 February 2006

Hove-Madsen L, Prat-Vidal C, Llach A, Ciruela F, Casado V, Lluis C, Bayes-Genis A, Cinca J, Franco R. Adenosine A2A receptors are expressed in human atrial myocytes and modulate spontaneous sarcoplasmic reticulum calcium release. Cardiovasc Res. 2006;72:292-302.

Huser, J., S. L. Lipsius, et al. (1996). "Calcium gradients during excitation contraction coupling in cat atrial myocytes." J Physiol **494 (Pt 3)**: 641-651.

Iwasaki Y., Nishida K, Kato T, Nattel S. Atrial Fibrillation Pathophysiology. Circulation. 2011;124:2264-2274

Johnson E.A,. & Mckinnon M.G. Effect of acetylcholine and adenosine on cardiac cellular potentials.Nature, 1956. 178,1174-1175

Kabell G, Buchanan LV, Gibson JK, Belardinelli L. Effects of ad- enosine on atrial refractoriness and arrhythmias. *Cardiovasc Res*. 1994;28:1385–1389.

K.S. Song, P.E. Scherer, Z.L. Tang, T. Okamoto, S. Li, M. Chafel, C. Chu, D.S. Kohtz, M. P. Lisanti, Expression of caveolin-3 in skeletal, cardiac, and smooth muscle cells: caveolin-3 is a component of the sarcolemma and co-fractionates with dystrophin and dystrophin-associated glycoproteins, J. Biol. Chem. 271 (1996) 15160–15165.

Kaftan, E., A. R. Marks, et al. (1996). "Effects of rapamycin on ryanodine receptor/Ca(2+)-release channels from cardiac muscle." Circ Res **78**(6): 990- 997.

Kapicka, C. L., Montamat, S. C., Olson, R. D., Musser, B., Mudumbi, R. V.,& Vestal, R. E. (2003). Species comparison of adenosine A_1 receptors in isolated mammalian atrial and ventricular myocardium. Life Sci 72, 2825–2838.

Khairy, P. and S. Nattel (2002). "New insights into the mechanisms and management of atrial fibrillation." CMAJ **167**(9): 1012-1020.

Kirk MM, Izu LT, Chen-Izu Y, McCulle SL, Wier WG, Balke CW et al. Role of the transverse-axial tubule system in generating calcium sparks and

calcium transients in rat atrial myocytes. J Physiol 2003;547:441–451.

Klabunde R E 2011Cardiovascular Physiology Concepts (Philadelphia, PA: Williams & Wilkins).

Kleinman HK, Cannon FB, Laurie GW, Hassell JR, Aumailley M, Terranova VP, et al. Biological activities of laminin. J Cell Biochem. 1985;27:317–25.

Knollmann, B.C. & Roden, D.M. A genetic framework for improving arrhythmia therapy. 2008. Nature, 451(7181), pp.929–36.

Kockskämper, J. & Pieske, B., 2006. Phosphorylation of the cardiac ryanodine receptor by Ca2+/calmodulin-dependent protein kinase II: the dominating twin of protein kinase A? Circulation research, 99(4), pp.333–5.

Kurachi Y, Nakajima T, Sugimoto T. On the mechanism of activation of muscarinic K+ channels by adenosine in isolated atrial cells: involvement of GTP-binding proteins. Pflügers Archiv. 1986, Volume 407, Issue 3, pp 264–274.

Kuschel, M. et al., 1999. Gi Protein-mediated Functional Compartmentalization of Cardiac β2 -Adrenergic Signalling. Journal of Biological Chemistry, 274, pp.22048–22052.

Lammerant J & Becse,I. Left ventricular contractility and developed tension in the intact dog submited to an intracoronary infusion of adenosine. 1973J. Physiol., 229, 41-49.

Lasley, R.D.,. Adenosine receptors and membrane microdomains. 2011Biochimica et biophysica acta, 1808(5), pp.1284–9.

Lavoie C, Mercier JF, Salahpour A, Umapathy D, Breit A, Villeneuve LR, Zhu WZ, Xiao RP, Lakatta EG, Bouvier M, Hébert TE. Journal of Biological Chemistry. 2002; 277:35402.

Lee D.I., Zhu G., Sasaki T., Cho G.S., Hamdani N., Holewinski R., Jo S.H., Danner T., Zhang M., Rainer P.P., Bedja D., Kirk J.A., Ranek M.J., Dostmann W.R., Kwon C., Margulies K.B., Phosphodiesterase 9A controls nitric-oxide-independent cGMP and hypertrophic heart disease. 2015. Nature 519, 472–476

Leimbach WN Jr, Wallin BG, Victor RG, Aylward PE, Sundlöf G, Mark AL Direct evidence from intraneural recordings for increased central sympathetic outflow in patients with heart failure. Circulation. 1986 May; 73(5):913-9.

Levick Scott P., Murray David B.,. Janicki Joseph S, Gregory L. Brower. Sympathetic Nervous System Modulation of Inflammation and Remodeling in the Hypertensive Heart. 2010. Hypertension.55:270-276.

Li X, Liu M, Sun R, Zeng Y, Chen S, Zhang P (2016) Protective approaches against myocardial ischemia reperfusion injury. Exp Ther Med 12(6):3823–3829

Liang BT and Gross GJ. Direct preconditioning of cardiac myocytes via opioid receptors and KATP channels. *Circ Res* **84**: 1396–1400, 1999.

Light PE, Bladen C, Winkfein RJ, Walsh MP, and French RJ. Molecular basis of protein kinase C-induced activation of ATP-sensitive potassium channels. *Proc Natl Acad Sci USA* **97**: 9058–9063, 2000.

Linden J, Hollen CE, Patel A: The mechanism by which adenosine and cholinergic agents reduce contractility in rat myocardium. Correlation with cyclic adenosine monophos- phate and receptor densities. *Ore Res* 1985;56:728-735

Lipp P, Huser J, Pott L, Niggli E (1996) Spatially non-uniform Ca signals induced by the reduction of transverse tubules in citrate-loaded guinea-pig ventricular myocytes. *J Physiol (Lond)* **497**:589–597.

Llach A, Molina CE, Prat-Vidal C, Fernandes J, Casadó V,Ciruela F, Lluís C, Franco R, Cinca J, Hove-Madsen . Abnormal calcium handling in atrial fibrillation is linked to up-regulation of adenosine A2A receptors. 2011.European heart journal, 32(6), pp.721–9.

Lloyd-Jones DM, Larson MG, Leip EP, et al. Lifetime risk for developing congestive heart failure: the Framingham Heart Study. Circulation. 2002;106:3068-72.

Lohse, M.J., Engelhardt, S. & Eschenhagen, T., 2003. What is the role of beta-adrenergic signalling in heart failure? Circulation research, 93(10), pp.896–906.

Lompre, A. M., Hajjar, R. J., Harding, S. E., Kranias, E. G., Lohse, M. J., and Marks, A. R. (2010). Ca2+ cycling and new therapeutic approaches for heart failure. Circulation 121, 822–830. doi: 10.1161/CIRCULATIONAHA.109. 890954

Londos, C., Cooper, D. M. & Wolff, J. Subclasses of external adenosine receptors. *Proc. Natl Acad. Sci. USA* **77,** 2551–2554 (1980)

Lou Q, Hansen BJ, Fedorenko O, Csepe TA, Kalyanasundaram A, Li N, Hage LT, Glukhov AV, Billman GE, Weiss R, Mohler PJ, Györke S, Biesiadecki BJ, Carnes CA, Fedorov VV. Upregulation of adenosine A1 receptors facilitates sinoatrial node dysfunction in chronic canine heart failure by exacerbating nodal conduction abnormalities revealed by novel dual-sided intramural optical map- ping. *Circulation*. 2014;130:315–324.

Louch WE, Louch WE, Mørk HK, Sexton J,Strømme TA, Laake P, Sjaastad I,Sejersted OM T-tubule disorganization and reduced synchrony of Ca2+ release in murine cardiomyocytes following myocardial infarction. 2006.*J Physiol (Lond)* **574**:519–533.

Lundgren E, Gullberg D, Rubin K, Borg TK, Terracio MJ, Terracio L. In vitro studies on adult cardiac myocytes: attachment and biosynthesis of collagen type IV and laminin. J Cell Physiol. 1988;136:43–53.

Lyon AR, MacLeod KT, Zhang Y, Garcia E, Kanda GK, Lab MJ, et al. Loss of T-tubules and other changes to surface topography in ventricular myocytes from failing human and rat heart. Proc Natl Acad Sci U S A. 2009; 106:6854–9.

M Böhm, R Brückner, I Hackbarth, B Haubitz, R Linhart, W Meyer, B Schmidt, W Schmitz and H Scholz. Adenosine inhibition of catecholamine-induced increase in force of contraction in guinea-pig atrial and ventricular heart preparations. Evidence against a cyclic AMP- and cyclic GMP-dependent effect.Journal of Pharmacology and Experimental Therapeutics August 1984, 230 (2) 483-492;

Mackenzie J. Diseases of the Heart. 3rd ed. London, UK: Oxford Medical Publications; 1914.

Mackenzie L., Bootman, M.J. Berridge, P. Lipp, Predetermined recruitment of calcium release sites underlies excitation–contraction coupling in rat atrial myocytes, J. Physiol. 530 (2001) 417–429.

Maczewski M., A. Beresewicz, The role of adenosine and ATP-sensitive potassium channels in the protection afforded by ischemic preconditioning against the post-ischemic endothelial dysfunction in guinea-pig hearts, J. Mol. Cell. Cardiol. 30 (1998) 1735–1747.

Manning W.J., Silverman D.I., Katz S.E., Riley M.F., Come P.C., Doherty R.M., Munson J.T., Douglas P.S.. Impaired left atrial mechanical function after cardioversion: relation to the duration of atrial fibrillation, J Am Coll Cardiol , 1994, vol. 23 (pg. 1535-1540)

Manning W.J., Silverman D.I., Katz S.E., Riley M.F., Doherty R.M., Munson J.T., Douglas P.S.. Temporal dependence of the return of atrial mechanical function on the mode of cardioversion of atrial fibrillation to sinus rhythm, Am J Cardiol , 1995, vol. 75 (pg. 624-626)

Matherne GP, Linden J, Byford AM, Gauthier NS, Headrick JP . Transgenic A1 adenosine receptor overexpression increases myocardial resistance to ischemia. *Proc Natl Acad Sci U S A*. 1997;94:6541– 6546.

McNutt N.S., Fawcett D.W., The ultrastructure of the cat myocardium. II. Atrial muscle, J. Cell Biol. 42 (1969) 46–67.

Melenovsky V, Borlaug BA, Rosen B, Hay I, Ferruci L, Morell CH, Lakatta EG, Najjar SS, Kass DA. Cardiovascular features of heart failure with preserved ejection fraction versus nonfailing hypertensive left ventricular hypertrophy in the urban Baltimore community: the role of atrial remodeling/dysfunction. *J Am Coll Cardiol*. 2007;**49**:198–207.

Meyer TE, Chung ES, Perlini S, Norton GR, Woodiwiss AJ, Lorbar M, Fenton RA, Dobson JG Jr. Antiadrenergic effects of adenosine in pressure overload hypertrophy. *Hypertension*. 2001;37:862– 868.

Miura T, Liu Y, Kita H, Ogawa T, and Shimamoto K. Roles of mitochondrial ATP-sensitive K+ channels and PKC in anti-infarct tolerance afforded by adenosine A1 receptor activation. *J Am Coll Cardiol* 35: 238–245, 2000.

Mongillo M., Tocchetti C.G., Terrin A., Lissandron V., Cheung Y.F., Dostmann W.R., Pozzan T., Kass D., Paolocci N., Houslay M.D., Zaccolo M. (2006) Compartmentalized phosphodiesterase-2 activity blunts beta-adrenergic cardiac inotropy via an NO/cGMP- dependent pathway. 98 (2) 226-34

Musser, B., Morgan, M. E., Leid, M., Murray, T. F., Linden, J., & Vestal, R. E. (1993). Spe- cies comparison of adenosine and β-adrenoceptors in mammalian atrial and ven- tricular myocardium. Eur J Pharmacol 246, 105–111.

Netter FH, M.D. Atlas of human anatomy. Section III, Thorax, plastes 167-230; 2011.

Newby AC, Worku Y, Meghji P, Nakazawa M, Skladanowski A: Adenosine: A retaliatory metabolite or not? News Physiol Sci 1990;5:67-70

Newby AC, Worku Y , Holmquist CA. Adenosine formation. Evidence for a direct biochemical link with energy metabolism. Advances in Myocardiology [01 Jan 1985, 6:273-284]

Nikolaev V.O., Moshkov A., Lyon A.R., Miragoli M., Novak P., Paur H., Lohse M.J., Korchev Y.E., Harding S.E., Gorelik J. (2010) Beta2-adrenergic receptor redistribution in heart failure changes cAMP compartmentation. Science. 327 (5973) 1653-7

Nikolaev, V. O., Bunemann, M., Schmitteckert, E., Lohse, M. J., and Engelhardt, S. (2006). Cyclic AMP imaging in adult cardiac myocytes reveals far-reaching β1- adrenergic but locally confined β2 -adrenergic receptor-mediated signaling. Circ. Res. 99, 1084–1091. doi: 10.1161/01.

Newman T.M., N.J. Severs, Coated vesicles are implicated in the post-fusion retrieval of the membrane of rat atrial secretory granules, Cell Tissue Res. 268 (1992) 463–469.

Ohler A, Weisser-Thomas J, Piacentino V, Houser SR, Tomaselli GF, O'Rourke B. Two-photon laser scanning microscopy of the transverse-axial tubule system in ven- tricular cardiomyocytes from failing and non-failing human hearts. Cardiol Res Pract 2009;2009:802373.

Ohnishi A, Li P, Branch RA, Biaggioni IO, and Jackson EK (1988) Adenosine in renin-dependent renovascular hypertension. Hypertension 12:152–161.

Oliveira RF, Terrin A, Di Benedetto G, Cannon RC, Koh W, et al. The Role of Type 4 Phosphodiesterases in Generating Microdomains of cAMP: Large

Scale Stochastic Simulations. 2010.PLoS ONE 5(7): e11725. doi: 10. 1371/ journal.

Olsson RA, Pearson JD. Cardiovascular purinoceptors. Physiol Rev. 1990 Jul;70(3):761-845.

Orchard C. H., Pásek M, Brette F. The role of mammalian cardiac t-tubules in excitation–contraction coupling: experimental and computational approaches. 2009. Experimental Physiology. Volume 94, Issue 5. Pages 509–519

Palade GE, Bruns RR Structural modulations of plasmalemmal vesicles. J Cell Biol. 1968 Jun; 37(3):633-49

Palade, G.E., 1953. an Electron Microscope Study of the Mitochondrial Structure. Journal of Histochemistry & Cytochemistry, 1(4), pp.188–211.

Perera, R. K., and Nikolaev, V. O. (2013). Compartmentation of cAMP signalling in cardiomyocytes in health and disease. Acta Physiol (Oxf). 207, 650–662. doi: 10.1111/apha.12077

Perlini S, Arosio B, Parmeggiani L, Santambrogio D, Palladini G Tozzi R, Gatti C, Annoni G, Meyer T and Ferrari A. Adenosine A1 receptor expression during the transition from compensated pressure overload hypertrophy to heart failure Journal of Hypertension: February 2007 - Volume 25 - Issue 2 - p 449–454

Pogwizd, S. M., Schlotthauer, K., Li, L., Yuan, W. & Bers, D.M. Arrhythmogenesis and contractile dysfunction in heart failure: roles of sodium–calcium exchange, inward rectifier potassium current and residual -adrenergic responsiveness. *Circ. Res.* **88,** 1159–1167 (2001).

Prystowsky EN, Katz AM. Atrial fibrillation. In: Topol ES, editor. Textbook of Cardiovascular Medicine. Philadelphia: Lippincott-Raven, 1998: 1827–61.

Rankin AC, Brooks R, Ruskin JN, McGovern BA. Adenosine and the treatment of supraventricular tachycardia. *Am J Med*. 1992;92:655–664.

Richards, M.A. et al., 2011. Transverse tubules are a common feature in large mammalian atrial myocytes including human. Am J Physiol Heart Circ Physiol, 301(5), pp.1996–2005.

Robin E., Sabourint J, Benoit R., Pedretti S., Raddatz E. Adenosine A1 receptor activation is arrhythmogenic in the developing heart through NADPH oxidase/ERK- and PLC/PKC-dependent mechanisms. 2011.Journal of molecular and cellular cardiology, 51(6), pp.945–54.

Rogel, A., Bromberg, Y., Sperling, O. & Zoref-Shani, E. Phospholipase C is involved in the adenosine-activated signal transduction pathway conferring protection against iodoacetic acid-induced injury in primary rat neuronal cultures. *Neurosci. Lett.* **373,** 218–221 (2005).

Rosen, M. R. & Schwartz, P. J. The'Sicilian Gambit'-A new approach to the classification of antiarrhythmic drugs based on their actions on arrhythmogenic mechanisms. European Heart Journal 12, 1112-1131 (1991).

Rothberg KG, Heuser JE, Donzell WC, Ying YS, Glenney JR, Anderson RG Caveolin, a protein component of caveolae membrane coats Cell. 1992 Feb 21; 68(4):673-82.

Schotten, S. Verheule, P. Kirchhof, A. Goette, Pathophysiological mechanisms of atrial fibrillation: a translational appraisal, Physiol. Rev. 91 (2011) 265–325.

Schrader J., Baumann, G. & Gerlach, E. Adenosine as an inhibitor of myocardial effects of catecholamines. 1977. PflugersArch.,372,29-35.

Schrader J., Baumann, G. & Gerlach, E. Sites and mode of action of adenosine in the heart IVentricularmyocardium In Physiological and Regulatory Functions of Adenosine and Adenine Nucleotides .ed. 1979 Baer, H.P.& Drummond,G.I.pp.137-144.NewYork: Raven Press.

Schroder J. Metabolism of Adenosine and Site of Production in the Heart. Boston: Martinus Nijhoff 1983

Shah, A., Kechejian S.J., Kavaler F. & Fisher, V.J. Effects of adenine nucleotides on contractility of normal and postischemic myocardium1974. Am. HeartJ.,87, 740-749.

Silverthorn DU (2010) Cardiovascular physiology In Benjamin Cummings Human Phisiology (4th ed). San Francisco : Pearson. 464-500.

Simionescu N . Cellular aspects of transcapillary exchange. Physiol Rev. 1983 Oct; 63(4):1536-79.

Sipido, K.R. & Cheng, H., 2013. T-tubules and ryanodine receptor microdomains: on the road to translation. Cardiovascular research, 98(2), pp.159–61.

Smyrnias I, Mair W, Harzheim D, Walker SA, Roderick HL, Bootman MD. Compari- son of the T-tubule system in adult rat ventricular and atrial myocytes, and its role in excitation-contraction coupling and inotropic stimulation. Cell Calcium 2010;47: 210 – 223.

Soeller, C. and M. B. Cannell . Examination of the transverse tubular system in living cardiac rat myocytes by 2-photon microscopy and digital image- processing techniques. 1999.Circ Res 84(3): 266-275.

Song LS, Sobie EA , McCulle S , Lederer W. J. , Balke VW and Cheng H Orphaned ryanodine receptors in the failing heart. (2006) *Proc Natl Acad Sci USA* **103**:4305–4310.

Song Y, Belardinelli L. The American Journal of Physiology. 1996; 271:C1233.

Sonnenblick EH, Ross J, Covell JW, Spotnitz HM and Spiro D. The Ultrastructure of the Heart in Systole and Diastole.Circulation Research. 1967;21:423-431, originally published October 1, 1967

Sprenger, J. U., and Nikolaev, V. O. (2013). Biophysical techniques for detection of cAMP and cGMP in living cells. Int. J. Mol. Sci. 14, 8025–8046. doi: 10.3390/ijms14048025

Strickberger SA, Man KC, Daoud EG, Goyal R, Brinkman K, Knight BP, Weiss R, Bahu M, Morady F. Adenosine-induced atrial arrhyth- mia: a prospective analysis. *Ann Intern Med*. 1997;127:417–422.

Szentmiklósi A. J., Németh M., Szegi J., Papp J. Gy., Szekeres L. Effect of adenosine on sinoatrial and ventricular automaticity of the guinea-pig. 1980 Naunyn- Schmiedebergs Arch. Pharmac., 311, 147-149.

Tang, X. L., H. X. Wang, et al. (1998). "Reduced responsiveness of [Ca2+]i to adenosine A1- and A2-receptor stimulation in the isoproterenol-stimulated ventricular myocytes of spontaneously hypertensive rats." J Cardiovasc Pharmacol **31**(4): 493-498

Tawfik HE, Schnermann J, Oldenburg PJ, Mustafa SJ Tebbenjohanns J, Schumacher B, Pfeiffer D, Jung W, Lüderitz B. Dose and rate-dependent effects of adenosine on atrial ac- tion potential duration in humans. J Interv Card Electrophysiol. 1997;1:33–37.

Tawfik Huda E., Schnermann J., Oldenburg Peter J., Mustafa S. Jamal. Role of A1 adenosine receptors in regulation of vascular tone. American Journal of Physiology - Heart and Circulatory Physiology.2005 Vol. 288 no. 3, H1411-H1416

Teng, B., Ledent, C., & Mustafa, S. J.Up-regulation of A_{2B} adenosine receptor in A_{2A} adenosine receptor knockout mouse coronary artery. 2008. J Mol Cell Cardiol 44, 905–914.

Teng, B., Qin, W., Ansari, H. R., & Mustafa, S. J. Involvement of p38-mitogen activated protein kinase in adenosine receptor-mediated relaxation of coronary artery.2005. Am J Physiol Heart Circ Physiol 288, H2574–H2580.

Thomas, J. A. and B. H. Marks.Plasma norepinephrine in congestive heart failure. 1978. Am J Cardiol **41**(2): 233-243.

Trafford, A. W., J. D. Clarke, et al. (2013). "Calcium signalling microdomains and the t- tubular system in atrial mycoytes: potential roles in cardiac disease and arrhythmias." Cardiovasc Res **98**(2): 192-203.

Van Calker, D., Muller, M. & Hamprecht, B. Adenosine regulates via two different types of receptors, the accumulation of cyclic AMP in cultured brain cells. *J. Neurochem.* **33,** 999–1005 (1979).

Van den Berg, M. P., I. C. van Gelder, et al. Impact of atrial fibrillation on mortality in patients with chronic heart failure. 2002. Eur J Heart Fail **4**(5): 571-575.

Vandeput F, Wolda SL, Krall J, Hambleton R, Uher L, McCaw KN, Radwanski PB, Florio V, Movsesian MA. (2007) Cyclic Nucleotide Phosphodiesterase PDE1C1 in Human Cardiac Myocytes*. J. Biol. Chem.,* 282, 32749-32757*.*

Vivek Garg Jundong Jiao Keli Hu. Regulation of ATP-sensitive K+ channels by caveolin-enriched microdomains in cardiac myocytes. Cardiovascular Research, Volume 82, Issue 1, 1 April 2009, Pages 51–58

Vlahovich N., Kee AJ, Van der Poel C, Kettle E, Hernandez-Deviez D, Lucas C, Lynch GS, Parton RG, Gunning PW, Hardeman EC. (2009) Cytoskeletal tropomyosin Tm5NM1 is required for normal excitation–contraction coupling in skeletal muscle. *Mol. Biol. Cell*. 20, 400– 409.

Vliegen, H.W., van der Laarse, A., Cornelisse, C.J., Eulderink, F. (1991). Myocardial changes in pressure overload-induced left ventricular hypertrophy. A study on tissue composition, polyploidization and multinucleation. *Eur. Heart J.* 12, 488-94.

Voigt, N., Zhou, X. B., Dobrev, D. Isolation of Human Atrial Myocytes for Simultaneous Measurements of Ca2+ Transients and Membrane Currents. *J. Vis. Exp.* (77), e50235,

Wagner E, Lauterbach MA, Kohl T, Westphal V, Williams GS, Steinbrecher JH, et al. Stimulated emission depletion live-cell super-resolution imaging shows proliferative remodeling of T-tubule membrane structures after myocardial infarction. Circ Res. 2012; 111:402–14.

Wallukat, G. Herz (2002) 27: 683. https://doi.org/10.1007/s00059-002-2434-z

Wei S, Guo A, Chen B, Kutschke W, Xie YP, Zimmerman K, Weiss RM, Anderson ME, Cheng H, Song LS. (2010) T-tubule remodeling during transition from hypertrophy to heart failure. *Circ. Res*. 107(4):520-31

Welles CC, Ku IA, Kwan DM, Whooley MA, Schiller NB, Turakhia MP. Left atrial function predicts heart failure hospitalization in subjects with preserved ejection fraction and coronary heart disease: longitudinal data from the Heart and Soul Study. *J Am Coll Cardiol*. 2012;**59**:673–680.

West ,A.,Belardinelli ,L.& Berne,R.M. Antagonistic effects of adenosine and aminophylline on ventricular automaticity. 1982. Fedn. Proc., 41, 1384.

Wettschureck N, Offermanns S. Mammalian G proteins and their cell type specific functions. Physiol Rev. 2005;85(4):1159–204.

Williams, C. cAMP detection methods in HTS: selecting the best from the rest. *Nat. Rev. Drug Discov.* **3**, 125–135 (2004)

Woodman S.E, Park D.S., Cohen A.W., Cheung M.W., Chandra M., Shirani J., Tang B., Jelicks L.A., Kitsis R.N., Christ G.J., Factor S.M., Tanowitz H.B., Lisanti M.P. (2002) Caveolin- 3 knock-out mice develop a progressive cardiomyopathy and show hyperactivation of the p42/44 MAPK cascade. *J.*

Biol. Chem. 277 (41) 38988-97

Xiang, Y. Compartmentalization of beta-adrenergic signals in cardiomyocytes. 2011. *Circ. Res*. 109(2), 231–44.

Xiao RP, Hohl C, Altschuld R, Jones L, Livingston B, Ziman B, Tantini B, Lakatta EG J Biol Chem. 1994 Jul 22; 269(29):19151-6.

Xiao, R. P. and E. G. Lakatta (1993). "Beta 1-adrenoceptor stimulation and beta 2- adrenoceptor stimulation differ in their effects on contraction, cytosolic Ca2+, and Ca2+ current in single rat ventricular cells." Circ Res **73**(2): 286-300.

Xu J, He J, Castleberry AM, Balasubramanian S, Lau AG, Hall RA. Journal of Biological Chemistry. 2003; 278:10770. [PubMed: 12529373]

Yeh YH, R. Wakili, X.Y. Qi, D. Chartier, P. Boknik, S. Kaab, U. Ravens, P. Coutu, D. Dobrev, S. Nattel, Calcium-handling abnormalities underlying atrial arrhythmogenesis and contractile dysfunction in dogs with congestive heart failure, Circ. Arrhythm. Electrophysiol. 1 (2008) 93–102.

Yu, F.-X. et al., 2011. Protective effects of adenosine in rabbit sinoatrial node ischemia-reperfusion model in vivo: control of arrhythmia by hyperpolarization-activated cyclic nucleotide-gated (HCN)4 channels. Molecular biology reports, 38(3), pp.1723–31.

Zaccolo M and Pozzan T. Discrete Microdomains with High Concentration of cAMP in Stimulated Rat Neonatal Cardiac Myocytes Science 01 Mar 2002 Vol. 295, Issue 5560, pp. 1711-1715

Zaccolo, M. cAMP signal transduction in the heart: understanding spatial control for the development of novel therapeutic strategies. 2009. Br. J. Pharmacol. 158, 50–60. doi: 10.1111/j.1476-5381.2009.00185.x

Zhao, Z., Francis, C. E., & Ravid, K. An A3-subtype adenosine receptor is highly expressed in rat vascular smooth muscle cells: its role in attenuating adenosine- induced increase in camp. 1997.Microvasc Res 54, 243–252.